Dissertations   Theses and Dissertations

1984

Central Neural Organization of the Respiratory Modulation of Sympathetic Nerve Activity

Caroline Ann Connolly
Loyola University Chicago

CENTRAL NEURAL ORGANIZATION OF THE RESPIRATORY

MODULATION OF SYMPATHETIC NERVE ACTIVITY

by

Caroline Ann /Connelly

A Dissertation Submitted to the Faculty of the Graduate

School of Loyola University of Chicago in Partial

Fulfillment of the Requirements for the Degree of

Doctor of Philosophy

August

1984

I dedicate this work to my family and friends
who shared in the celebration of each achievement
along the way.

ACKNOWLEDGEMENTS

I want to thank the Department of Physiology for the excellent graduate training which I have received. This program has provided me with a firm foundation upon which to build a successful research and teaching career.

I express sincere respect and thanks to my advisor, Dr. Robert D. Wurster. His enthusiasm, scientific curiosity, creativity, depth of knowledge, broad perspective, and boundless energy serve as an inspiration to all who know him. He provided me with the intellectual environment and independence to learn how to think as a scientist. He encouraged independence, yet was always available to help if it was necessary. His example of dedication and hard work will continue to influence me throughout my own career.

I also offer thanks to Mira Milosavljevic for her histological work, David Defily for use of his statistics programs, and the secreterial staff for all of their assistance. In addition, my thanks to Dr. John Trimble and Dr. Charles Robinson for use of the Rockland Real-Time Spectrum Analyzer.

VITA

Caroline Ann Connelly, daughter of Nanette and the late Robert J. Connelly, was born on April 24, 1955 in Chicago, Illinois.

Caroline attended elementary and high schools in West Chicago, Illinois. She graduated from West Chicago Community High School in June of 1973.

In August of 1973, Caroline entered the University of Illinois at Champaign-Urbana. In May of 1977, she graduated with a Bachelor of Science degree in Biology with a minor in Chemistry.

In July of 1978, Caroline entered graduate school at Loyola University in the Department of Physiology. Her dissertation work was completed under the direction of Dr. Robert D. Wurster. The author is a student member of the Society for Neuroscience and the American Physiological Society.

Caroline has accepted a post-doctoral research position with Dr. John Remmers, M.D., at the University of Calgary located in Calgary, Alberta, Canada.

PUBLICATIONS

1.   CONNELLY, C.A. and R.D. Wurster. Spinal organization of respiratory influences on sympathetic nerve discharge patterns in cat. Soc. for Neurosci. Abstracts. 8: 78, 1982.

2.   CONNELLY, C.A. and R.D. Wurster. Effects of hyperventilation on respiratory periodicity of sympathetic nerves. Fed. Proc. 42: 1125, 1983.

3.   CONNELLY, C.A. and R.D. Wurster. Pneumotaxic center influences on the respiratory periodicity of sympathetic nerves. Soc. for Neurosci. Abstracts 9: 180, 1983.

4.   CONNELLY, C.A. and R.D. Wurster. Effects of midline medullary lesions on the respiratory modulation of sympathetic nerve activity. Fed. Proc. 43: 402, 1984.

5.   CONNELLY, C.A. and R.D. Wurster. Midline medullary and cerebellar lesion effects on respiratory modulation of sympathetic activity. Soc. for Neurosci. Abstracts: 1984.

Caroline Ann Connelly

CENTRAL NEURAL ORGANIZATION

OF THE RESPIRATORY MODULATION

OF SYMPATHETIC NERVE ACTIVITY

Central neural organization of pathways and structures influencing the respiratory modulation of sympathetic nerve activity was investigated in five independent studies. Inferior cardiac sympathetic and phrenic nerve activities were recorded in alpha-chloralose anesthetized, vagotomized, paralyzed, artificially ventilated cats. Arterial blood pressure, blood gases, pH, and body temperature were monitored and maintained within normal limits. In some studies, laryngeal nerve, intercostal nerve, or brainstem respiratory unit activities were also recorded. Baroreceptor reflex integrity was assessed before and after lesions or other procedures.

The first study assessed the respiratory nature of sympathetic oscillations related to phrenic nerve activity. It was concluded that respiratory modulation of sympathetic activity was due to central respiratory input and that carotid sinus baroreceptor mediated inputs may explain the presence of apparently independent sympathetic rhythms in previous studies.

The second study assessed spinal locations of

descending pathways responsible for the respiratory modulation of sympathetic activity. It was concluded that influences mediating the respiratory modulation of sympathetic activity descend bilaterally in the dorsolateral funiculus of the spinal cord.

Effects of medial cerebellar lesions on sympathetic rhythmicity were assessed in the third study. This control study indicated that removal of medial cerebellar structures did not affect rhythmicity of sympathetic nerve activity, baroreceptor responses, or respiration.

Since pontine parabrachial areas have known influences on both respiratory and cardiovascular systems, effects of pontine parabrachial stimulation and lesions on respiratory modulation of sympathetic activity were assessed in the fourth study. The stimulation studies indicated that parabrachial area influences on sympathetic activity were not gated through respiratory inputs on sympathetic activity. After pontine lesions, sympathetic activity was enhanced at the onset and inhibited at the termination of apneustic phrenic nerve activity.

The fifth study assessed whether midline medullary pathways and structures were necessary for respiration and the respiratory modulation of sympathetic activity. It was concluded that midline medullary lesions eliminated the respiratory modulation of sympathetic activity by decreasing

the population of rhythmically active brain stem respiratory units.   Other   influences   on   sympathetic   activity   (e.g. baroreceptor and supramedullary stimulation) remained intact after midline medullary lesions.

TABLE OF CONTENTS

vii

LIST OF ILLUSTRATIONS

Appendix Figure

CHAPTER I

INTRODUCTION

Interactions between respiratory and cardio-
vascular control systems have been the focus of several
recent symposia (104, 168, 184). Such research issues
bridging the interface between two fundamental areas not
only clarify interactions between two systems, but also aid
our understanding of each individual system. The purpose of
this dissertation was to characterize central nervous system
interactions between respiratory and cardiovascular control
systems by studying the respiratory modulation of
sympathetic activity.

The dissertation has been organized such that
general reviews of the sympathetic nervous system and neural
regulation of respiration precede the five self-contained
studies. The rationale and specific literature pertinent to
each study are provided in each of the five individual
sections. The five studies are then summarized prior to
listing the final conclusions.

CHAPTER II

GENERAL LITERATURE REVIEW

A. SYMPATHETIC NERVOUS SYSTEM

Cardiovascular function is regulated by sympathetic and parasympathetic branches of the autonomic nervous system. Anatomical and functional aspects of the sympathetic nervous system, as it relates to cardiovascular control, will be discussed in this section of the literature review.

1. Anatomical Organization

The sympathetic branch of the autonomic nervous system is composed of pre- and post-ganglionic nerves. Preganglionic sympathetic nerves originate primarily in the intermediolateral (IML) column of the thoracolumbar spinal cord (148). In addition, sympathetic preganglionic cell bodies have been identified in the lateral funiculus, central autonomic, and intercalated areas of the spinal cord (148). Preganglionic sympathetic nerves from T1 to T9

spinal levels project to the ipsilateral stellate ganglion (148) where they synapse with post-ganglionic sympathetic nerves, including the inferior cardiac nerves which were recorded in these dissertation studies.

The activity of sympathetic nerves is affected by descending brain stem inputs frequently referred to as central sympathetic pathways. In a classic 1863 study, Bernard (24) originally concluded that the brain was necessary for blood pressure control after observing marked decreases in blood pressure following cervical spinal cord transection. Subsequent serial transection studies in rabbits by Dittmar in 1870 (52) and Owsjannikow in 1871 (149) indicated that the caudal one-third of the pons and rostral two-thirds of the medulla are the principle brain stem sites responsible for maintaining blood pressure. In 1946, Alexander (5) did similar transections while recording cervical and inferior cardiac sympathetic nerves in the cat. Alexander found that sympathetic nerve activity decreased with blood pressure after cervical spinal transection. In more recent studies of spinal cord transected cats, some recovery of sympathetic nerve activity was observed with time (9, 19). However, even after recovery, rhythmicity of sympathetic activity was altered following loss of the descending inputs in those studies (19). Thus, lesion studies support the concept that cardiovascular function is

modulated by brain stem structures.

Stimulation studies further verified that supraspinal structures influence sympathetic nerves. Ranson and Billingsley in 1916 (157) and Wang and Ranson in 1939 (186) mapped out pressor and depressor regions by stimulating points on the dorsal brain stem while noting cardiovascular responses. Projection of specific brain stem structures to sympathetic preganglionic cell bodies has been suggested by more recent studies. Brain stem stimulation studies (94, 181) indicated evoked sympathetic activity following stimulation of such areas as the periventricular grey, nucleus reticularis ventralis, and nucleus reticularis parvocellularis. In addition, those studies indicated that brain stem projections to sympathetic nerves are bilateral. Other stimulation studies have indicated supraspinal inputs to sympathetic nerves from a number of structures, including the hypothalamus (1), pontine parabrachial areas (144), medial cerebellar nuclei (1, 2, 139, 140), and cingulate cortex (120) among others.

Brain stem neurons with cardiovascular related activity have been reported by numerous investigators (67, 75, 106, 156, 166, 177). Gootman, Cohen, Piercy, and Wolotsky (75) used cross-correlograms to identify brain stem unit activity related to that of splanchnic sympathetic activity in cats. Using spike-triggered averaging, Gebber

and Barman (67) located neurons in the classic pressor region of the lateral medullary reticular formation which had activity patterns correlated with ipsilateral inferior cardiac sympathetic nerves in cats. Spike triggered averaging has also been used to identify neurons in the hypothalamus (14) and medullary raphe nuclei (142) with activities related to sympathetic nerve discharges.

Anatomical techniques have also been used to determine brain stem projections to the sympathetic preganglionic nerves. Horseradish peroxidase (HRP) studies have allowed retrograde tracing of brain stem projections to the IML (110, 138). Miura, Onai, and Takayama (138) reported HRP-labeled cells distributed in the medulla (72.1%), pons (10.2%), midbrain (8.5%), and hypothalamus (9.2%) following HRP injection into the IML. Labeled cells were most concentrated in the medullary reticular formation (37.8%), median raphe (26.9%), and pontine reticular formation (10.2%). Medullary cell groups with bilateral projections to the IML were found in the median raphe, nucleus tractus solitarius, vestibular nuclei, and ventromedial reticular formation. Brain stem catecholamine projections to the intermediolateral column of the thoracolumbar cord have also been described (8, 33, 46, 131).

Tracts descending from supraspinal regions which

control sympathetic activity are located in dorsal and
ventral regions of the spinal cord (1, 62, 88, 89, 100).
When Illert and Seller (89) stimulated spinal pathways in
cats with spinal cord transections at C1-C2 levels, they
identified depressor pathways in the ventrolateral cord
which inhibited sympathetic activity and decreased blood
pressure. Using similar methods, pressor pathways have been
localized in the dorsolateral funiculus region of the spinal
cord (62, 88).

2. Functional Aspects

a. Respiratory-Related Activity

        Respiratory related rhythms were observed in the
first recordings of sympathetic nerves by Adrian, Bronk, and
Phillips in 1932 (3). Subsequently, other investigators
have described rhythms of apparent respiratory origin in
sympathetic discharge patterns (41, 72, 108, 127, 146, 154,
155, 180). Cohen and Gootman (41) noted parallel changes in
splanchnic sympathetic and phrenic rhythms with alterations
in end-tidal carbon dioxide in paralyzed, alpha-chloralose
anesthetized and decerebrate cats. Additionally, Preiss,
Kirchner and Polosa (154) observed increases in inspiratory
discharges of cervical sympathetic single fibers following

increases in end-tidal carbon dioxide levels in pentobarbitol anesthetized cats. Levy, DeGeest and Zieske (112) concluded in a 1966 study that the respiratory modulation of sympathetic activity caused rhythmic fluctuations in heart rate and ventricular contractility coinciding with respiration in vagotomized dogs. Other than coordination of respiratory and cardiovascular systems, the functional significance of respiratory rhythms in sympathetic nerve discharges is not thoroughly understood at this time.

b. Baroreceptor Influences

Cardiac-related rhythms were also observed in the first sympathetic nerve recordings by Adrian, Bronk, and Phillips (3). Cardiac-related sympathetic activity is attributed to baroreceptor-mediated inhibition of sympathetic activity occurring with each arterial pressure pulse and is eliminated after sino-aortic baroreceptor denervation, as reviewed by Spyer (174). Baroreceptor mediated inhibition of sympathetic activity was initially described by Kezdi and Geller (101). Using an isolated carotid sinus model in the dog, Kezdi and Geller determined that the time delay from carotid sinus pressure change to inhibition of renal or splanchnic sympathetic activity

ranged from 0.15 to 0.36 seconds. They reported that the time delay from carotid sinus pressure change to the reflex blood pressure change was 3.5 seconds.

A 2-6 cycle/second sympathetic rhythm, unrelated to the cardiac cycle, has been reported after decerebration and sinoaortic baroreceptor denervation in cats (67). This independent sympathetic rhythmicity has been interpreted to indicate an intrinsic central sympathetic oscillator (66). Using the central sympathetic oscillator model, cardiac-related sympathetic rhythmicity has been explained as baroreceptor entrainment of the 2-6 cycle/second central sympathetic oscillator.

c. <u>Chemoreceptor Influences</u>

Stimulation of carotid body chemoreceptors results in peripheral vasoconstriction and bradycardia mediated by autonomic nerves (25, 48). Bernthal, Motley, Schwind and Weeks (25) originally observed vasoconstrictor responses in the hindlimb and submaxillary gland of dogs following injection of sodium cyanide into vascularly isolated carotid sinus regions. The vasoconstriction was eliminated after sympathectomy. In a later study, Daly and Scott (48) perfused dog isolated carotid sinuses with hypoxic blood from donor dogs. The resultant vasoconstriction in the

artificially ventilated dogs was eliminated by administration of hexamethonium, substantiating that the vascular response was mediated by sympathetic nerves. Bradycardia resulting from carotid body stimulation was decreased, but not eliminated, after vagotomy. The small bradycardia response which remained after cervical vagotomy was abolished after eliminating sympathetic influences by application of a local anesthetic to the stellate ganglion. Thus, sympathetic activity to the heart is decreased in response to carotid body stimulation. However, all neuronal traffic through the stellate ganglion is not decreased in response to carotid body stimulation. Hypoxic stimulation of the carotid bodies causes pulmonary vasoconstriction which is also mediated by sympathetic nerves via the stellate ganglion (47). Thus, differential activation of sympathetic pathways results from carotid body stimulation.

Chemoreceptors located on the ventral surface of the brain stem also influence sympathetic activity (60). In contrast to the peripheral chemoreceptors, which are sensitive to hypoxia, medullary chemoreceptors affecting sympathetic activity are pH (169) and drug (61) sensitive. Schlaefke, See and Loeschke (169) reported small but significant increases in arterial blood pressure following localized surface application of low pH solutions (pH = 7.0) to ventral medullary chemoreceptor regions in vagotomized,

sinoaortic denervated cats. Surface application of
inhibitory pharmacological agents (e.g. glycine) to the
ventral medullary chemoreceptor regions causes blood
pressure depression (77). Amendt, Czachurski, Dembowsky,
and Seller (6) have determined that the ventral medullary
chemosensitive area projects to the intermediolateral cell
column. Guertzenstein and Silver (77) reported that
bilateral lesions of the ventral medullary surface resulted
in marked mean blood pressure depression of 52 mmHg (77).
Thus, it has been hypothesized that the ventral
chemoreceptive surface of the medulla is a vasomotor center
which plays a key role in maintenance of arterial pressure.

Responses of sympathetic preganglionic neurons to
systemic hypoxia (pO2 < 40 mmHg) in the absence of
peripheral chemoreceptors have also been described (4, 164,
165). Alexander (4) and Rohlicek and Polosa (164) reported
that hypoxia caused excitation of sympathetic nerves in
spinal preparations. In contrast, sympathetic fibers were
either excited or inhibited by hypoxia in sino-aortic
denervated cats with intact central nervous systems (165).
Rohlicek and Polosa (165) reported that the effects of
hypoxia on sympathetic firing rate were not usually seen
until systemic pO2 levels were extremely low, e.g. pO2 = 20
mmHg.

B. NEURAL CONTROL OF RESPIRATION

Following a general description of the anatomical organization of some key central nervous system structures and pathways involved with respiration, two basic models for respiratory rhythmogenesis will be briefly discussed.

1. Anatomical Organization

a. Dorsal Respiratory Group

The site of respiratory rhythm generation was first localized to the medulla by brain stem transection studies (111, 121, 122, 123, 124). With the advent of more sophisticated neuroanatomical and neurophysiological techniques, roles for specific medullary nuclei in the control of respiration have been elucidated. Medullary nuclei with respiratory activities have been subdivided into dorsal and ventral respiratory group classifications (135).

As reviewed by Long and Duffin (119), dorsal respiratory group inspiratory neurons are located in the ventrolateral subnucleus of the nucleus of the solitary tract (nTS) in densely packed, bilateral columns which are parallel to the neuraxis. The columns extend 2.0 to 3.0 mm rostral to the obex, 2.0 to 3.0 mm lateral to the midline

and are 0.6 to 2.6 mm below the dorsal medullary surface. In a 1973 study von Euler et. al. (56) identified dorsal respiratory group neurons physiologically before injecting Procion yellow dye intracellularly to determine their morphological characteristics. The Procion yellow labeled neurons were either stellate or fusiform shaped with dendrites oriented in both dorsomedial and ventrolateral directions. Somal diameters ranged from 20 to 60 um.

In a more recent study, Berger et. al (22) injected ventrolateral nTS inspiratory neurons intracellularly with horseradish peroxidase to better characterize axonal and dendritic arborizations. Somal dimensions in that study were reported to be 30 um. The dendrites were observed to course longitudinally, parallel, and ventral to the nTS. Axons of the injected nTS neurons were generally found in the contralateral ventral medulla, rostral to the level of their cell bodies. Axonal bifurcations of nTS projections in the medulla were observed in three cases. Following bifurcation in one case, an axonal branch was reported to enter the contralateral medulla while the other branch projected caudally in the ipsilateral medulla. Those results were consistent with autoradiographic (117) and physiological cross-correlation data (42) indicating that nTS neurons project bilaterally, with a contralateral predominance, from the medulla to phrenic motor nerves in

the spinal cord.

In a classic 1958 study, Baumgarten and Kanzow (18) described the inspiratory respiratory units located in the vicinity of the nTS. Those nTS neurons, which always fired in phase with phrenic nerve discharges and were inhibited by lung inflations, were designated as R-alpha neurons. The other type of inspiratory cells found in the nTS, characterized by the fact that lung inflations enhanced their activity, were designated as R-beta neurons. A study by von Euler et. al. (56) initially indicated that the R-alpha cells project to the spinal cord whereas R-beta neurons are restricted to the brain stem. However, a more recent study by Lipski, Kubin, and Jodkowski (113) has indicated that the R-beta neurons also project to the spinal cord. Inspiratory neurons of the dorsal respiratory group are reported to be the source of respiratory input to spinal phrenic and external intercostal inspiratory neurons (56, 57). In addition to the inspiratory cells, a limited number of expiratory cells and "P" (respirator pump) cells have also been reported in the dorsal respiratory group (21, 56).

b. Ventral Respiratory Group

The ventral respiratory group extends from the rostral border of the medulla to the C1 spinal level. It is

comprised of respiratory neurons in the Botzinger complex (i.e. retrofacial nucleus region), nucleus retroambigualis, and nucleus ambiguus.

The most rostral portion of the ventral respiratory group, the Botzinger complex, contains exclusively expiratory neurons (135). The Botzinger complex in the cat is located between 3.5 to 5.5 mm rostral to the obex, 2.9 to 3.3 mm lateral to the midline, and 3 to 5 mm below the dorsal surface of the medulla (119). Projections of Botzinger complex axons to contralateral nTS inspiratory neurons have been demonstrated using anatomical tracing techniques (32, 96). In addition, Merrill et. al. (136) provided physiologic evidence that stimulation of Botzinger complex expiratory neurons produced inhibitory post-synaptic potentials in intracellularly recorded contralateral nTS inspiratory neurons. Botzinger expiratory neurons also have collateral arbors in the ipsilateral nTS and project bilaterally to inspiratory and expiratory regions of the nucleus retroambigualis. A study by Fedorko (59) indicated that eighty-three percent of the Botzinger neurons project to the spinal cord. Fifty percent of the expiratory neurons cross to the contralateral rostral medulla before descending in the spinal cord.

Respiratory cells of the nucleus retroambigualis are located in bilateral columns which extend from 3 mm rostral

to the obex to the first cervical spinal level. The bilateral columns are located 3 to 5 mm lateral to the midline and 3 to 5 mm below the dorsal surface of the medulla. The region rostral to the obex contains primarily inspiratory cells whereas expiratory cells are concentrated caudal to the obex. A mixed population of inspiratory and expiratory cells are found in the nucleus retroambigualis at the level of the obex (135). Antidromic mapping studies by Merrill (134) indicated that 90% of the nucleus retroambigualis inspiratory neurons cross the rostral medullary midline before descending in the contralateral spinal cord in the ventrolateral white matter, dorsolateral funiculus or most medial aspects of the ventral column. Merrill demonstrated that axons of the expiratory nucleus retroambigualis neurons cross the medulla caudal to the obex and then descend in the ventral spinal cord. Uncrossed spinal projections of nucleus retroambigualis expiratory neurons have not been demonstrated.

Inspiratory and expiratory neurons of the nucleus ambiguus extend from the obex to 3 mm rostral to the obex. They are 3 to 5 mm lateral to the midline and 3 to 5 mm below the dorsal surface of the medulla. Subnuclei of the nucleus ambiguus have axons which project ipsilaterally to the various laryngeal and pharyngeal muscles.

c. Post-Inspiratory Neurons

Post-inspiratory neurons, as described by Richter (160, 161), are interposed between the nucleus retroambigualis and nTS rostral to the obex. Activity of post-inspiratory neurons coincides with the period of phrenic nerve afterdischarge, occurring between inspiratory and active expiratory phases of the respiratory cycle. Although anatomical projections of post-inspiratory neurons have not been elucidated, physiological evidence has suggested that they may be involved in respiratory rhythmogenesis (160, 161).

d. The Pons

Neurons in the pons have a strong influence on respiration, but are not considered necessary for rhythmic breathing (30, 83, 185). Lesions of the dorsolateral rostral pons or transections of the pons result in an apneustic (i.e. prolonged inspiratory duration) breathing pattern (26, 121, 122, 123, 124). The prolonged inspiration after pontine lesions was originally interpreted to mean that the pons provided expiratory facilitory input necessary for normal breathing. Another interpretation was that the respiratory pacemaker was located in the pons. To test the

pontine pacemaker hypothesis, Cohen sought to determine if pontine respiratory unit activity continued in dorsolateral pontine regions after isolation from the medulla (.37). However, in that study Cohen found no periodic discharges in isolated pontine segments and concluded that pontine respiratory unit activity was derived from the medulla. Neuroanatomical results have verified that nTS inspiratory neurons in the medulla have reciprocal connections with pontine parabrachial areas (32, 102).

e. Spinal Pathways

Bulbospinal respiratory pathways to phrenic and intercostal respiratory motoneurons arise primarily from contralateral brain stem respiratory neurons which decussate in the medulla and then course in ventrolateral regions of the spinal cord (36, 151).

2. Respiratory Rhythmogenesis

Pacemaker cell and neuronal network theories have each been proposed to explain the generation of central respiratory rhythmicity (119, 137, 189). Although there is evidence for pacemaker cell control of respiratory movements in invertebrates (132), there is a lack of experimental

evidence for respiratory pacemakers in mammals. Instead, current models explaining central respiratory rhythmogenesis are based on neuronal networks.

Salmoiraghi and Burns are credited with the reciprocal inhibition model of central rhythm generation (31). The model consists of reciprocal inhibition between inspiratory and expiratory neurons, along with local re-excitation among each group of neurons. According to this model, inspiratory neuron discharges inhibit expiratory neuron discharges until excitability of the inspiratory neurons decreases due to accomodation. Once the inspiratory neuron discharge terminates, expiration ensues with the disinhibition of expiratory neurons. However, until a recent study by Merrill, Lipski, Kubin and Fedorko (136), there was no experimental evidence indicating monosynaptic inhibitory connections of expiratory neurons with inspiratory neurons.

Wyman has proposed an off-switch model to explain respiratory rhythmogenesis (189). Central respiratory output is divided into an augmenting inspiratory discharge, a rapid inhibition of the discharge (off-switch) and a pause during expiration. According to the model, lung inflation, temperature, CO_2, and dorsolateral rostral pontine influences on the augmenting inspiratory discharge are mediated through a common off-switch mechanism. The off-switch neurons responsible for the termination of

inspiration are a theoretical population of neurons separate from the expiratory neurons. Some investigators have suggested that a group of respiratory neurons which discharge during late inspiration may constitute part of the off-switch mechanism. The mechanism of the augmenting inspiratory discharge is also not understood. Richter has postulated that the augmenting inspiratory discharge is due to a gradual withdrawal of inhibitory input to inspiratory neurons (161). However, the mechanism underlying central respiratory rhythm generation is still a controversial issue among respiratory neurophysiologists.

CHAPTER III

EFFECTS OF HYPERVENTILATION ON RESPIRATORY MODULATION
OF SYMPATHETIC NERVE ACTIVITY

A. INTRODUCTION

Blood pressure waves and slow sympathetic rhythms
with respiratory frequencies of apparent non-respiratory
origin have been described (13, 104, 105, 107). Separate
central sympathetic and respiratory oscillators, which may
be reciprocally entrained to each other, have been recently
postulated to explain independent slow sympathetic rhythms
(13). Unlike the respiratory oscillator, central
sympathetic oscillators were postulated to be relatively
unaffected by chemoreceptor input. The hypothesis was based
on the observation in some animals of a slow "respiratory"
periodicity remaining in the sympathetic nerve discharge
following hyperventilation beyond cessation of phrenic nerve
activity. An alternate hypothesis contends that respiratory
cells are primarily responsible for slow sympathetic
oscillations with respiratory frequencies (3, 41, 72, 91,
153, 154, 155, 180) and that seemingly independent slow

20

sympathetic rhythms may be explained by more classic mechanisms, possibly involving baroreceptors (91, 146, 180).

In the present study, the nature of slow sympathetic rhythmicity was reexamined using spectral analysis of sympathetic nerve frequencies. Spectral peak frequencies of sympathetic activity were assessed to determine if any changes in sympathetic rhythmicity occurred during hyperventilation-induced phrenic and external intercostal nerve quiescence. Blood pressure and sympathetic nerve responses to baroreceptor input were tested using bilateral carotid occlusions and ECG-triggered computer summation of sympathetic activity, respectively. Blood pressure, blood pressure responses to bilateral carotid occlusion tests, blood gases, and pH were compared for differences between control, hyperventilation, recovery, and expiratory hold (ventilator transiently turned off) stages.

B. METHODS

1. Preparation

Nine cats were anesthetized with chloroform followed by intravenous infusion of alpha-chloralose (40-60 mg/kg). Femoral artery catheters were inserted for blood pressure, (Statham P23Db pressure transducer) and pH, pO_2, and pCO_2 measurements (Radiometer-Copenhagen BMS3-C Blood Microsystem). After tracheotomy, end-expiratory %CO_2 was continuously monitored (Beckman LB1 analyzer). Positive pressure artificial ventilation was begun after neuro-muscular blockade with continuous succinyl choline infusion (6 mg/kg/hr). A cannula was inserted into the trachea for measurement of intratracheal pressure (Statham P23Db pressure transducer) as an indicator of ventilator activity. Cervical vagi and aortic depressor nerves were cut to eliminate vagal stretch receptor and aortic baro- and chemoreceptor influences on sympathetic activity. Inflatable occluders (Rhodes Medical Instruments) were placed around the carotid arteries for bilateral carotid occlusion tests of reflex sympathetic activation during control, hyperventilation, recovery, and twenty second expiratory hold maneuvers. Normal values for blood gases and pH were defined as $pO_2 \geq 100$ mmHg, $pCO_2 = 20-35$ mmHg, and pH

= 7.34. Control blood gas and pH values were in the normal range or were adjusted to normal ranges prior to the experimental procedure by infusion of 8.4% sodium bicarbonate or adjustment of ventilator rate and pressure. Rectal temperature was maintained at 38 ± 1 C with a servo-regulated heating pad.

Each cat was secured in a stereotaxic head frame (David Kopf Instruments). The pelvic iliac crests and a thoracic spine were clamped to a hanging frame to minimize ventilator induced movement artifacts.

2. Nerve and Electrocardiogram Recordings

A skin and muscle flap extending from the left ear to the second thoracic spine was pulled laterally and attached to a curved horizontal rod to create two oil pools; a rostral one for the phrenic nerve and a caudal one for the inferior cardiac sympathetic and T1 external intercostal nerves. To isolate the left inferior cardiac sympathetic and external intercostal nerves, dorsal muscle layers were scraped away from the first and second ribs and the heads of the two ribs were removed. The bodies of the ribs were laterally retracted to expose the T1 spinal nerve rostrally and the stellate ganglion ventrocaudally. The T1 intercostal nerve was cut distally and the epineural sheath was

routinely removed. The caudally coursing inferior cardiac sympathetic nerve was cut distally and desheathed in some preparations. Rostrally, the phrenic nerve was isolated as it exited from the fourth cervical nerve root, cut distally, and desheathed.

Left phrenic, inferior cardiac sympathetic, and external intercostal nerves were placed on bipolar platinum electrodes for differential recording (Grass P9 amplifiers). Nerve signals were monitored on a storage oscilloscope and photographed at various stages in each experiment. After leaky integration, (Grass Model 7P3 A Integrator, low pass filter time constant = 0.5 sec.) the signals were displayed on the oscillograph and stored on magnetic tape (Precision Instruments model 6200 tape recorder) for later analysis.

To allow comparison between this study and a similar investigation which used different signal filtering methods (13), the inferior cardiac sympathetic nerve signal in one cat was simultaneously recorded on two amplifiers and integrators with differing preamplifier frequency filter settings (Fig. 3-1). Low and high 1/2 amplitude filter settings for Amplifier A were 10 Hz and 2 KHz, respectively. Frequency filter settings for the other eight experimental cats were the same as Amplifier A. Amplifier B was set at low and high 1/2 amplitude filter settings of 0.5 Hz and 2

Figure 3-1

The oscilloscope picture (Top) illustrates phrenic nerve activity, sympathetic nerve activity after signal filtering method A (Symp. A) and sympathetic nerve activity after signal filtering method B (Symp. B). Amplification methods and frequency filter characteristics used to produce Symp. A and Symp B. recordings are diagrammatically illustrated below. RC characteristics of a sympathetic nerve fiber on a bipolar electrode are depicted using standard electronic symbols for resistance and capacitance.

PHRENIC N. 100 μV

SYMP. A 200 μV

SYMP. B 250 μV

I SEC

AMP A
LOW 1/2 AMP = 10 HZ
HIGH " = 2 KHZ
→ SYMP. A

AMP B
LOW 1/2 AMP = 0.5 HZ
HIGH " = 2 KHZ.
→ SYMP. B

SYMP. N.
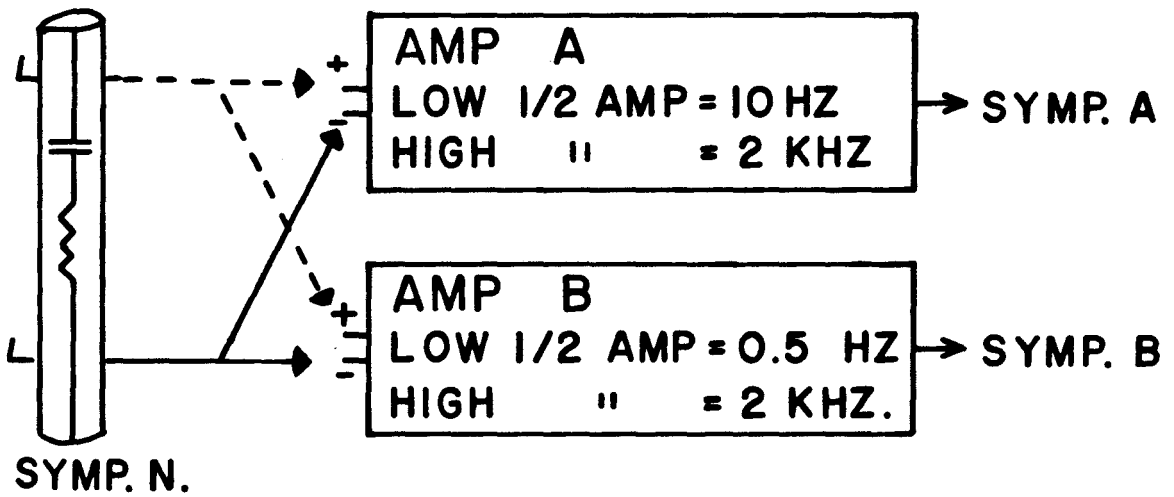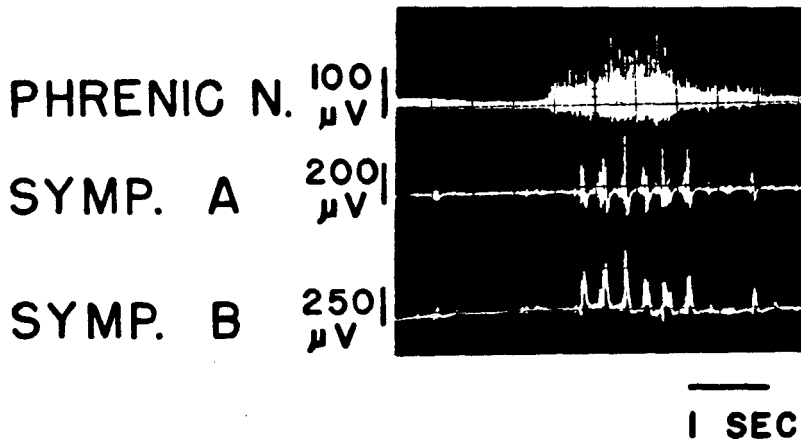
KHz, respectively. The Amplifier B settings allowed passage of very slow signals. The slower frequency signals present in the Symp. B recordings were derived from summation of multifiber nerve activity due to impedence properties of the nerve (See Appendix I). Figure 3-1 (Top) illustrates that bursts of sympathetic activity were similarly represented, irrespective of the signal filtering method used.

Lead II Electrocardiograms (ECG) were recorded for analysis of cardiac related (2 to 6 Hz) sympathetic activity using ECG (R-wave) triggered computer summation (described below).

3. Procedure

Control measurements of 1) pH, 2) arterial pO_2, 3) arterial pCO_2, 4) end-expiratory CO_2, 5) blood pressure, and 6) blood pressure responses to bilateral carotid occlusion tests were recorded. The cats were then hyperventilated to induce apnea by increasing the depth of artificial positive pressure ventilation, keeping the ventilator rate constant. The six variables were measured during apnea, and then the ventilator depth was decreased back to the control settings to allow recovery of phrenic nerve activity. Cats were considered to be in the recovery stage only after arterial blood gases and pH values returned to control levels.

Recovery from hyperventilation was frequently induced by transiently discontinuing artificial ventilation for twenty second periods (expiratory hold maneuvers). The six variables were also measured during recovery and expiratory hold stages.

4. Spectral Analysis

Presence of slow sympathetic respiratory rhythmicity was qualitatively assessed during control, hyperventilation, recovery and expiratory hold stages of the procedure. In addition, spectral analysis (Rockland Real-Time Spectrum Analyzer FFT 512/S) was used to determine the effect of hyperventilation on the slow frequency characteristics of sympathetic nerve activity. Prior to spectral analysis, the sympathetic nerve signals were low-pass filtered (Grass Integrator TC = 0.5 sec) to facilitate assessment of the slow frequency components due to rhythmic bursts of sympathetic activity coinciding with the respiratory frequency ("Respiratory Peaks"). Although higher freqency components of sympathetic activity (e.g. cardiac-related activity indicated by a "Cardiac Peak") were attenuated or eliminated by the low-pass filtering technique, the low frequency bursts of sympathetic activity ("Respiratory Peaks") were more readily detected after low-pass filtering

the input signal. Thus, this application of spectral analysis was specifically used to detect the presence or absence of "Respiratory Peaks" in this experiment. It should be noted that the higher background spectral amplitude in the lower frequencies is attributed to the low-pass signal filtering methods prior to spectral analysis, and should not be mistakenly interpreted as more physiological activity in the low rather than high frequency range. The spectral amplitude (millivolts) of sympathetic nerve activity at the respiratory frequency (amplitude of the "Respiratory Peak") was measured during control, hyperventilation, and recovery stages of the experiment and those results statistically compared for all cats.

5. Computer Summation Analysis

The presence of cardiac related sympathetic activity during control, hyperventilation and recovery stages of the experiment was determined by ECG triggered computer summation (Nuclear Chicago Data Retrieval Computer) of amplified, integrated sympathetic activity (four hundred sweeps). The area (millivolt-seconds) of the computer summed activity was divided by its duration (seconds) to correct for any differences due to variation in cardiac cycle time. ECG triggered sympathetic activity (area/time)

was quantitatively expressed in millivolts. Areas and durations of computer summed activity were measured using a graphics tablet (Bausch and Lomb) connected to a digital computer (Apple II Plus).

6. Statistics

Differences between control, hyperventilation, recovery and expiratory hold values for blood pressure, blood pressure responses to bilateral carotid occlusion tests, pH, and blood gases were statistically evaluated using analysis of variance followed by tests for least significant differences (69, 163). Differences between control, hyperventilation and recovery values for ECG triggered sympathetic activity (area/time), end expiratory CO_2, and spectral amplitudes of sympathetic nerve activity (millivolts) in the respiratory frequency range were also statistically compared using the same tests. Significance was defined at $P < 0.05$. Values are expressed as means $\pm$ standard error (SE) of the mean.

C. RESULTS

Richter (160) divided the central nervous rhythm of respiration into three phases based on activities of phrenic and intercostal nerves. Inspiratory, post-inspiratory, and expiratory phases of the respiratory cycle were designated as phases 1, 2, and 3, respectively. The term, post-inspiratory, was originally introduced by Gautier, Remmers and Bartlett (65) to describe the passive expiratory stage coinciding with the period of phrenic nerve afterdischarge occurring between inspiration and active expiration. Figure 3-2 illustrates that characteristic patterns of respiratory-related rhythms in sympathetic activity corresponded well with the three phases of respiration designated by Richter. Sympathetic activity was enhanced with inspiration during phase 1 of the respiratory cycle. The strong inhibition of sympathetic activity at the onset of the post-inspiratory period (phase 2) was a prominent synchronizing point between phrenic and sympathetic activities. Following the period of inhibition during post-inspiration, sympathetic nerves characteristically resumed activity during the expiratory phase (phase 3). Although exact patterns of sympathetic activity vary somewhat in different cats, elements of the phase 1, 2, and 3 influences just described are ordinarily

Figure 3-2

Oscillograph recordings indicate respiratory modulation of sympathetic nerve activity in a paralyzed, artifically ventilated cat. Integrated inferior cardiac sympathetic (Integ. Symp.), integrated phrenic (Integ. Phren.), raw inferior cardiac sympathetic (Symp.), and raw phrenic (Phren.) nerve recordings are illustrated.

INTEG. SYMP.

INTEG. PHREN.

5 SEC

SYMP. 125 μV

375 PHREN. μV
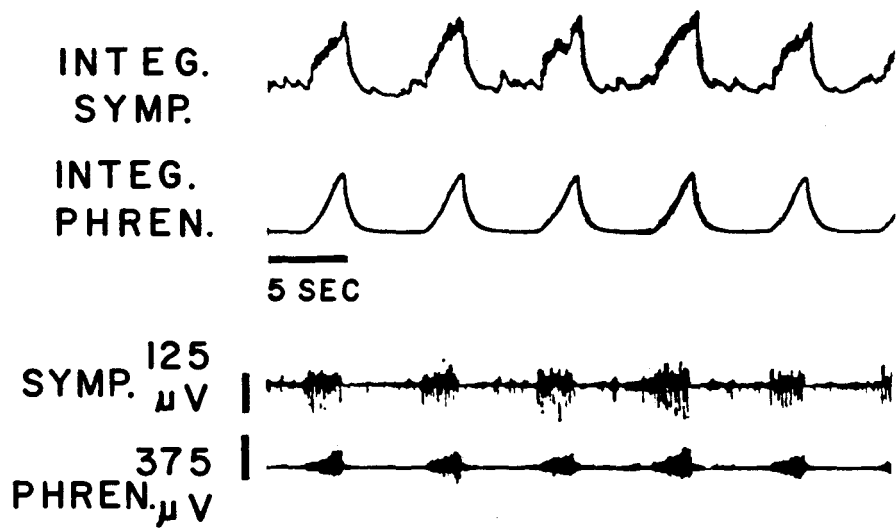
present to varying degrees.

Effects on central respiratory activity, sympathetic activity and blood pressure during hyperventilation, expiratory hold, and after recovery are depicted for one of the cats in Fig. 3-3. As control recordings indicated, external intercostal, phrenic, and sympathetic nerve activities had synchronized respiratory-related rhythms prior to hyperventilation. As for all the cats, control blood pressure was above 100 mmHg. Little or no effect of the ventilator on sympathetic activity or blood pressure was observed since the cats were artificially ventilated with high frequency, low volume inflations. Artificial ventilator activity was indicated by intratracheal pressure recordings. When higher frequency (e.g. 60 oscillations/min) ventilator-related sympathetic rhythms were observed in some cats, they were clearly distinguished from lower frequency (e.g. 12 breaths/min) rhythms of central nervous system origin.

Raw and integrated sympathetic nerve recordings in Figure 3-3 illustrate changes in sympathetic rhythms due to hyperventilation, expiratory hold and after recovery to normoventilation conditions. As hyperventilation gradually reduced phrenic and intercostal nerve activities to quiescence, sympathetic nerve activity simultaneously lost the slow regular rhythmic oscillations related to

Figure 3-3

Oscillograph tracing during (left to right) control, hyperventilation, expiratory hold, and recovery stages. Integrated external intercostal nerve, integrated inferior cardiac sympathetic nerve, integrated phrenic nerve, raw sympathetic nerve, raw phrenic nerve, blood pressure, and intratracheal pressure recordings are illustrated (Top to Bottom).
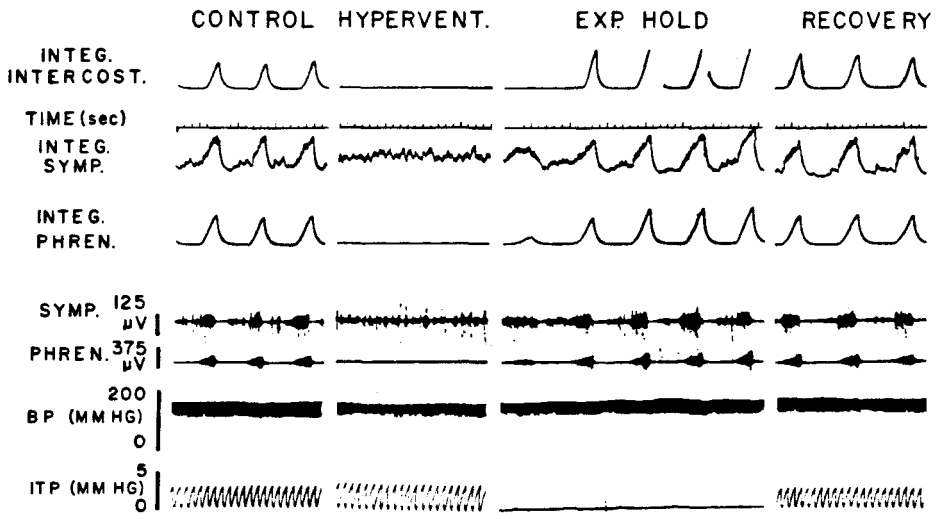
respiration.   Specifically, the enhancement of sympathetic activity coinciding with inspiration during phase 1 of the respiratory cycle and the characteristic inhibitory period related to post-inspiration were absent during hyperventilation.   Phrenic, external intercostal, and respiratory-related sympathetic rhythms returned during the expiratory hold maneuver immediately following hyperventilation.   Enhancement of sympathetic activity during inspiration and inhibition with the onset of post-inspiration were even more prominent than in control recordings.   Subsequent recordings, after recovery from all experimental maneuvers, were observed to be no different from control.

Figure 3-4 (Top) illustrates spectral analysis of sympathetic activity obtained from one cat. During the control period and after recovery from hyperventilation, labeled respiratory peaks indicated the presence of regularly occurring sympathetic rhythms with respiratory frequencies. Absence of the respiratory peak in sympathetic activity during hyperventilation indicated that regularly occurring sympathetic rhythms with respiratory frequencies were not present during phrenic nerve quiescence resulting from hyperventilation.   The cardiac peak, which reflected baroreceptor influences on sympathetic activity, was unaffected by hyperventilation.   Spectral analysis of

Figure 3-4

Spectral analysis from a single cat (Top) and mean values for spectral amplitude at the respiratory frequency for 9 cats (Bottom) indicate loss of the respiratory peak during hyperventilation. The asterisk indicates a significant ($P <$ 0.001) decrease in mean spectral amplitude during hyperventilation.
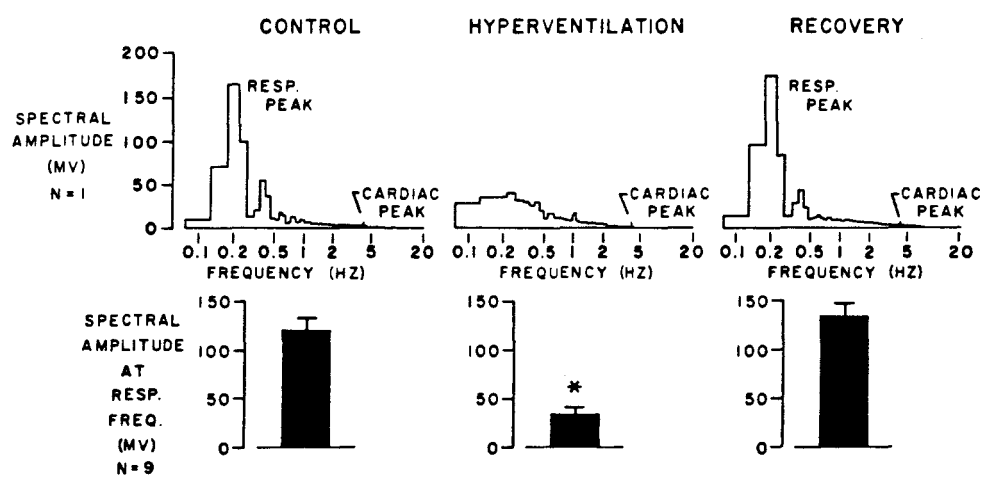
sympathetic activity from all cats was grouped for statistical analysis by comparing spectral amplitude (millivolts) at the respiratory frequency during control, hyperventilation and recovery stages of the procedure. Spectral amplitude at the respiratory frequency during hyperventilation was significantly ($P < 0.001$) decreased from amplitudes measured during control and recovery stages (Fig. 3-4, Bottom). The spectral analysis data substantiated qualitative observations indicating that respiratory rhythms in sympathetic activity were due to central respiratory inputs which were attenuated or absent during hyperventilation.

Figure 3-5 illustrates the effect of hyperventilation on arterial $pO2$, $pCO2$, and pH in a typical cat with sympathetic nerve activity recorded using two different filter methods, A or B. The hyperventilation procedure caused increases in $pO2$ and pH and a decrease in $pCO2$. Two separate oscilloscope pictures illustrated the absence of slow regularly occurring rhythms in sympathetic activity during hyperventilation. Sympathetic bursts occasionally coincided with ventilator activity and were sometimes grouped into irregular bursts of activity such as those illustrated in Fig. 3-5 (Top). Effects of hyperventilation on sympathetic nerve activity were equally represented using either of the signal filter methods, A or

Figure 3-5

Oscilloscope pictures illustrate typical phrenic nerve, sympathetic nerve and intratracheal pressure (ITP) recordings during control, hyperventilation, and recovery stages (Top). In this cat, inferior cardiac sympathetic nerve activity was simultaneously recorded using two signal filtering methods, A and B. Both recording methods provided similar representations of sympathetic nerve activity. The pO2, pCO2 and pH values recorded during control, hyperventilation, and recovery stages are also illustrated for this cat (Bottom).

	CONTROL	HYPERVENTILATION	RECOVERY
pO_2 (mmHG)	109	132	108
pCO_2 (mmHG)	34	20	28
pH	7.35	7.49	7.34
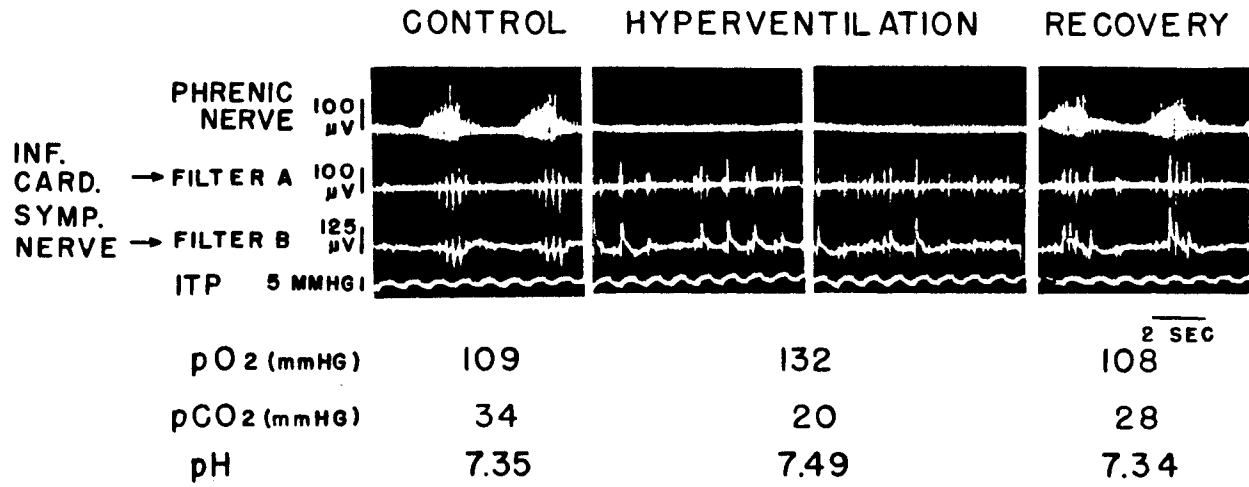
B.

Blood gases, pH and end-expiratory CO2 were within normal ranges during control and recovery stages of the procedure (Fig. 3-6). During hyperventilation and expiratory hold procedures, pO2, pCO2, pH, and end-expiratory CO2 were significantly ($P < 0.05$) different from control and recovery values.

Responses to bilateral carotid occlusion indicated that sympathetic responses to baroreceptor input were not affected by hyperventilation or expiratory hold maneuvers. Figure 3-7 illustrates sympathetic and phrenic nerve responses to bilateral carotid occlusion (indicated by dark horizontal bars) during normoventilation, hyperventilation, recovery and expiratory hold. Irrespective of the ventilatory state, background sympathetic activity was enhanced during bilateral carotid occlusion and markedly inhibited upon release of the occlusion. During normoventilation, recovery, and expiratory hold states, respiratory modulation of sympathetic activity was superimposed on increased background activity during occlusion. Stimulation of carotid sinus baroreceptors (upon release of the occluders) also inhibited phrenic nerve activity and increased the duration of expiration until the next breath. At the point of occluder release, baroreceptor mediated inhibition masked any respiratory influences on

Figure 3-6

End-tidal CO2 and arterial pO2, pCO2, and pH measurements during control (CON), hyperventilation (HPV), recovery (REC) and expiratory hold (EXP HOLD) stages are illustrated. Asterisks indicate significant ($P < 0.05$) differences from control.
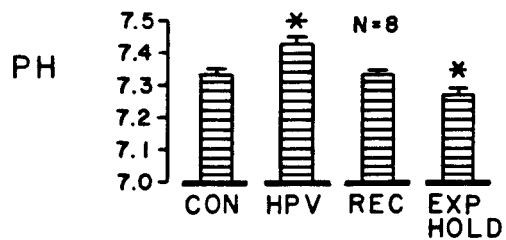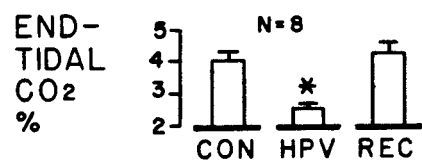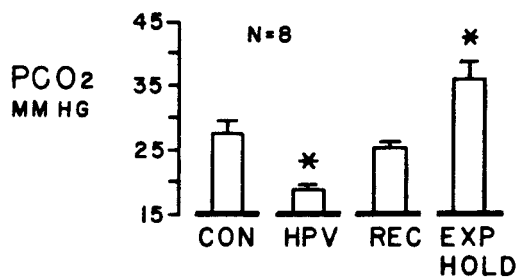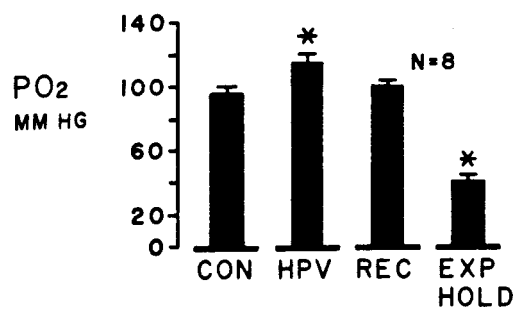
Figure 3-7

Oscillograph recordings illustrate the effect of bilateral carotid occlusion (dark horizontal bars) on integrated (INTEG.) and raw inferior cardiac sympathetic (SYMP.) and phrenic (PHREN.) nerve activities during normoventilation (NORMOVENT.), hyperventilation (HYPERVENT.), recovery, and expiratory hold (EXP. HOLD) stages.

NORMOVENT. HYPERVENT.

INTEG.
INF. C. SYMP.

INTEG.
PHREN.

SYMP. 125
μV

PHREN. 376
μV

RECOVERY EXP. HOLD

10 SEC
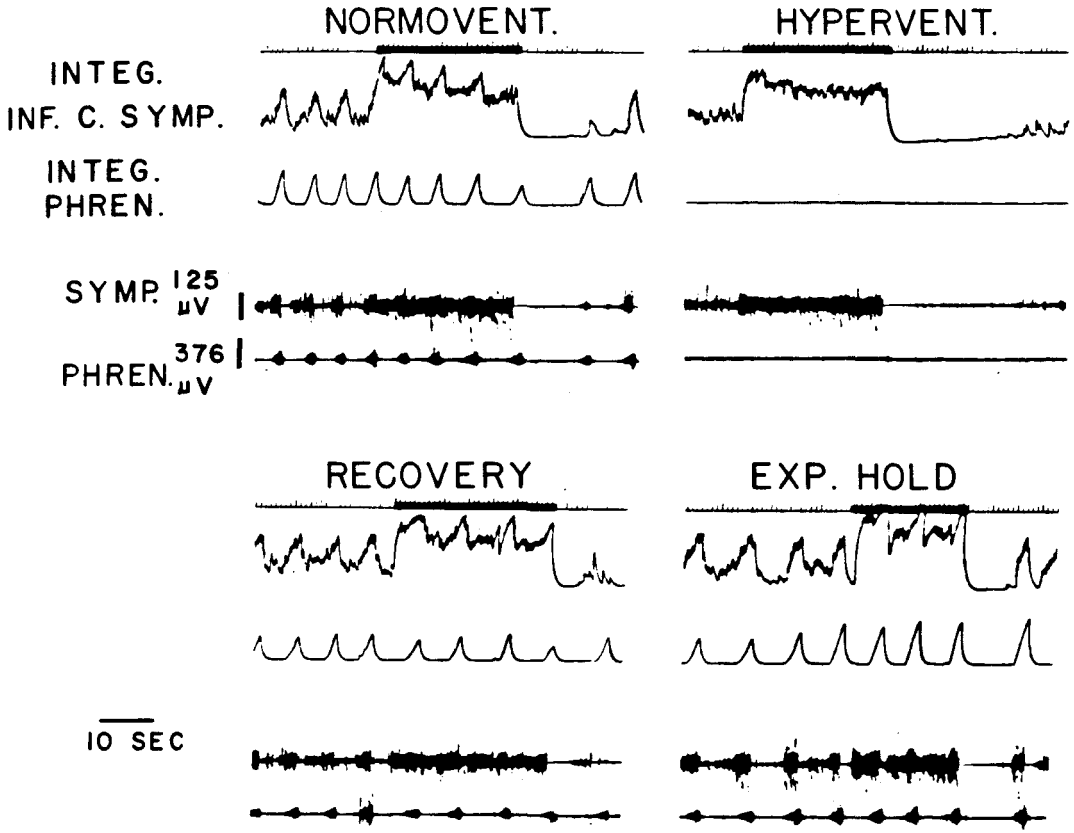
sympathetic activity even though attenuated phrenic nerve activity was still present.

Electrocardiogram triggered computer summation of sympathetic activity allowed more systematic evaluation of baroreceptor entrained cardiac rhythms in sympathetic nerve discharges. ECG triggered computer summated activities from one cat (Fig. 3-8, Top) and mean area/time (mV), calculated from computer summated activites of eight cats (Fig. 3-8, Bottom), indicated that cardiac related sympathetic activity was unaffected by hyperventilation. There were no significant (P > 0.05) differences between mean area/time during control, hyperventilation, or recovery states.

Figure 3-9 illustrates that mean blood pressures and blood pressure increases due to bilateral carotid occlusion were not significantly (P > 0.05) different during control, hyperventilation, recovery and expiratory hold states.

Figure 3-8

Cardiac-related sympathetic activity was assessed using ECG-triggered computer summation of integrated sympathetic activity during control, hyperventilation and recovery stages. A computer summation from one cat is illustrated (Top). Oblique lines under each computer summation indicate typical areas which were measured, divided by cardiac cycle times, and then statisically compared for differences between control, hyperventilation, and recovery stages (Bottom) in eight cats. There were no significant (P < 0.05) differences.
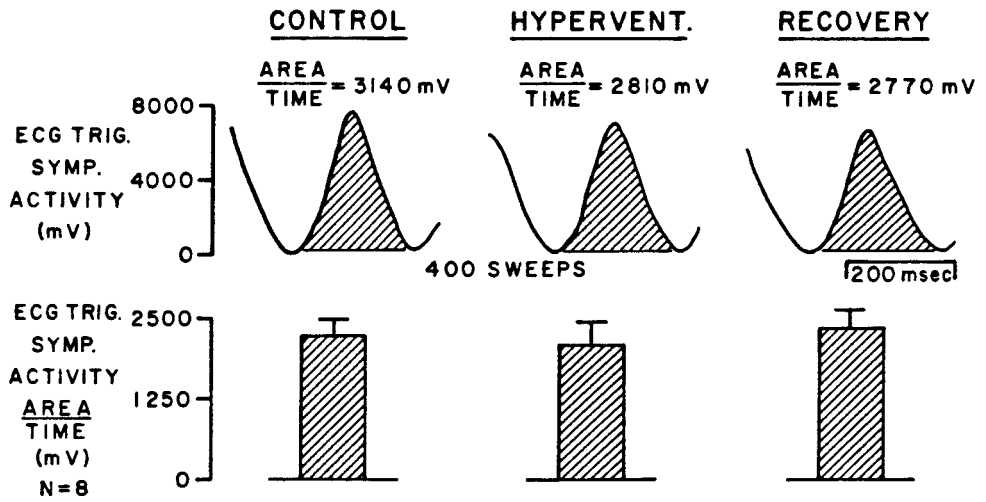
Figure 3-9

Mean blood pressure (Solid Bars, Left Scale) and blood pressure increases during bilateral carotid occlusion (Open Bars, Right Scale) were compared during control (CON), hyperventilation (HPV), recovery (REC), and expiratory hold (EXP HOLD) stages. There were no significant (P < 0.05) differences.
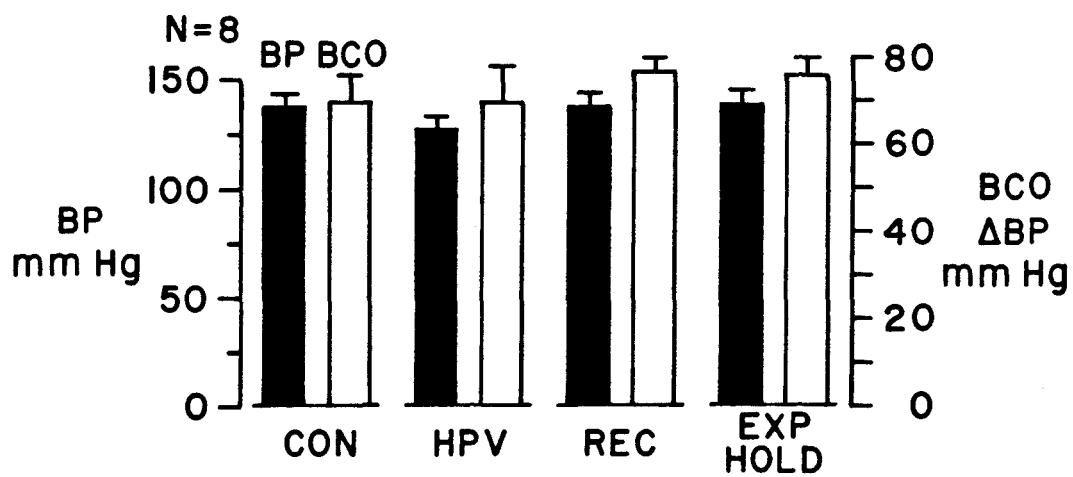
D. DISCUSSION

Respiratory-related rhythms have been observed in sympathetic nerve activity since the first recordings of sympathetic nerves by Adrian in 1932 (3). Subsequent studies by other investigators (41, 72, 154, 155) substantiated that the observed slow sympathetic rhythms were respiratory-related. Respiration (phrenic nerve) triggered computer summation of sympathetic activity indicated that slow sympathetic rhythms were linked with respiration (41, 154). Respiratory-related sympathetic rhythms, synchronous with phrenic nerve activity, were enhanced by increasing arterial pCO_2 to stimulate central inspiratory activity (CIA) and diminished by decreasing arterial pCO_2 to inhibit CIA (41, 155). Of sixty-four spontaneously firing units that Preiss, Kirchner, and Polosa (154) isolated from the sympathetic cervical trunk, forty-one had peak discharge frequencies during inspiration. Twenty of the sympathetic units were not correlated with respiration and three units fired during expiration. The sub-population of sympathetic units which fired during inspiration closely followed the phrenic nerve activity pattern. There were synchronous changes in the activity of sympathetic inspiratory neurons when phrenic nerve frequency was altered by hyperventilation or by electrical stimulation of laryngeal nerve or lung stretch receptor afferents in the

vagus nerve to cause apnea (68, 153). Only sympathetic units with respiratory modulated activities were affected by reflexes altering central respiratory activity, indicating that effects on sympathetic inspiratory units resulted from respiratory center connections.

The concept that CIA affects sympathetic activity to produce respiratory-related sympathetic rhythms was challenged by Barman and Gebber in 1976 (13). They reported that slow rhythms with respiratory frequencies were present in external carotid post-ganglionic sympathetic nerve activities of some cats after hyperventilation-induced apnea. Rhythms were assessed by comparing bursts of sympathetic activity recorded on the oscillograph. In an earlier study, Cohen and Gootman (41) had used respiration triggered computer summation of splanchnic sympathetic activity to illustrate the attenuation of respiratory-related sympathetic rhythms during hyperventilation. Barman and Gebber (13) contended that slow sympathetic rhythms unrelated to respiration would not be indicated by respiration triggered computer summation and that Cohen and Gootman's oscillographic nerve activity recordings during hypocapnia appeared to contain slow sympathetic rhythms similar in form and frequency to those linked with phrenic activity during normocapnia. Barman and Gebber concluded that "slow rhythms within sympathetic and phrenic nerve

discharges arise from independent oscillators."

Results from a 1958 study by Koepchen and Thurau (107) were used to extend the independent oscillator theory. Briefly, Koepchen and Thurau recorded blood pressure and phrenic nerve activity in chloralose-morphine anesthetized dogs with carotid sinus and aortic arch baroreceptors intact. The dogs were artificially ventilated with 100% oxygen so that relationships between blood pressure oscillations and phrenic nerve activity could be assessed with the ventilator off (to eliminate lung stretch receptor effects) for brief periods following neuromuscular blockade with succinyl choline. In two dogs, blood pressure oscillations of 25-50 mmHg with frequencies of approximately eight oscillations/min were desynchronized from phrenic nerve activity which was depressed and irregular following rapid injection of succinyl choline. Koepchen and Thurau's observations have been more recently interpreted to indicate the uncoupling of two independent oscillators affecting sympathetic and phrenic activities (105, 107).

In the present study, no regularly occurring slow sympathetic rhythms with frequencies in the respiratory range were observed during hyperventilation induced apnea, although irregular bursts of sympathetic activity could be distinguished (Fig.3-5). Spectral analysis of sympathetic nerve frequencies confirmed the absence of regularly

occurring slow sympathetic rhythms during hyperventilation in nine cats. In fact, instantaneous spectral analysis recordings observed during data analysis clearly indicated the synchronous disappearance of the respiratory peak in sympathetic activity as phrenic nerve activity was gradually attenuated to quiescence during hyperventilation. The respiratory peak in sympathetic nerve spectral analysis returned with the reappearance of phrenic nerve activity after hyperventilation was discontinued. These results are supportive of numerous previous reports that respiratory related oscillations were eliminated from sympathetic activity by hyperventilation-induced apnea (41, 91, 108, 146, 155, 180). Cardiac vagal neurons which discharge rhythmically during expiration have been similarly reported to lose respiratory-related activity during hyperventilation (174).

Results from the present and previous studies suggest that the independent sympathetic oscillator theory may not provide an appropriate explanation for respiratory-related sympathetic rhythms. Also, Barman and Gebber's results (13) and Koepchen and Thurau's results (107) may be alternatively explained by mechanisms not requiring an independent sympathetic oscillator. Baroreceptor mechanisms, for example, may provide alternative explanations for blood pressure and sympathetic

nerve oscillations with slow frequencies unrelated to respiration since carotid sinus nerves were intact whenever "independent sympathetic oscillators" were demonstrated (13, 107). Prior to Barman and Gebber (13), Okada and Fox (146) demonstrated that, until carotid sinus nerves were sectioned, ventilator-related rhythms with respiratory frequencies were present in splanchnic sympathetic activity of vagotomized dogs during hyperventilation-induced apnea. The carotid sinus nerve mediated ventilator effects on sympathetic activity occurred in the absence of marked ventilator-related oscillations in femoral artery blood pressure recordings. Pneumothoracotomy reduced ventilator-related blood pressure oscillations and sympathetic rhythms. Janig, Kummel, and Wiprich (91) also noted ventilator related sympathetic rhythms, attributing them to phasic unloading of baroreceptors with ventilator-induced blood pressure changes and/or afferent input from pulmonary receptors. Ventilator-related bursts of sympathetic activity during hyperventilation are illustrated in Figure 3-5 from the present study. Although carotid sinus nerves were intact in the present study, higher frequency ventilator-related bursts of sympathetic activity could not be mistaken for lower frequency independent sympathetic rhythms of presumed central oscillatory origin. In addition, baroreceptor responses during hyperventilation were clearly

unaltered from control responses (Figs. 3-7, 3-8, and 3-9). Even after baroreceptor denervation, artificial ventilator influences may be mediated by intercostal afferents. Thus, it is possible that regularly occurring independent slow sympathetic oscillations could be artificial ventilation-induced sympathetic rhythms mediated by carotid sinus nerves or intercostal afferents.

Koepchen and Thurau's observation (107) of blood pressure waves independent from phrenic nerve activity may have also involved baroreceptor feedback rather than an intrinsic sympathetic oscillator dissociated from the respiratory oscillator. The ventilator influence was not a factor in Koepchen and Thurau's preparation since the lungs were not inflated during the particular maneuver used to elicit the "independent sympathetic oscillator." Instead, large amplitude blood pressure fluctuations coupled with baroreceptor negative feedback delay loops created ideal conditions for pressoreceptor-autonomic oscillations as described by Guyton and Harris in 1951 (78). Blood pressure waves (8 cycles/min) with amplitudes of 25 to 50 mmHg were induced by rapid succinyl choline injection causing transient large (50-100 mmHg) increases in blood pressure during the depolarization stage of drug action. Briefly, the pressoreceptor-autonomic oscillation mechanism is as follows: 1) Baroreceptors are stimulated by elevated

arterial pressure. 2) Reflex stimulation of vagal efferent activity and inhibition of sympathetic activity cause heart rate and blood pressure to decrease. 3) Due to delayed response times, the blood pressure decreases to low levels before baroreceptor unloading causes reflex stimulation of sympathetic activity and inhibition of vagal efferent activity. 4) Blood pressure is subsequently elevated to high levels, stimulating baroreceptors and causing the cycle to repeat. Koepchen and Thurau's preparation provided ideal conditions for such baroreceptor-mediated oscillations to occur, particularly since vagus and carotid sinus nerves were intact and the amplitude of blood pressure fluctuation was so large. Results from the current study indicate that strong baroreceptor-mediated influences on sympathetic activity predominated over respiratory influences. Hence, Koepchen and Thurau's early illustration of independent respiratory and sympathetic oscillators of central nervous system origin can be alternatively explained with classic baroreceptor mechanisms.

Mayer's waves and the mechanism underlying their formation have been largely ignored in recent descriptions of slow sympathetic rhythms independent from respiration. Although Mayer's waves are defined as blood pressure waves of a slower frequency (1-5 cycles/min) than respiratory-related (Traube-Hering) blood pressure waves,

the difference has not always been distinguished (107). The following theory involving CNS ischemia has been proposed (79, 98) to explain Mayer's waves: 1) CNS ischemia stimulates sympathetic activity. 2) Blood pressure increases due to increased sympathetic activity and relieves the ischemia. 3) After the ischemic stimulus for sympathetic activity is removed, sympathetic activity and blood pressure decrease. 4) The CNS becomes ischemic again and the cycle repeats. Blood gas and pH measurements in the present study gave no indication of CNS ischemia (Fig. 3-6). However, CNS ischemia may occur but not be indicated when only end-expiratory CO_2 is measured during an experiment. For example, if air passes into the bone sinuses during craniotomy and air emboli form in the lungs, gas exchange may be impaired such that a normal end-expiratory CO_2 is indicated only when the animal is severely hypoventilated. Even with normal blood gases, localized regions of ischemic CNS could account for observations of independent sympathetic rhythms (12).

Changing phase relations between sympathetic and phrenic nerve activities have also been interpreted as evidence for variable entrainment between separate sympathetic and respiratory oscillators (2). However, phase shifts between sympathetic and phrenic nerve activity patterns can be explained by other mechanisms. Specific

populations of respiratory cells may vary their input to the sympathetic nervous system depending on physiological conditions. Subtle variations of respiratory patterns in sympathetic activity may be explained by varying inputs from inspiratory, post-inspiratory, expiratory, and phase-spanning respiratory cells which have been recorded in the medulla and pons (38, 160). Inspiratory cells may enhance sympathetic activity, while post-inspiratory cells inhibit and phase spanning cells further modulate activity. Phase relations between phrenic and sympathetic discharges also appear to shift as a function of respiratory frequency and baroreceptor sensitivity. For example, strong central inspiratory stimulation of sympathetic activity can cause transient blood pressure increases which feedback inhibit sympathetic activity before the termination of inspiration, altering apparent phase relations between phrenic and sympathetic discharges.

In summary, an independent sympathetic oscillator, relatively insensitive to chemoreceptor drive, has been hypothesized by some investigators to explain observations of slow sympathetic rhythms with respiratory frequencies of apparent non-respiratory origin (13). Although alternative mechanisms have been discussed, the existence of separate sympathetic and respiratory oscillators is difficult to prove or disprove if the oscillators are mutually entrained

under most physiologic conditions. Results from the present study and many others (3, 41, 72, 91, 153, 154, 155, 180) are not supportive of the independent slow sympathetic oscillator theory. Instead of generating its own independent slow frequency rhythm, the sympathetic nervous system may process rhythmic and arrhythmic inputs from central and peripheral sources, as diagramatically illustrated in Fig. 3-10. Summation of multiple inputs may result in a net rhythmic or arrythmic output, varying with the state of the organism. Complicated rhythms may result from combined influences of central respiratory input, artificial ventilator input, pressoreceptor-autonomic baroreceptor feedback loops, and, in certain cases, Mayer's waves. However, during enhanced chemoreceptor stimulation of CIA (e.g. expiratory hold maneuvers), central respiratory input would predominate over other influences. In conclusion, influences from the central respiratory cells best explain the respiratory modulation of sympathetic activity.

Figure 3-10

Depending on the physiologic conditions, summation of peripheral (e.g. baroreceptor) and central (e.g. respiratory oscillator) inputs may result in net rhythmic or arrhythmic sympathetic nerve discharge patterns.
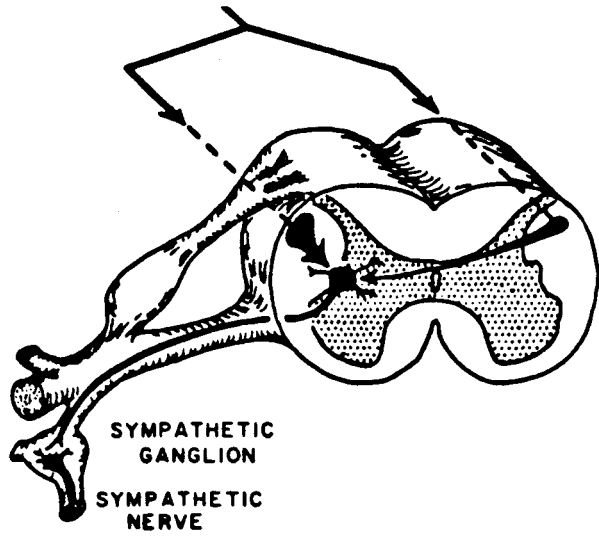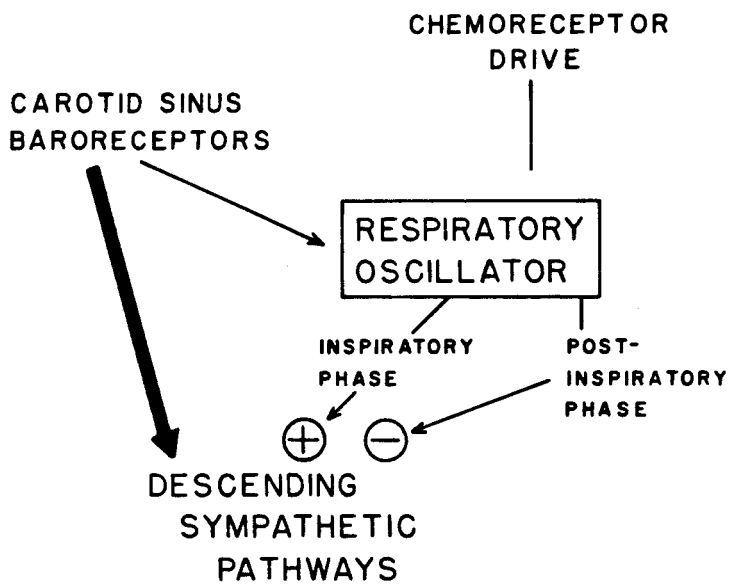
CHAPTER IV

SPINAL PATHWAYS MEDIATING RESPIRATORY INFLUENCES

ON SYMPATHETIC NERVES

A. INTRODUCTION

Brain stem respiratory neurons descend in the ventral half of the spinal cord (7, 21, 36, 57, 151) before terminating on phrenic (C4-C5) and intercostal (T1-T10) nerves innervating the diaphragm and external intercostal muscles, respectively. Descending pathways affecting sympathetic preganglionic activity have been located in both dorsolateral and ventral regions of the spinal cord (62, 88, 89). Previous studies have addressed the issue of spinal cord interactions between phrenic and sympathetic nerves in spinalized animals (74). However, no study has yet examined the spinal organization of descending respiratory influences on sympathetic nerves.

Two purposes of the present study were to determine 1) if ventral spinal cord pathways affecting thoracic respiratory neurons are necessary for the respiratory modulation of sympathetic nerve activity and/or 2) whether

ventral or dorsolateral spinal sympathetic pathways (88, 89) relay respiratory-related activity to preganglionic neurons. In this study, multiple spinal cord lesions were placed at C6-C7 spinal cord levels while recording external intercostal (T1) and phrenic (C4-C5) respiratory nerves and the inferior cardiac sympathetic nerve (T1-T2) in chloralose anesthetized cats. Using computer summation, the respiratory modulation of sympathetic activity was quantitatively assessed before and after each lesion. Bilateral carotid occlusion (BCO) responses were used to test baroreceptor reflex activation of sympathetic nerve activity.

B. METHODS

1. Preparation

Sixteen cats were anesthetized with chloroform followed by intravenous infusion of 40-60 mg/kg alpha-chloralose (12). Femoral artery catheters were inserted for blood pressure (Statham P23Db pressure transducer), and pH, pO2, and pCO2 measurements (Radiometer-Copenhagen BMS3-C Blood Microsystem). After tracheotomy, end-expiratory %CO2 was continuously monitored (Beckman LB1 analyzer). Positive pressure artificial ventilation was begun after neuromuscular blockade with continuous succinyl choline infusion (6 mg/kg/hr). A cannula was inserted into either the intrapleural space or the trachea for measurement of intrapleural or intratracheal pressure (Statham P23Db pressure transducer) as an indicator of ventilator activity. Cervical vagi and aortic depressor nerves were cut to eliminate vagal stretch receptor and aortic baro- and chemoreceptor influences on sympathetic activity. Inflatable occluders (Rhodes Medical Instruments) were placed around the carotid arteries to test bilateral carotid occlusion responses before and after each spinal cord lesion. When indicated, blood pressure, pH and/or blood gases were adjusted to normal ranges with dextran,

8.4% sodium bicarbonate infusions or adjustment of ventilator rate and pressure. Normal blood gas and pH values were defined as $pO_2 \geq 100$ mmHg, $pCO_2 = 20-35$ mmHg, and pH = 7.34. Cat rectal temperature was maintained at 38 $\pm$ 1 C with a servo-regulated heating pad.

Each cat was secured in a stereotaxic head frame (David Kopf). The pelvic iliac crests and a thoracic spine were clamped to a hanging frame to minimize ventilator induced movement artifacts. A dorsal laminectomy exposed the C6-C7 segments of the spinal cord. The dura was left intact until lesions were made.

2. Left Phrenic, Inferior Cardiac Sympathetic and External Intercostal Nerve Recordings

A skin and muscle flap extending from the left ear to the second thoracic spine was pulled laterally and attached to a curved horizontal rod to create two oil pools; a rostral one for the phrenic and a caudal one for the inferior cardiac sympathetic and T1 external intercostal nerves. To isolate the left inferior cardiac sympathetic and external intercostal nerves, the scapula was retracted exposing the ribs. Dorsal muscle layers were then carefully scraped away from the first and second ribs. The heads of the two ribs were removed before laterally retracting the

bodies of the ribs to expose the T1 spinal nerve rostrally and the stellate ganglion ventrocaudally. The T1 intercostal nerve was cut distally and the epineural sheath routinely removed. The caudally coursing inferior cardiac sympathetic nerve was cut distally and desheathed in some preparations. Rostrally, the phrenic nerve was isolated as it exited from the fourth cervical nerve root, cut distally and desheathed.

Left phrenic, inferior cardiac sympathetic, and external intercostal nerves were placed on bipolar platinum electrodes for differential recording (Grass P9 amplifiers). Nerve signals were monitored on a storage oscilloscope and photographed at various stages in each experiment. After rectification and leaky integration, (Grass Model 7P3 A Integrator, low pass filter time constant = 0.5 sec.) the signals were displayed on the oscillograph and stored on magnetic tape (Precision Instruments model 6200 tape recorder) for later analysis.

3. Lesions

C6-C7 spinal cord lesions were made with fine dissecting scissors, a sharp dissecting knife and a blunt spatula to interrupt descending pathways to sympathetic and intercostal nerves (T1-T2 level). Since all of the lesions were caudal to the C5 spinal level, phrenic nerve activity

was maintained as a continuous monitor of central respiratory drive. Intercostal nerve activity was recorded to monitor central respiratory input to thoracic spinal levels. Following each lesion, respiratory rhythmicity of intercostal and sympathetic nerve activity was analyzed (computer summation method described below) and compared to control activity.

The sixteen cats were divided into two groups based on the lesion sequence they received. The cumulative lesions were displaced from each other by several millimeters to allow histological verification of each lesion following the experiment. Group I (eight cats) received ventral cord lesions first, followed by sequential lesions leading to total spinal cord transection. Figure 4-1 illustrates the lesion sequence for Group I: A) ventral hemisection, B) left hemisection, C) right dorsolateral funiculus (DLF) region and/or D) right hemisection and E) midline lesion between right and left hemisection. Group II (eight cats) initially received dorsal lesions. Figure 4-2 illustrates the lesion sequence for Group II: F) unilateral right (four cats) or left (four cats) dorsolateral funiculus (DLF) G) the contralateral dorsolateral funiculus, H) dorsal hemisection, and I) total spinal cord transection.

Figure 4-1

C6-C7 spinal cord lesion sequence for Group I cats.

<u>A</u>, ventral hemisection; <u>B</u>, left hemisection; <u>C</u>, right DLF lesion; <u>D</u>, right hemisection; <u>E</u>, midline lesion between right and left hemisections.

C4-C5

LESION **A**

PHRENIC
NEUROGRAM

LESION B

LESION D
C6-C7

LESION C

INTERCOSTAL
NEUROGRAM

INF. CARD. SYMP.
NEUROGRAM

LESION
E

T1-T2
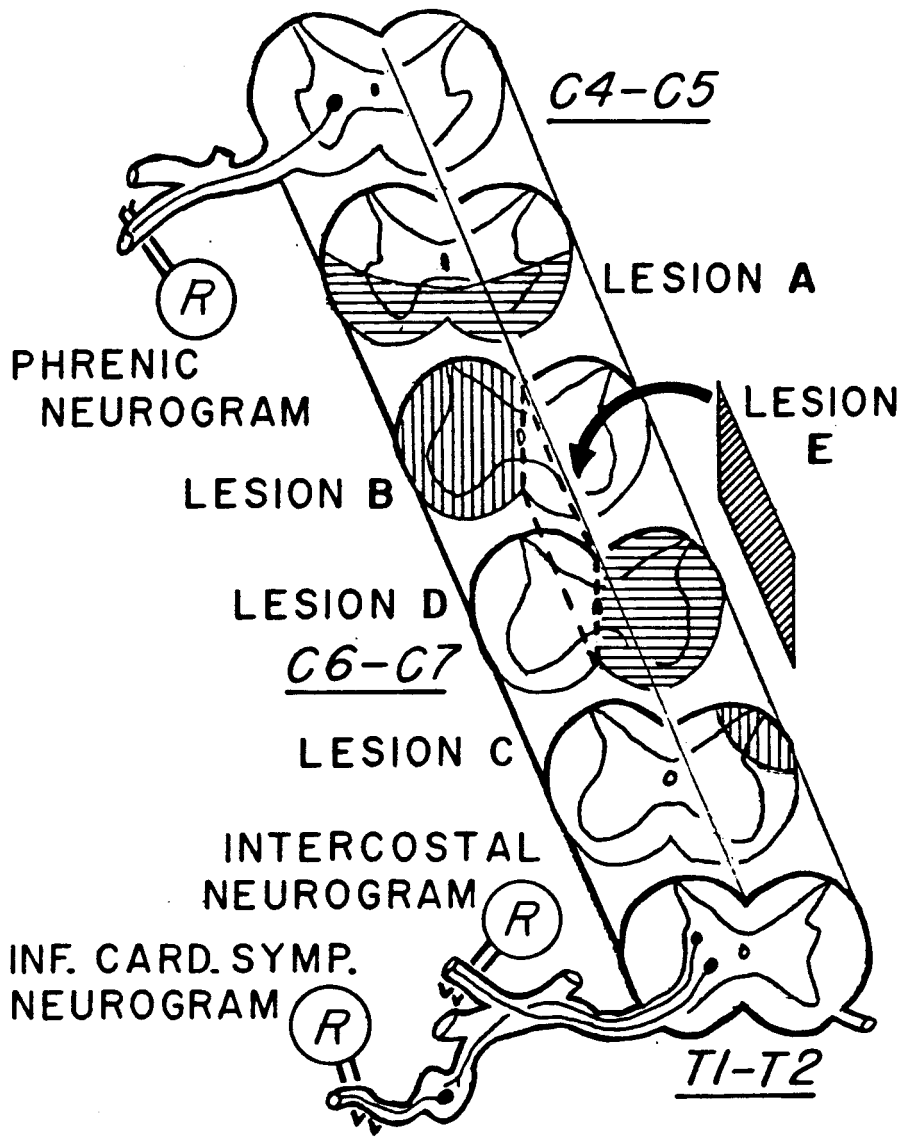
Figure 4-2

C6-C7 spinal cord lesion sequence for Group II cats.
F, unilateral DLF lesion; G, contralateral DLF lesion; H,
dorsal hemisection; I, total transection.

C4–C5

LESION F

PHRENIC
NEUROGRAM

LESION G

LESION H

C6–C7

LESION I

INTERCOSTAL
NEUROGRAM

INF. CARD. SYMP.
NEUROGRAM

T1–T2
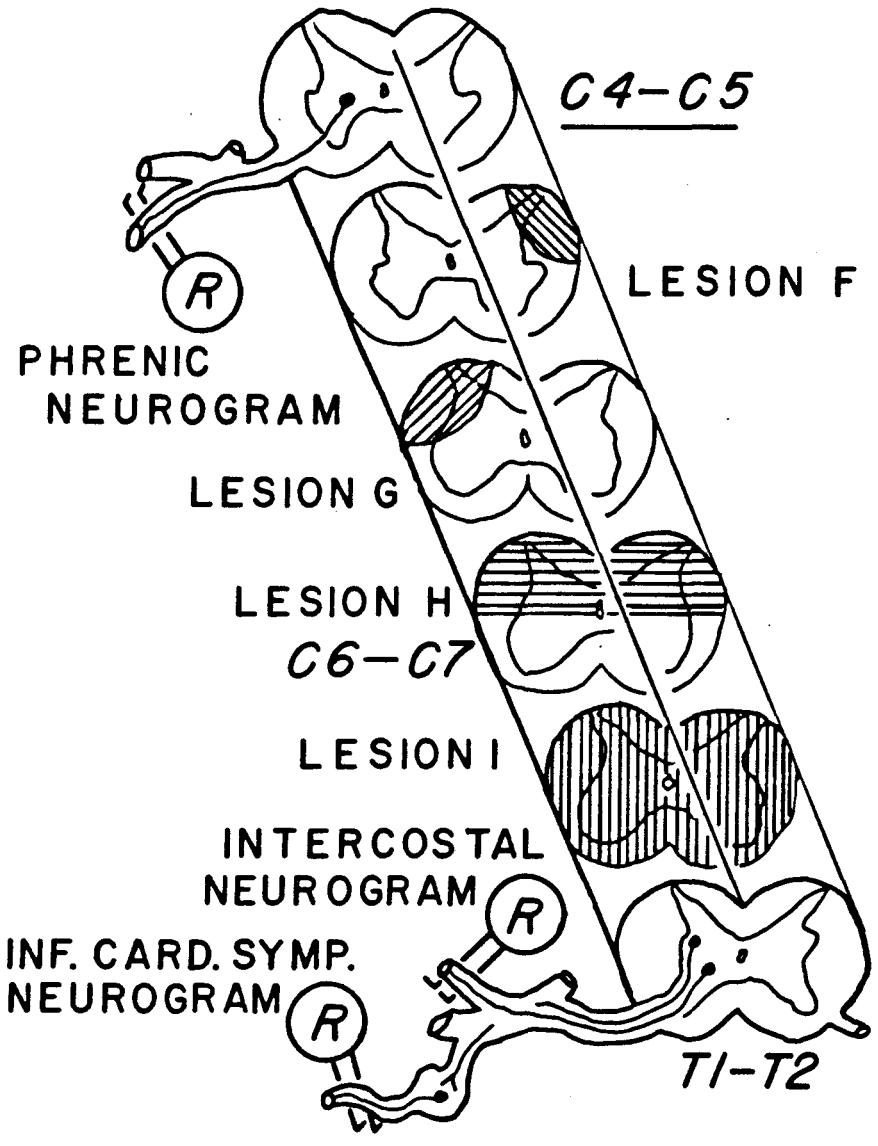
4. Computer Summation

Computer summation techniques were used to analyze effects of spinal cord lesions on the respiratory modulation of sympathetic nerve activity. Amplified integrated sympathetic activity (millivolts) was processed using respiration (ie. phrenic nerve signal) triggered computer summation (Nuclear Chicago Data Retrieval Computer). Computer summated (twenty sweeps) phrenic and sympathetic nerve activities were analyzed before and after lesions. Areas of computer summated sympathetic activity were measured using a graphics tablet (Bausch and Lomb) connected to a digital computer (Apple II plus). Net sympathetic inspiratory amplitude (NSIA) was then calculated to quantitate the respiratory modulation of sympathetic nerve activity (Fig. 4-3):

NSIA= (Area Insp/ TI) - (Area Exp/ TE)

Area Insp= computer-summed area (twenty sweeps) of amplified integrated sympathetic activity during inspiration (millivolt-seconds)
Area Exp= computer-summed area (twenty sweeps) of amplified integrated sympathetic activity during expiration (millivolt-seconds)

Figure 4-3

Diagrammatic illustration of data analysis method used to determine NSIA (net sympathetic inspiratory amplitude) as described in the text.

COMPUTER SUMMATED INTEGRATED PHRENIC N. ACTIVITY

INSP.
EXP.
TIME →

T_{exp} | T_{insp}

COMPUTER SUMMATED INTEGRATED SYMP. N. ACTIVITY

MEAN INSP. AMPLITUDE

NET SYMPATHETIC INSP. AMPLITUDE

MEAN EXP. AMPLITUDE $AREA_{exp.}$ $AREA_{insp.}$
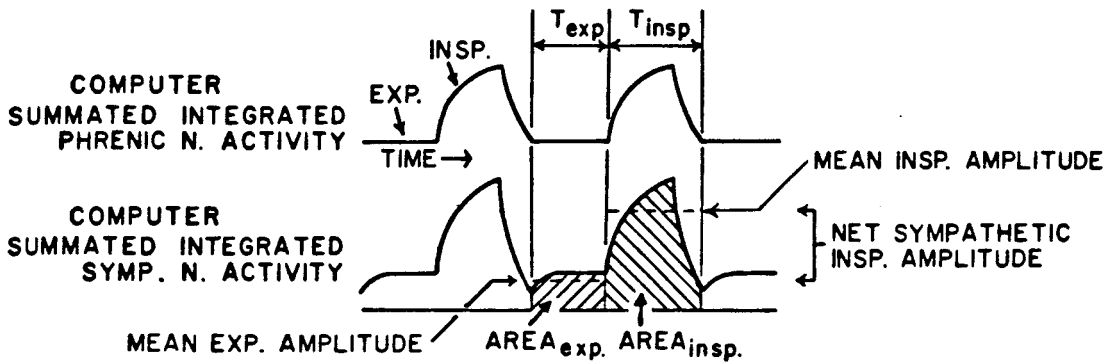
$$\text{MEAN EXP. AMPLITUDE} = \frac{AREA_{exp.}}{T_{exp.}}$$

$$\text{MEAN INSP. AMPLITUDE} = \frac{AREA_{insp.}}{T_{insp.}}$$

$$\text{NET SYMPATHETIC INSP. AMPLITUDE} = \text{MEAN INSP. AMPLITUDE} - \text{MEAN EXP. AMPLITUDE}$$

$TI=$ duration of inspiration (seconds)

$TE=$ duration of expiration (seconds)

When sympathetic activity has a respiratory related discharge, the derived net sympathetic inspiratory amplitude is a positive value. Net sympathetic inspiratory amplitude approaches zero when no respiratory modulation is present and phrenic nerve triggered sympathetic activity summates into a relatively straight horizontal line. As an alternative to only presenting single cat data, the NSIA analysis procedure was devised as a quantitative means to assess the respiratory modulation of sympathetic activity after specific lesions in all of the cats.

5. Histology

The spinal cords were placed in 10% buffered formalin for at least 3 days and then embedded in paraffin. Every fifth ten micron thin serial section was stained for fibers and cell bodies by the Kluver-Barrera method (103). The slides were projected onto paper to trace the locations of spinal cord lesions.

6. Statistics

Control values for net sympathetic inspiratory amplitude (NSIA), blood pressure and blood pressure responses to bilateral carotid occlusion tests were statistically compared with values obtained after each spinal cord lesion. Data were analyzed using analysis of variance followed by tests for least significant differences (69, 163). $P < 0.05$ indicated statistical significance. Values are expressed as means $\pm$ standard error (SE) of the mean.

C. RESULTS GROUP I

1. Control Activity

Sympathetic activity was linked to phrenic and external intercostal nerve activities prior to the spinal lesions (Fig. 4-4, RAW DATA, CONTROL). Sympathetic activity was increased during inspiration and diminished or quiescent during post inspiratory and expiratory phases of the respiratory cycle. Respiration triggered computer summation confirmed that such slow oscillations in sympathetic activity were respiratory-related (Fig. 4-4, COMP. DATA, CONTROL). Respiratory modulation of sympathetic activity was quantitated by determining net sympathetic inspiratory amplitude (NSIA). Mean NSIA for eight cats was 146 ± 39 millivolts prior to any spinal cord lesions (Fig. 4-5, CONTROL).

Blood pressure and bilateral carotid occlusion responses of a Group I cat are presented in Figure 4-4. Mean blood pressure and bilateral carotid occlusion responses for the eight Group I cats were 124 ± 6 mm Hg and 68 ± 5 mm Hg, respectively (Fig. 4-5, CONTROL).

Figure 4-4

Data from Cat #6 illustrates effects of Group I lesions A,B,C,D, and E. (Top to Bottom) RAW DATA: left phrenic, external intercostal (T2) and inferior cardiac sympathetic nerve activities, COMP. DATA: respiration triggered computer summation (20 sweeps) of phrenic and sympathetic nerve activites, BP/MEAN: pulsatile/and mean blood pressures, BCO BP/MEAN: pulsatile/and mean blood pressures during bilateral carotid occlusion, SYMP. BCO RESPONSE: reflex response of inferior cardiac sympathetic nerve to bilateral carotid occlusion. Time scales are depicted by arrows to the lower right of the RAW DATA and COMP. DATA photographs.

CAT #6

RAW DATA	CONTROL	**A** VENTRAL HEMI.	**B** LEFT HEMI.	**C** RIGHT DLF	**D & E** RIGHT HEMI. & MIDLINE
PHRENIC N. 200 µV]					
INTERCOS. N. 200 µV]					
SYMP. N. 50 µV]					→4S←
COMP. DATA PHRENIC N. SYMP. N.					←6S→
BP MEAN (MM HG)	170/140 155	160/130 145	140/105 125	130/100 120	125/95 115
BCO BP MEAN (MM HG)	270/190 230	265/185 205	220/175 192	165/125 140	135/105 120
SYMP. BCO RESPONSE	PRESENT	PRESENT	PRESENT	ABSENT	ABSENT
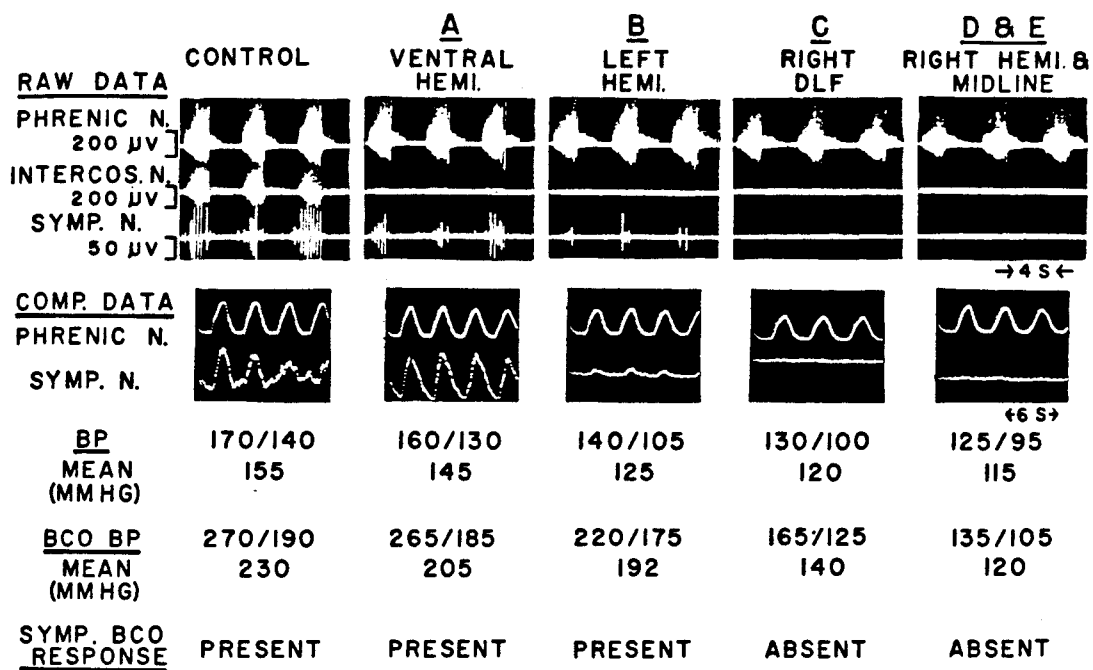
Figure 4-5

Effects of Group I lesions on net sympathetic inspiratory
amplitude (Top), mean blood pressure (Bottom, solid bar,
left ordinate scale), and blood pressure increases during
bilateral carotid occlusions (Bottom, open bar, right
ordinate scale). Bars depict mean $\pm$ SE for the number of
cats indicated in parentheses. The symbols *,0, and +
indicate significant differences of $P < 0.05$ when the group
indicated was compared to control, A, and B, respectively.
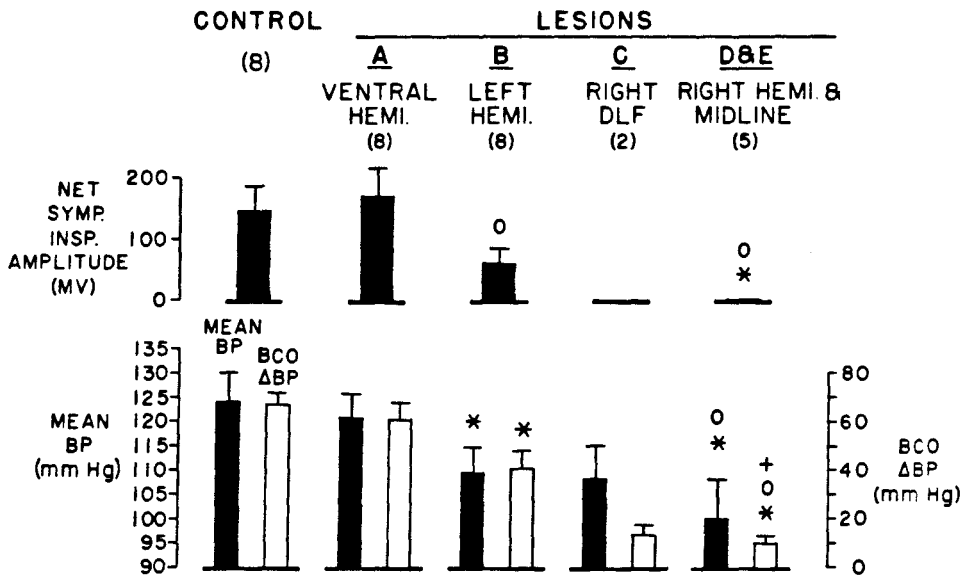
2. Ventral Hemisection (Lesion A)

Ventral hemisections at the C6 level of the spinal cord were extended until intercostal nerve activity ceased (Fig. 4-4A). Ventral hemisections were considered complete when intercostal nerve activity did not return during chemoreceptor stimulation induced by transient cessation of artificial ventilation (15 to 20 seconds). Phrenic nerve activity remained intact since the ventral lesions were caudal to the C4-C5 spinal levels of phrenic motor neurons. The ventral hemisections were histologically verified (Fig. 4-6A). In all cases dorsolateral funiculus regions of the spinal cord were intact following ventral hemisections. Raw and computer summation data indicated that the respiratory modulation of sympathetic activity was retained after ventral hemisections interrupted descending respiratory pathways to external intercostal nerves (Fig. 4-4A). Mean NSIA was not significantly different from control, indicating that the respiratory modulation was intact after ventral hemisection (Fig. 4-5A). The slight increase of mean NSIA reflects a more predominant respiratory-related rhythm in sympathetic nerve activity (Fig. 4-4A, COMP. DATA) after ventral hemisections in 50% of the cats.

Blood pressure and blood pressure responses to bilateral carotid occlusion were not significantly altered

Figure 4-6

Group I C6-C7 spinal cord lesions A,B,C,D, and E are depicted by the stippled areas. The triangles indicate two cats with blood pressures at or below 50 mm Hg following right hemisection.

LESIONS

A VENTRAL HEMI.	B LEFT HEMI.	C RIGHT DLF	D RIGHT HEMI.	E MID-LINE

CAT #

CAL └────┘5 mm
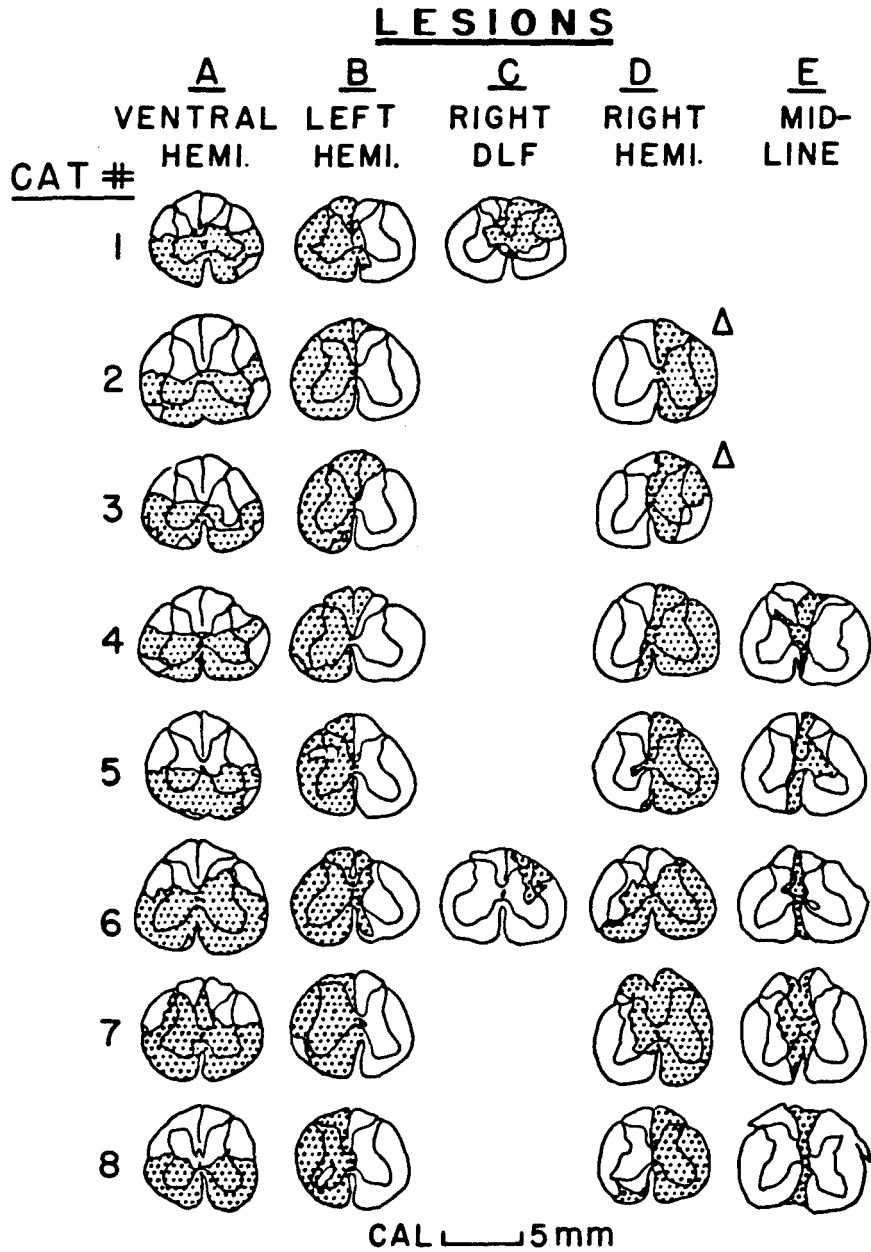
from control (Figs. 4-4A, 4-5A).

3. Left Hemisection (Lesion B)

Combined ventral and left hemisections (lesions A and B) decreased overall sympathetic activity. However, attenuated sympathetic activity retained the respiratory modulation (Figs. 4-4B, 4-5B). Phrenic nerve activity remained intact since lesions were caudal to C4-C5 spinal levels. Histological analysis indicated that only pathways descending contralaterally in the dorsal quadrant of the C6-C7 spinal cord level were intact following combined left and ventral hemisections (Figs. 4-6A, 4-6B). Mean NSIA (60.9 $\pm$ 25 millivolts) indicated a significant reduction of the respiratory modulation after left spinal cord hemisection (Fig. 4-5B). Since overall sympathetic activity was attenuated, the decreased NSIA was attributed to overall loss of descending inputs to sympathetic nerves and not exclusive loss of respiratory projections. Loss of some descending inputs also resulted in significantly (P < 0.05) lower mean blood pressures and blood pressure responses to bilateral carotid occlusions (Figs. 4-4B, 4-5B).

4. Right DLF (Lesion C)

Results from two cats were obtained after right dorsolateral funiculus lesions were added to preceding lesions A and B (Fig. 4-6A, 4-6B, 4-6C). After additive lesions A, B, and C, the spinal cord was nearly transected. Typical responses, as shown in Fig. 4-4C, indicated that the effective transection at C6-C7 spinal levels caused acute cessation of sympathetic activity, lowered mean blood pressure to 120 mm Hg and decreased the bilateral carotid occlusion response to 20 mm Hg. Phrenic nerve function remained intact. Mean NSIA (zero millivolts) reflected an absence of sympathetic respiratory modulation coinciding with loss of supraspinal influences on sympathetic nerve activity (Fig. 4-5C). NSIA and blood pressure responses after right DLF lesions were not included in the statistical analysis since this specific data was obtained for only two cats.

5. Right Hemisection and Midline Lesion (Lesions D and E)

When additively combined with the previous lesions, lesions D and E resulted in effective spinal cord transection (Fig. 4-6). Data was not used when overly traumatic lesions caused blood pressure to fall to 50 mm Hg

in two cats, indicated by the triangle superscript in figure 4-6D. Results were obtained from the other five cats which received right hemisections followed by midline spinal lesions (Figs. 4-4D and E, 4-5D and E). NSIA (2.19 $\pm$ 1.14 millivolts) was significantly reduced (P < 0.05) from control and post left hemisection values, reflecting the absence of sympathetic activity and its respiratory modulation after additive lesions A,B,C,D, and E. Significantly decreased mean blood pressure and bilateral carotid occlusion responses of 10 $\pm$ 3 mm Hg indicated that supraspinal inputs to sympathetic nerves were essentially interrupted by the series of cumulative lesions (Figs. 4-5D, 4-5E).

D. RESULTS GROUP II:

1. Control Activity

Data from a Group II cat is presented in Figure 4-7. Prior to Group II lesions in eight cats, the marked respiratory modulation of sympathetic nerve activity was quantitatively indicated by an NSIA of 272 ± 39 millivolts (Fig. 4-8, CONTROL). Mean blood pressure was 141 ± 5 mm Hg and bilateral carotid occlusion responses were 69 ± 4 mm Hg.

2. Unilateral DLF (Lesion F)

Cats 9 through 12 initially received right DLF lesions and cats 13 through 16 initially received left DLF lesions (Fig. 4-9F). NSIA after unilateral DLF lesions (223 ± 45 millivolts) was not significantly different from control. Intercostal and phrenic nerve activities remained intact, indicating that the unilateral dorsal lesions did not adversely affect ventral spinal cord pathways caudal or rostral to the C6-C7 spinal lesion. However, blood pressure and bilateral carotid occlusion responses were significantly decreased (P < 0.05). The slight attenuation of blood pressure (123 ± 5 mm Hg) and carotid occlusion responses (55 ± 5 mm Hg) indicated that some pathways to sympathetic

Figure 4-7

Data from Cat #16 indicates responses to Group II lesions
F,G,H, and I. (Top to Bottom) RAW DATA: left external
intercostal (T2), inferior cardiac sympathetic, and phrenic
nerve activities, intratracheal pressure, COMP. DATA:
respiration triggered computer summation (20 sweeps) of
phrenic and sympathetic nerve activities, BP/MEAN:
pulsatile/ and mean blood pressures, BCO BP/MEAN: pulsatile/
and mean blood pressures during bilateral carotid occlusion,
SYMP. BCO RESPONSE: reflex response of left inferior cardiac
sympathetic nerve to bilateral carotid occlusion. Time
scales are depicted by arrows to the lower right of the RAW
DATA and COMP. DATA photographs.

CAT # 16

RAW DATA	CONTROL	F. UNILAT. DLF	G. BILAT. DLF	H. DORSAL HEMI.	I. TRANSECT.

INTERCOS. N. 200 µV]
SYMP. N. 100 µV]
PHRENIC N. 400 µV]
ITP, 4 mm Hg]

→ 4 S ←

COMP. DATA
PHRENIC N.

SYMP. N.

→ 6 S ←

	CONTROL	UNILAT. DLF	BILAT. DLF	DORSAL HEMI.	TRANSECT.
BP MEAN (MM HG)	170/135 145	170/120 140	155/100 125	150/100 120	135/80 100
BCO BP MEAN (MM HG)	265/200 225	250/185 205	170/120 140	160/115 135	150/105 120
SYMP. BCO RESPONSE	PRESENT	PRESENT	ABSENT	ABSENT	ABSENT

Figure 4-8

Effects of Group II lesions on net sympathetic inspiratory amplitude (Top), mean blood pressure (Bottom, solid bar, left ordinate scale), and blood pressure increases during bilateral carotid occlusion (Bottom, open bar, right ordinate scale). Bars depict mean $\pm$ SE for the number of cats indicated in parentheses. The symbols *, 0, and + indicate significant differences of $P < 0.05$ when the group indicated was compared to control, F, and G, respectively.
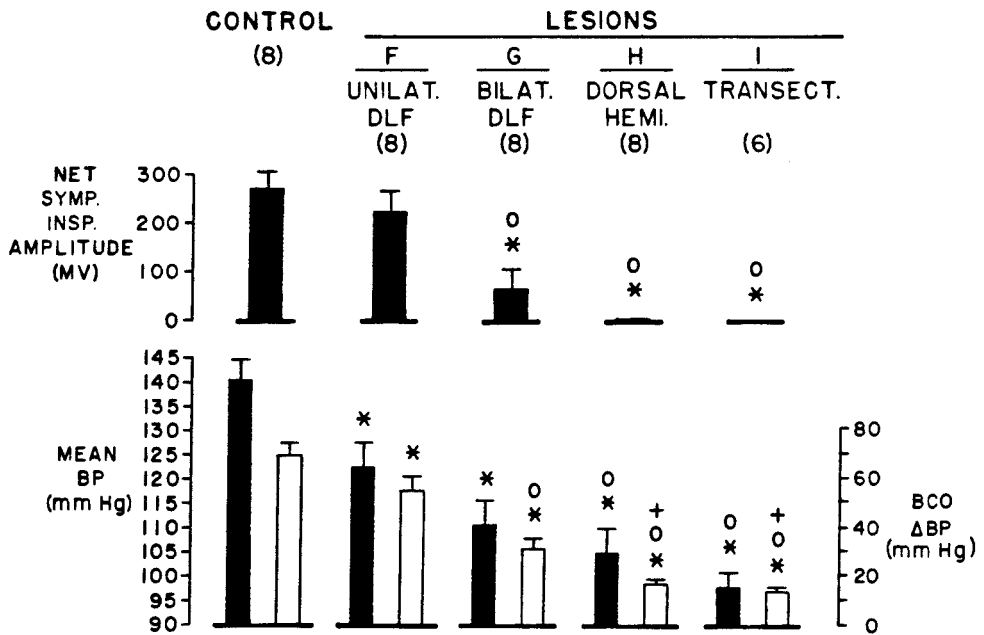
Figure 4-9

Group II C6-C7 spinal cord lesions are depicted by the stippled areas. An asterisk to the upper right of a section indicates the specific lesion in the sequence causing loss of respiratory-modulated sympathetic activity and BCO responses.

LESIONS

| | F
UNILAT.
DLF | G
CONTRA.
DLF | H
DORSAL
HEMI. | I
TRAN-
SECT. |

CAT #

9, 10, 11, 12, 13, 14, 15, 16

CAL |——| 5 mm
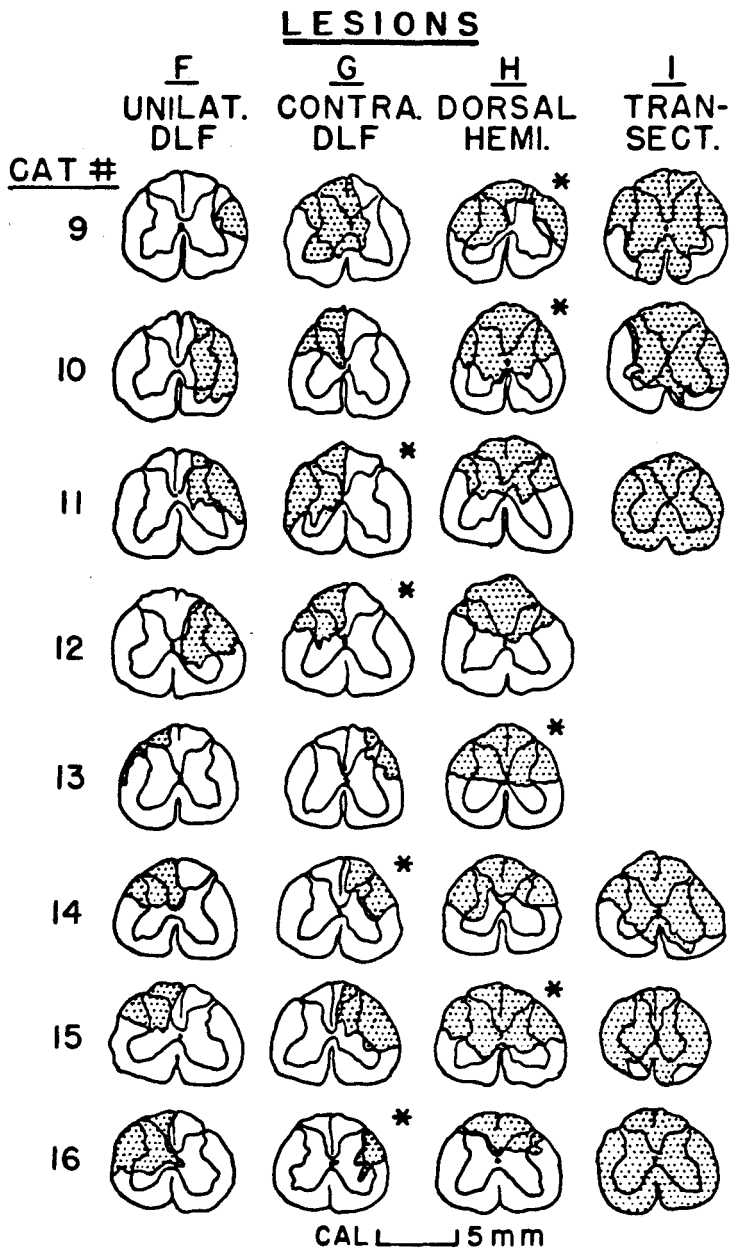
nerves were affected by the lesions, although the respiratory modulation was unaffected.

3. Bilateral DLF (Lesion G)

Following bilateral dorsolateral funiculus lesions (lesions F and G), the respiratory modulation of sympathetic nerve activity and responses to bilateral carotid occlusions were eliminated in four of the eight cats. As indicated by histological analysis (Figs. 4-9F and 4-9G, asterisks), DLF pathways were completely interrupted in those four cats (cats 11,12,14,and 16). In Figure 4-9, an asterisk to the upper right of a spinal cord section indicates the lesion stage where respiratory modulation of sympathetic activity and bilateral carotid occlusion responses were eliminated. Portions of the DLF pathways remained intact in the other four cats which retained the respiratory modulation of sympathetic activity after attempted bilateral DLF lesions (Fig. 4-9F and G, no asterisks). Phrenic and intercostal nerve activities were intact after bilateral DLF lesions eliminated the respiratory modulation of sympathetic nerve activity (Fig. 4-7G). Ventral respiratory pathways were, therefore, not affected by interruption of dorsal spinal cord pathways to sympathetic nerves. Mean NSIA was significantly ($P < 0.05$) decreased, reflecting that the

respiratory modulation of sympathetic nerve activity was reduced after bilateral DLF lesions eliminated descending pressor pathways to sympathetic nerves (Fig. 4-8G). Although mean blood pressure was significantly reduced from control, adequate levels were maintained (110 ± 5 mm Hg). Bilateral carotid occlusion responses were significantly attenuated after elimination of major descending pathways to sympathetic nerves located in the DLF.

4. Dorsal Hemisection (Lesion H)

Respiratory modulation of sympathetic activity was eliminated only after dorsal hemisection in cats 9,10,13, and 15. The dorsolateral funiculus pathways were not completely interrupted in these four cats until after this lesion stage (Fig. 4-9H, asterisks). Minimal bilateral carotid occlusion responses after dorsal hemisection (17 ± 2 mm Hg) further indicated the interruption of descending DLF pathways to sympathetic nerves. Since bilateral DLF lesions were previously complete in cats 11,12,14, and 16 (Figs. 4-9F, 4-9G), dorsal hemisections had no further effect on respiratory modulation of sympathetic activity or carotid occlusion responses in those cats (Fig. 4-7H). There were no differences in mean blood pressure or NSIA between bilateral DLF and dorsal hemisection lesion stages (Figs. 4-8G, 4-8H).

Bilateral carotid occlusion responses after dorsal hemisection were significantly lower than those after bilateral DLF lesions. Differences in bilateral carotid occlusion responses were attributed to some intact DLF pathways in cats 9,10,13, and 15 prior to dorsal hemisection.

4. Transection (Lesion I)

Spinal cord transections were extended ventrolaterally until intercostal nerve activity ceased due to interruption of descending respiratory pathways located in the ventrolateral spinal cord (Fig. 4-7I and Fig. 4-9I). Results were obtained in six of the eight Group II cats. Phrenic nerve activity remained intact, since the effective C6-C7 transection was caudal to the C4-C5 spinal level of phrenic motoneurons. Sympathetic nerves were either quiescent or exhibited low levels of non-rhythmic activity after the lesions (Fig. 4-7I). NSIA indicated no sympathetic respiratory modulation and was not significantly different after transection, bilateral DLF lesions or dorsal hemisections (Fig. 4-8I). Blood pressure and bilateral carotid occlusion responses were also not different from those after bilateral disruption of descending DLF pathways (Fig. 4-8I).

E. DISCUSSION

The main issue addressed by this study was the location of descending spinal pathways responsible for the respiratory rhythmicity of sympathetic nerve activity described by previous investigators (3, 41, 154). Descending pathways affecting sympathetic nerve activity have been described in dorsolateral (1, 62, 88, 99, 100) and ventral (50, 88, 89) regions of the spinal cord. When Kerr and Alexander (100) made ventral hemisections of the spinal cord, blood pressure was either unaffected or slightly increased.   Illert and Seller (89) determined that stimulation of ventral pathways depressed blood pressure and inhibited sympathetic nerve activity. In addition, they determined that those inhibitory pathways were not necessary for baroreceptor inhibition.

In the present study, ventral hemisections interrupted those descending pathways to sympathetic nerves just described (50, 89) and also motor pathways to external intercostal nerves (7). As in previous investigations (89, 100), blood pressure and bilateral carotid occlusion responses in the present study were not adversely affected by ventral spinal cord hemisections.   The respiratory modulation of sympathetic activity was unaffected or slightly enhanced after ventral hemisections. These results

indicate that 1) the inhibitory ventral spinal pathways described by Illert and Seller (89) are not necessary for respiratory modulation of sympathetic activity and 2) the respiratory modulation of sympathetic nerve activity is not mediated by the same ventral spinal cord pathways conveying central respiratory information to external intercostal nerves.

Slight enhancement of respiratory influences on sympathetic activity may have occurred after ventral hemisections eliminated other non-respiratory ascending or descending influences mediated by ventral spinal cord pathways. For example, ventilator-related influences on sympathetic activity in vagotomized cats are possibly mediated by intercostal afferent information which ascends in the ventrolateral spinal cord to the brain stem (158). A more predominant influence by central respiratory drive may have resulted after ventral hemisection reduced ventilator-related influences on sympathetic activity.

Consistent with the results of others (62, 88, 100), bilateral lesions of dorsal descending DLF pathways to sympathetic nerves resulted in significantly reduced spontaneous sympathetic activity (RAW DATA, Fig. 4-4C,D & E, and Fig. 4-7G, H, & I) and absence of inferior cardiac sympathetic nerve response to bilateral carotid occlusion (SYMP. BCO RESPONSE, Fig. 4-4C and Fig. 4-7G). The

respiratory modulation of sympathetic activity was also eliminated when the bilaterally descending DLF pathways were completely interrupted. The results clearly indicated that, although spontaneous sympathetic activity gradually decreased as dorsal pathways were progressively interrupted, the respiratory modulation persisted until bilateral DLF pathways were completely eliminated. Intact intercostal nerve activity after the specific Group II dorsal lesions indicated that ventral respiratory pathways were relatively unaffected by contiguous dorsal lesions. Significantly reduced $(P < 0.05)$ mean blood pressures and blood pressure responses to bilateral carotid occlusion also indicated the absence of descending pressor pathways after bilateral DLF lesions.

The present study also investigated spinal decussation of descending pathways affecting sympathetic activity and its respiratory modulation. Most earlier studies indicated that descending pathways affecting sympathetic nerve activity are bilateral with an ipsilateral predominance (1, 71, 81, 82, 94, 99, 126). The evidence indicated that pathway decussations to the contralateral side occurred at brain stem and spinal levels. Histochemical evidence in support of spinal decussation also exists (33, 46, 131) but cannot confirm that the crossed monoamine pathways to the intermediolateral cell column

actually affect sympathetic nerve activity. Results from the present study provide direct functional evidence in support of spinal decussations of supraspinal pathways to sympathetic nerves. After ipsilateral DLF projections were eliminated, the maintained respiratory modulation of sympathetic activity and inferior cardiac sympathetic nerve response to bilateral carotid occlusion indicated spinal level decussations (Fig. 4-4B and Fig. 4-7F).

Results from earlier investigations and our present findings in support of spinal decussations may at first appear to conflict with previous results published by Foreman and Wurster (62). Foreman and Wurster concluded that no spinal decussation of descending DLF pathways occurred between second cervical and second thoracic segments of the spinal cord. However, the discrepancy between results may be due to differences between the inferior cardiac nerve and the T2 white ramus. Foreman and Wurster recorded sympathetic activity from the T2 white ramus which contains segmentally distributed preganglionic nerves originating from T2-T3 spinal levels (147, 148). In the present study the inferior cardiac sympathetic nerve was recorded. Differing from the T2 white ramus which contains segmentally distributed sympathetic preganglionic fibers, the inferior cardiac nerve originates from the stellate ganglion which receives ipsilateral preganglionic

sympathetic input from C8 through T8 spinal levels (147, 148). In addition, McLachlan and Oldfield (131) have reported that catecholaminergic axons, presumed to project from the brain stem to the intermediolateral cell column (8, 28), only crossed the midline from T7 through L2 spinal levels. That evidence suggests that T7-T8 level bulbospinal pathway decussations might be functionally indicated when recording from the inferior cardiac nerve, but not the T2 white ramus. Furthermore, it is not surprising that results obtained while recording the inferior cardiac nerve in the present study are consistent with results obtained in 1939 by Harrison, Wang, and Berry (81) using blood pressure and nictitating membrane responses as indicators of multisegmental sympathetic activation.

After C6-C7 spinal cord transection at the end of Group I and Group II experiments, intercostal nerve activity and the respiratory modulation of sympathetic activity were both absent. Placement of cervical lesions at C6-C7 spinal levels eliminated the possibility of recording spinal interactions between phrenic and preganglionic sympathetic cell bodies which may occur after high (C2-C3) spinal cord transection (74). Instead, these C6-C7 spinal cord transections tested 1) the effect of eliminating respiratory input from supraspinal and C4-C5 spinal sources and 2) the effect of losing other supraspinal inputs descending in

dorsal and ventral spinal pathways to sympathetic nerves. The absent or non-rhythmic low levels of spontaneous sympathetic activity observed after spinal cord transection (RAW DATA, Fig. 4-4D & E, and Fig. 4-7I) are consistent with observations of other investigators who have studied sympathetic activity in spinal animals (9, 19, 74, 130). The present results from the C6-C7 spinal cord transections further substantiated the initial results indicating that the respiratory modulation was due to descending bilateral DLF influences.

Specific origins of the bilateral descending DLF pathways mediating the respiratory modulation of sympathetic nerve activity were not determined by this study. Extracellular recordings of single medullary units with combined cardiac and respiratory-related activities by Gootman et. al.(75) and Koepchen et.al. (106) provided some initial evidence for a brain stem level of respiratory-sympathetic interaction. Results from the present study are compatable with those previous results suggesting that DLF pathways may acquire the respiratory influence at higher i.e. brain stem levels.

An additional possibility is that a respiratory pathway from the ipsilateral ventrolateral nucleus of the solitary tract (nTS) descends in the DLF and imparts its respiratory influence on sympathetic preganglionic cell

bodies. Loewy and Burton (117) provided histologic evidence for nTS projections to the thoracic intermediolateral cell column (bilateral) and to the ventral horn at the C5 spinal level of phrenic motor nerves (predominantly contralateral). They described ipsilateral nTS projections coursing in the dorsal columns and dorsolateral funiculus whereas contralateral nTS projections were via ventrolateral funiculus and ventral horn pathways. Central respiratory projections are known to arise from the contralateral ventrolateral nTS and project via ventral pathways to phrenic and intercostal motor nerves (7, 21, 57, 151) as the Loewy and Burton evidence confirms (117). Ipsilateral ventrolateral nTS projections descending in the dorsolateral funiculus to the intermediolateral cell column may relay respiratory influences to preganglionic sympathetic nerves. However, nTS projections cannot provide a sole explanation for anatomical origins of respiratory influences on sympathetic activity because respiratory-related sympathetic rhythmicity is intact after combined ventral and ipsilateral hemisections eliminate bilateral ventrolateral pathways and ipsilateral dorsolateral funiculus pathways.

Other supraspinal structures known to affect sympathetic activity, alter blood pressure and/or project to the intermediolateral cell column by way of descending DLF pathways include the hypothalamus (1, 81, 100), the

ventrolateral medulla (84, 85, 117, 138), the raphe nucleus (15, 29, 44, 84, 128, 183), the medial cerebellar (i.e. fastigial) nuclei (1), the cerebral cortex (99), and pontine parabrachial areas (84, 85, 138, 144, 179, 188). Additional studies are necessary to define the functional influences of these and other specific supraspinal structures and/or pathways on the respiratory modulation of sympathetic activity.

In summary, this study has determined that the respiratory modulation of sympathetic nerve activity is mediated by bilaterally descending pathways located in the dorsolateral funiculus of the spinal cord (Fig. 4-10). These results also functionally confirmed that descending pathways affecting inferior cardiac sympathetic activity decussate between C8 and T8 spinal cord levels. The present experiments were not designed to determine supraspinal levels of decussation and do not exclude the probability that multiple decussations occur at several levels. Possible supraspinal origins of the DLF pathways affecting sympathetic activity and its respiratory modulation were discussed. Sympathetic preganglionic cell bodies may receive some respiratory inputs from the ventrolateral nTS, but additional inputs are necessary to completely explain the present results. As suggested by evidence of Gootman et.al. (75) and Koepchen et. al. (106), pressor pathways to

Figure 4-10

Bilaterally. descending dorsolateral funiculus pathways with spinal level decussations are necessary for the respiratory modulation of sympathetic nerve activity.

BRAIN STEM RESPIRATORY-RELATED SYMPATHETIC ACTIVITY

SYMPATHETIC GANGLION
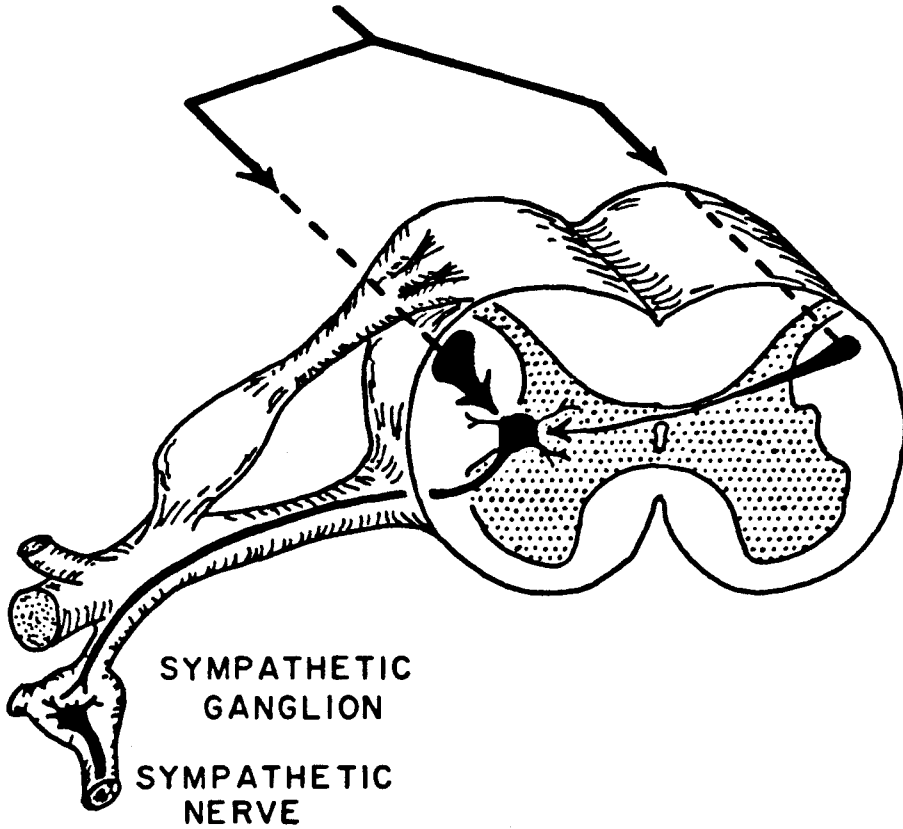
SYMPATHETIC NERVE

sympathetic nerves, also located in dorsolateral funiculus regions of the spinal cord, may acquire the respiratory modulation at brain stem levels. In conclusion, bilaterally descending DLF pathways may carry a combination of respiratory and respiratory modulated pressor influences mediating the respiratory modulation of sympathetic nerve activity.

CHAPTER V

EFFECTS OF MIDLINE CEREBELLAR LESIONS ON THE

RESPIRATORY MODULATION OF SYMPATHETIC NERVES

A. INTRODUCTION

The most medial of the deep cerebellar nuclei, known as fastigial or medial cerebellar nuclei, influence cardiovascular function. Achari and Downman (2) and Miura and Reis (139, 140) originally described arterial pressor and other autonomic responses to fastigial nucleus stimulation in anesthetized cats. Using glutamate injections to specifically excite cell bodies, Dormer, Foreman and Stone (55) verified that cerebellar pressor responses were specifically due to stimulation of fastigial nuclei and not axons of passage. Achari, Al-Ulbaidy and Downman (1) subsequently reported that medial cerebellar nucleus stimulation evoked discharges in inferior cardiac, splanchnic, and renal sympathetic nerves in chloralose anesthetized cats. Lesions of the restiform body, paramedian reticular nucleus and cervical dorsolateral spinal cord eliminate the evoked responses (1, 139, 140).

Although cerebellectomy does not eliminate respiratory rhythmicity (70, 172), stimulation of the anterior lobe of the medial cerebellum has inhibitory effects on inspiratory activity (49, 143).

The purpose of the present study was to determine if removal of medial cerebellar structures influenced the respiratory modulation of sympathetic nerve discharges. The respiratory modulation of sympathetic activity was assessed using respiration (phrenic nerve) triggered computer summation of phrenic and inferior cardiac sympathetic nerve activities in alpha-chloralose anesthetized cats. The computer summations, respiration, blood pressure and bilateral carotid occlusion responses were each compared before and after the midline structures of the cerebellum were removed by suction.

B. METHODS

1. Preparation

Eight cats were anesthetized with chloroform followed by intravenous infusion of alpha-chloralose (40-60 mg/kg). Femoral artery catheters were inserted for blood pressure (Statham P23Db pressure transducer), and pH, pO_2, and pCO_2 measurements (Radiometer-Copenhagen BMS3-C Blood Microsystem). After tracheotomy, end-expiratory $\%CO_2$ was continuously monitored (Beckman LB1 analyzer). Positive pressure artificial ventilation was begun after neuromuscular blockade with continuous succinyl choline infusion (6 mg/kg/hr). A cannula was inserted into the trachea for measurement of intratracheal pressure (Statham P23Db pressure transducer) as an indicator of ventilator activity. Cervical vagi and aortic depressor nerves were cut to eliminate vagal stretch receptor and aortic baro- and chemoreceptor influences on sympathetic activity. Inflatable occluders (Rhodes Medical Instruments) were placed around the carotid arteries for bilateral carotid occlusion tests of reflex sympathetic activation before and after midline cerebellar lesions. When indicated, blood pressure, pH and/or blood gases were adjusted to normal ranges with dextran, 8.4% sodium bicarbonate infusions or

adjustment of ventilator rate and pressure. Normal values for blood gases and pH were defined as $pO_2 \geq$ 100 mmHg, pCO_2 = 20-35 mmHg, and pH = 7.34. Cat rectal temperature was maintained at 38 ± 1 C with a servo-regulated heating pad.

Each cat was secured in a stereotaxic head frame (David Kopf Instruments). The pelvic iliac crests and a thoracic spine were clamped to a hanging frame to minimize ventilator induced movement artifacts. The cerebellum and dorsal surface of the medulla were exposed by an occipital craniotomy. Once the dura was cut, the brain was kept moist with warm mineral oil.

2. Left Phrenic and Inferior Cardiac Sympathetic Nerve Recordings

A skin and muscle flap extending from the left ear to the second thoracic spine was pulled laterally and attached to a curved horizontal rod to create two oil pools; a rostral one for the phrenic nerve and a caudal one for the inferior cardiac sympathetic nerve. To isolate the left inferior cardiac sympathetic nerve, the scapula was retracted exposing the ribs. Dorsal muscle layers were carefully scraped away from the first and second ribs and the heads of the ribs removed. The remaining bodies of the two ribs were then laterally retracted to expose the

stellate ganglion. The ventrocaudally coursing inferior cardiac sympathetic nerve was cut distally and desheathed in some preparations. Rostrally, the phrenic nerve was isolated as it exited from the fourth cervical nerve root, cut distally and desheathed.

Left phrenic and inferior cardiac sympathetic nerves were placed on bipolar platinum electrodes for differential recording (Grass P9 amplifiers). Nerve signals were monitored on a storage oscilloscope and photographed at various stages in each experiment. After rectification and leaky integration, (Grass Model 7P3 A Integrator, low pass filter time constant = 0.5 sec.) the signals were displayed on the oscillograph and stored on magnetic tape (Precision Instruments model 6200 tape recorder) for later analysis.

3. Lesions

Cerebellar lesions were made by suctioning the rostro-caudal extent of the medial cerebellum. When swelling or excessive bleeding occurred following the cerebellar lesion, the experiment was discontinued and the results were not used. Following the lesions, respiratory rhythmicity of sympathetic nerve activity was analyzed (computer summation methods described below) and compared to control activity.

4. Computer Summation

Computer summation techniques were used to analyze effects of midline cerebellar lesions on the respiratory modulation of sympathetic nerve activity. Amplified integrated sympathetic activity (millivolts) was processed using respiration (ie. phrenic nerve signal) triggered computer summation (Nuclear Chicago Data Retrieval Computer). Computer summated (twenty sweeps) phrenic and sympathetic nerve activities were analyzed before and after lesions. Areas of computer summated sympathetic activity were measured using a graphics tablet (Bausch and Lomb) connected to a digital computer (Apple II Plus). Net sympathetic inspiratory amplitude (NSIA) was then calculated to quantitate the respiratory modulation of sympathetic nerve activity (Fig. 5-1):

$$NSIA = (Area\ Insp/\ TI) - (Area\ Exp/\ TE)$$

Area Insp= computer-summed area (twenty sweeps) of amplified integrated sympathetic activity during inspiration (millivolt-seconds)

Area Exp= computer-summed area (twenty sweeps) of amplified integrated sympathetic activity during expiration

Figure 5-1

Diagrammatic illustration of data analysis method used to determine NSIA (net sympathetic inspiratory amplitude) as described in the text.

COMPUTER SUMMATED INTEGRATED PHRENIC N. ACTIVITY

INSP.

EXP.

TIME →

T_{exp} T_{insp}

COMPUTER SUMMATED INTEGRATED SYMP. N. ACTIVITY

MEAN INSP. AMPLITUDE

NET SYMPATHETIC INSP. AMPLITUDE

MEAN EXP. AMPLITUDE $AREA_{exp.}$ $AREA_{insp.}$

$$\text{MEAN EXP. AMPLITUDE} = \frac{AREA_{exp.}}{T_{exp.}}$$

$$\text{MEAN INSP. AMPLITUDE} = \frac{AREA_{insp.}}{T_{insp.}}$$

$$\begin{array}{l}\text{NET SYMPATHETIC}\\\text{INSP. AMPLITUDE}\end{array} = \begin{array}{l}\text{MEAN INSP. AMPLITUDE} -\\\text{MEAN EXP. AMPLITUDE}\end{array}$$

(millivolt-seconds)

T_I= duration of inspiration (seconds)

T_E= duration of expiration (seconds)

When sympathetic activity has a respiratory related discharge, the derived net sympathetic inspiratory amplitude is a positive value. Net sympathetic inspiratory amplitude approaches zero when phrenic nerve triggered sympathetic activity summates into a relatively straight horizontal line, indicating no respiratory modulation.

5. Histology

The cerebellum and brain stem were placed in 10% buffered formalin for at least 3 days and then embedded in paraffin. Every tenth ten micron thin serial section was stained for fibers and cell bodies by the Kluver-Barrera method (103). Slides of lesioned brain sections from rostral, intermediate and caudal regions containing deep cerebellar nuclei were projected onto paper and traced.

6. Statistics

Control values for net sympathetic inspiratory amplitude (NSIA), blood pressure, blood pressure responses

to bilateral carotid occlusion, respiration rate, and inspiratory duration were statistically compared with values obtained after midline cerebellar lesions using paired t tests (69, 163). Significance was defined at P less than 0.05. Values are expressed as means $\pm$ standard error (SE) of the mean.

C. RESULTS

Respiratory modulation of sympathetic nerve activity was apparent in control recordings from the eight cats. Presence of the respiratory modulation was confirmed by respiration triggered computer summation of sympathetic and phrenic nerve activities, as illustrated in Figure 5-2 (CONTROL). The control NSIA of 352 ± 37 MV reflected strong respiratory modulation of sympathetic activity prior to cerebellar lesions. Control blood pressure and bilateral carotid occlusion responses were 127 ± 7 mm Hg and 66 ± 9 mm Hg, respectively (Fig. 5-3, CONTROL).

Midline cerebellar lesions had no effect on respiratory modulation of sympathetic nerves, as indicated by no change in computer summated activity (Fig. 5-2) or NSIA after lesions (Fig. 5-3, Top). There were also no changes in mean blood pressure or blood pressure increases during bilateral carotid occlusion (Fig. 5-3, Bottom).

Group data from the eight cats indicated that respiration was not significantly altered after removal of medial cerebellar structures. Control respiration rate (11.4 ± 0.4 breaths/min) was insignificantly ($P > 0.05$) decreased to 9.9 ± 0.8 breaths/min after cerebellar lesions. Duration of inspiration was insignificantly ($P > 0.05$) increased from 2.9 ± 0.1 sec before lesions to 3.4 ± 0.3 sec

Figure 5-2

Respiration triggered computer summation (20 sweeps) of integrated sympathetic (Top) and phrenic (Bottom) nerve activities before (left) and after (right) midline cerebellar lesions.

Figure 5-3

Group data from eight cats indicating NSIA (Top), mean
arterial blood pressure (Bottom, Left Scale, Solid Bar), and
increases in mean blood pressure during bilateral carotid
occlusion (Bottom, Right Scale, Bar with Horizontal Stripes)
before (left) and after (right) midline cerebellar lesions.
Values indicated are means $\pm$ standard error of the mean.
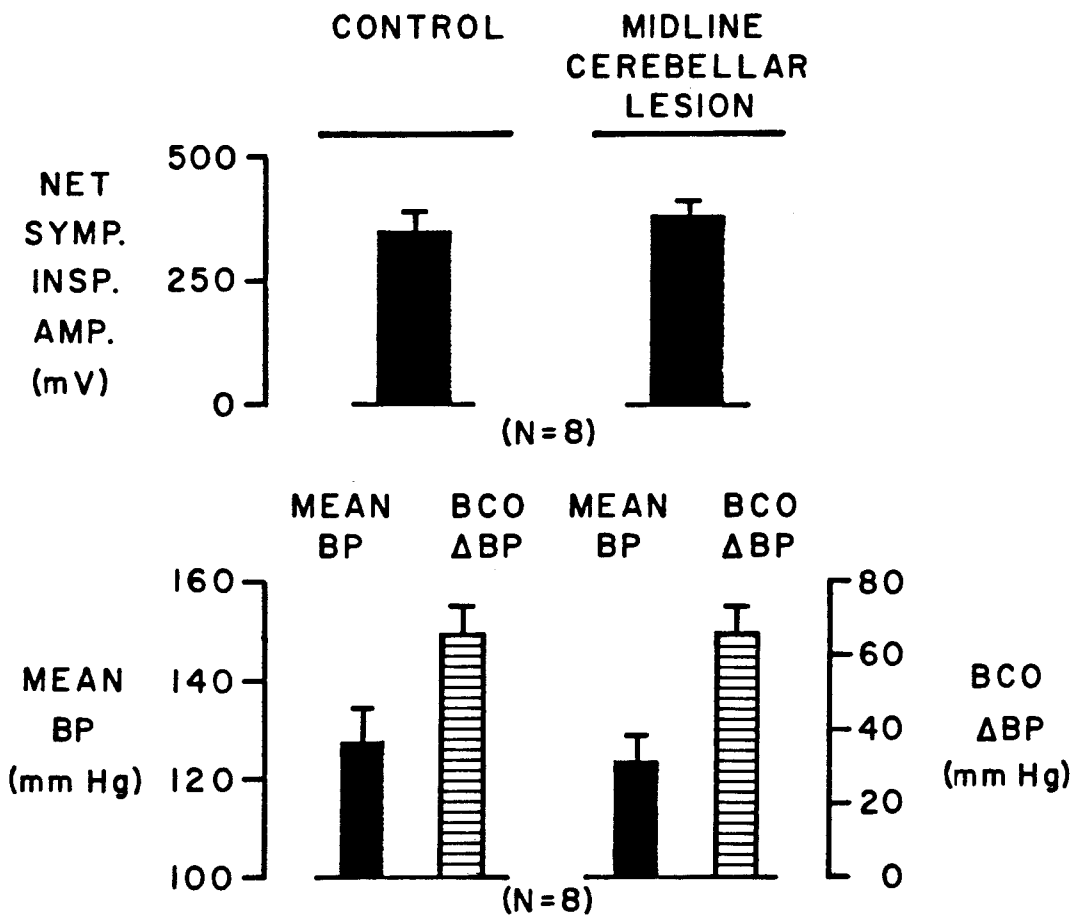
after medial cerebellar structures were removed. Respiratory rate was slightly decreased and inspiratory duration slightly increased after cerebellar lesions in three of the cats. No changes in respiration were observed in the other five cats after the lesions.

Figure 5-4 illustrates locations of the deep cerebellar nuclei identified after Kluver-Barrera staining in a control cat with no lesions. The identified medial cerebellar (CBM), interpositus (IN) and lateral cerebellar (CBL) nuclei are labeled in accordance with Berman's nomenclature (23).

Brain sections through the rostral, intermediate and caudal extent of the deep cerebellar nuclei indicated that medial cerebellar nuclei were completely eliminated by midline lesions in all but Cat #2 (Fig. 5-5). The vermal cortex was also largely destroyed by the lesions. Histological analysis confirmed that medullary and pontine regions immediately ventral to the lesioned cerebellum remained intact.

In summary, these results indicated that midline cerebellar lesions eliminating medial cerebellar nuclei caused no significant changes in respiration, respiratory modulation of sympathetic activity, mean arterial blood pressure or blood pressure increases during bilateral carotid occlusion.

Figure 5-4

Brain stem cross section from control cat with no cerebellar lesions to illustrate locations of deep cerebellar nuclei as seen after Kluver-Barrera staining. Abbreviations, according to Berman's nomenclature, are CBM, Medial Cerebellar Nucleus or Fastigial Nucleus; IN, Interpositus Nucleus; CBL, Lateral Cerebellar Nucleus.

CBM IN

CBL

5 mm
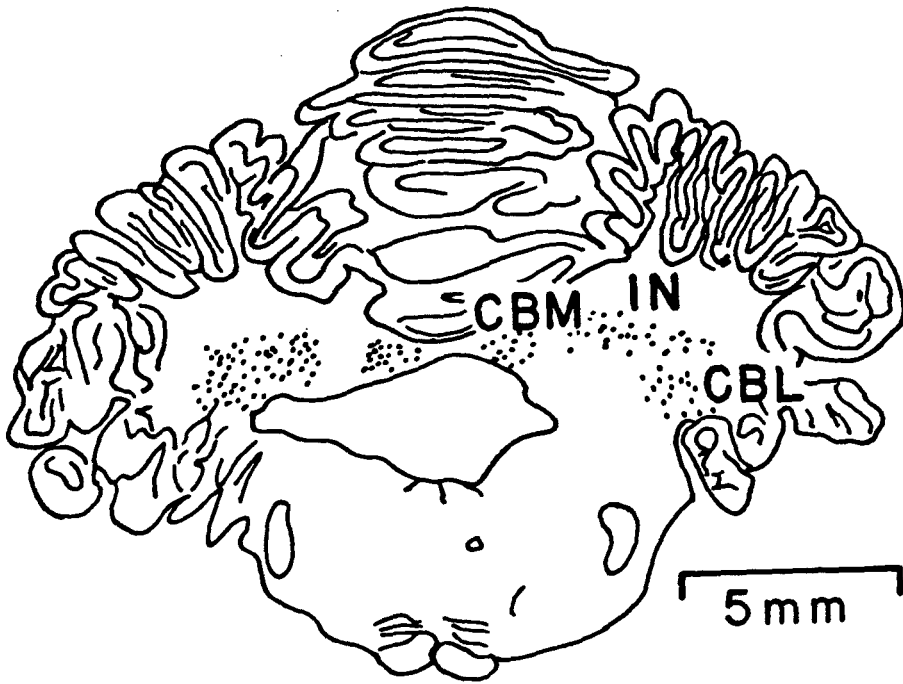
Figure 5-5

Brain stem cross sections after cerebellar lesions. Sections
through the rostral, intermediate and caudal zones of the
deep cerebellar nuclei are illustrated for each cat.

ROSTRAL　　CAUDAL

CAT
#

C1　CBL　IN

C2　IN CBL　CBM

C3　IN　CBL

C4　CBL　IN

C5　CBL　IN

C6　CBL　IN

C7　CBL

C8　CBL　CBL

10 mm
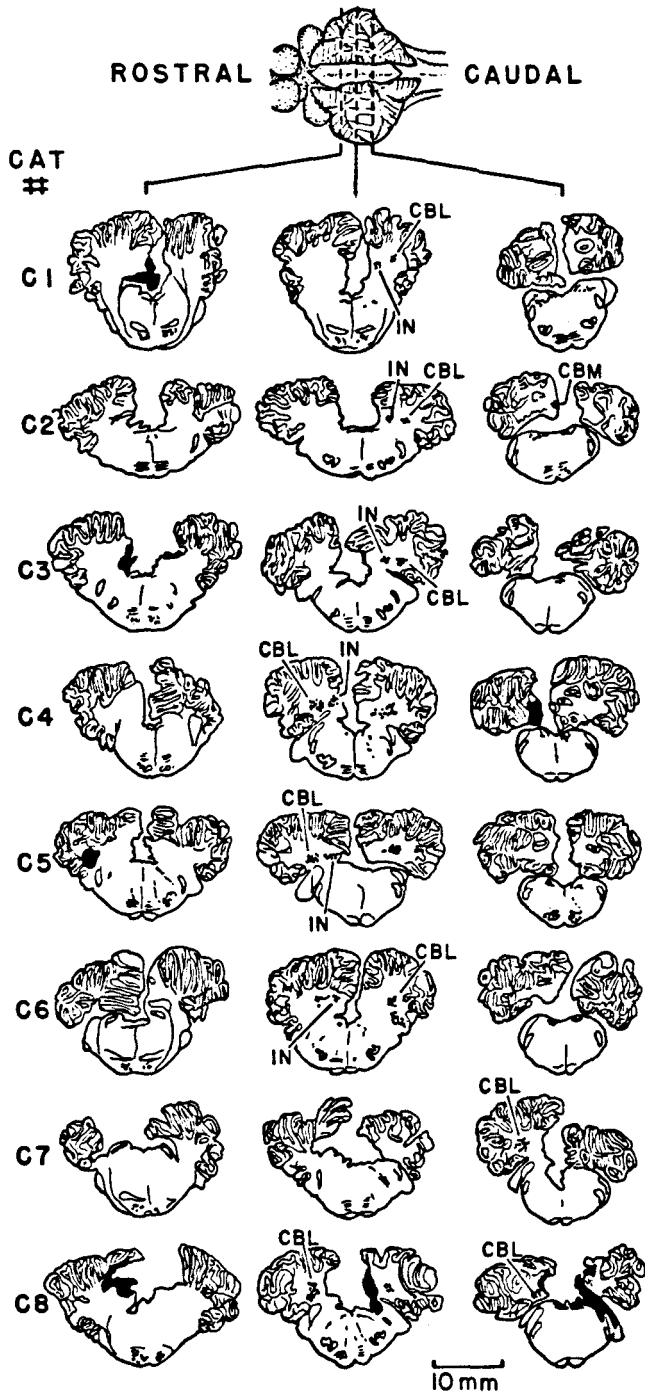
D. DISCUSSION

Other investigators have shown that cerebellar structures influence respiration and the autonomic nervous system. Moruzzi (143) and Decima and von Euler (49) previously reported that stimulation of the anterior lobe of the cerebellum inhibited respiratory activity. In a different study, Glasser, Tippet, and Davidian (70) showed that ablation or local anesthetic depression of the cerebellum resulted in prolonged inspiratory time. The rate of respiration was either unaltered or decreased by the lesions in their study. Respiratory rate and inspiratory time were unaffected by cerebellar lesions in the present study. Together, these data indicate that the cerebellum has a subtle inhibitory influence on inspiratory activity, but is not essential for respiratory rhythm generation. Cerebellar inhibition of inspiratory activity has a more predominant influence after destruction of pneumotaxic regions in the dorsolateral rostral pontine tegmentum (70).

Known autonomic effects resulting from stimulation of the cerebellar vermis were the major reason for this investigation of cerebellar influences on the respiratory modulation of sympathetic activity. In 1940, Moruzzi (143) reported that stimulation of vermal cortex in the anterior lobe of the cerebellum depressed blood pressure. Miura and

Reis (139, 140) and Achari and Downman (2) later determined that stimulation of medial cerebellar nuclei caused marked pressor responses due to increased sympathetic activity. Pressor or depressor responses resulted from stimulation of the medial cerebellar nuclei or cerebellar cortex, respectively. Injection of glutamate into regions of the cerebellum and brain stem by Dormer, Foreman and Stone (55) definitively proved that cerebellar pressor responses were specifically due to fastigial nuclei stimulation. Autonomic effects, other than just the pressor response, were indicated by cardiac arrythmias resulting from fastigial nucleus stimulation (86). Additional studies determined that cerebellar pressor responses were functionally involved in cardiovascular responses to orthostatic hypotension (53, 54, 87) hypotension induced by hemorrhage (125), and hypotension during endotoxic shock (125).

Although previous studies established that there were deficits in responses to orthostatic hypotension (53, 54, 87), hemorrhage (125) and endotoxic shock (125) after cerebellectomy, effects on sympathetic rhythms were never assessed. Inadvertant stimulation of fastigial nuclei or cerebellar cortex by nonspecific lesion-induced excitation of pathways or nuclei during and after removal of medial cerebellar structures could have potentially masked respiratory influences on sympathetic activity. However,

results from the present experiments indicated that midline cerebellar lesions, ablating medial cerebellar nuclei and vermal cortex, did not affect the respiratory modulation of sympathetic nerves (Fig. 5-2 and Fig. 5-3). Consistent with earlier observations by Lisander and Martner (116), the present experiments also indicated no effect of medial cerebellar lesions on blood pressure or bilateral carotid occlusion responses. Lisander and Martner (116) observed that the response pattern to fastigial nucleus stimulation resembled the pressor response to bilateral carotid occlusion, but that cerebellectomy did not affect bilateral carotid occlusion responses.

Direct projections from medial cerebellar nuclei to the intermediolateral gray matter of the spinal cord have been reported (20, 182, 187). There are also brain stem projections to nuclei with known autonomic influences, such as vestibular, lateral reticular and paramedian reticular nuclei (17, 20, 182). Physiologic evidence by Miura and Reis (139, 140) initially indicated that cerebellar pressor responses were relayed through brain stem paramedian reticular nuclei since responses were abolished by bilateral lesions in this region. Lesions of other brain stem nuclei, such as the lateral reticular nuclei, had no effect on the evoked response. Their physiologic results were substantiated by anatomically demonstrated projections of

medial cerebellar nuclei to paramedian reticular nuclei (17, 20, 182).   Results from an autoradiographic study in the monkey (17) indicated that fastigioreticular connections, including   those   to paramedian reticular nuclei, were entirely crossed.   Thus, available evidence best supports the conclusion that fastigial pressor responses are relayed through contralateral paramedian reticular nuclei which send projections to the spinal cord.

Achari, Al-Ubaidy and Downman (1) determined that descending spinal pathways mediating cerebellar pressor responses were located bilaterally in the dorsolateral funiculus. Results from Chapter IV (spinal cord study) indicated that the respiratory modulation of sympathetic nerve activity was also mediated by bilateral pathways descending in the dorsolateral funiculus of the spinal cord. The present study eliminated the possibility that cerebellar influences in descending dorsolateral funiculus pathways are necessary for the respiratory modulation of sympathetic activity.

It is significant that removal of medial cerebellar structures had no effect on respiration, the respiratory modulation of sympathetic activity, blood pressure, or baroreceptor responses in the present study. Medial regions of the caudal cerebellum are frequently removed using gentle suction or mechanically displaced to visually expose dorsal

aspects of the medulla for various types of experiments. For example, studies concerned with central control of respiration, central autonomic control and baroreceptor reflex connections in the brain stem frequently require displacement or removal of cerebellar structures for placement of electrodes in or near the nucleus of the solitary tract. Removal or mechanical displacement of just the medial cerebellar structures reduces the potential surgical trauma associated with complete cerebellectomy. The present study established that results from such studies are not inadvertantly influenced by removal of medial cerebellar structures.

CHAPTER VI

EFFECTS OF PONTINE PARABRACHIAL AREA STIMULATIONS
AND LESIONS ON SYMPATHETIC ACTIVITY

A. INTRODUCTION

Pontine parabrachial areas influence respiratory and cardiovascular functions. Extracellular recordings from parabrachial area neurons indicate discharge patterns related to respiratory and cardiac cycles (27, 43, 80). Neuroanatomical studies demonstrate direct connections from parabrachial areas to medullary cardiorespiratory centers (32, 51, 110, 138). Direct projections to the region of phrenic motoneurons (162) and sympathetic preganglionic cells in the spinal cord have also been reported (34, 110, 118).

Parabrachial area lesions induce an apneustic breathing pattern in vagotomized animals (26, 64, 176). Stimulation of the parabrachial region evokes activation or inhibition of phrenic discharges (16, 26, 39, 58). A cardiovascular pressor response of approximately fifty mmHg elevation in blood pressure is also elicited by high

137

frequency stimulation of this area (144).

The present study was designed to characterize pontine parabrachial area influences on sympathetic nerve activity in alpha-chloralose anesthetized cats. Phrenic and sympathetic nerves were recorded while stimulating ipsi- and contralateral pontine parabrachial areas during different phases of the respiratory cycle. Following parabrachial area lesions, the effect of apneustic breathing patterns on the respiratory modulation of sympathetic nerve activity was determined. Spectral analysis was used to assess slow frequency patterns in sympathetic nerve activity before and after pontine lesions.

B. METHODS

1. Preparation

Eleven cats were anesthetized with chloroform followed by intravenous infusion of alpha-chloralose (40-60 mg/kg). Femoral artery catheters were inserted for blood pressure, (Statham P23Db pressure transducer) and pH, pO2, and pCO2 measurements (Radiometer-Copenhagen BMS3-C Blood Microsystem). After tracheotomy, end-expiratory %CO2 was continuously monitored (Beckman (LB1) analyzer). Positive pressure artificial ventilation was begun after neuromuscular blockade with continuous succinyl choline infusion (6 mg/kg/hr). A cannula was inserted into the trachea for measurement of intratracheal pressure (Statham P23Db pressure transducer) as an indicator of ventilator activity. Cervical vagi and aortic depressor nerves were cut to eliminate vagal stretch receptor and aortic baro- and chemoreceptor influences on sympathetic activity. Inflatable occluders (Rhodes Medical Instruments) were placed around the carotid arteries for bilateral carotid occlusion tests of reflex sympathetic activation before and after pontine parabrachial area lesions. When indicated, blood pressure, pH and/or blood gases were adjusted to normal levels with dextran, 8.4% sodium bicarbonate infusions or adjustment of

ventilator rate and pressure. Rectal temperature was maintained at 38 $\pm$ 1 C with a servo-regulated heating pad.

Each cat was secured in a stereotaxic head frame (David Kopf). The pelvic iliac crests and a thoracic spine were clamped to a hanging frame to minimize ventilator induced movement artifacts. The dorsal surface of the medulla and cerebellum were exposed by an occipital craniotomy to allow insertion of stereotaxically positioned coaxial electrodes into the rostral pontine parabrachial areas corresponding to the pneumotaxic center. Once the dura was cut, the dorsal surface of the brain was kept moist with warm mineral oil.

2. Left Phrenic and Inferior Cardiac Sympathetic Nerve Recordings

A skin and muscle flap extending from the left ear to the second thoracic spine was pulled laterally and attached to a curved horizontal rod to create two oil pools; a rostral one for the phrenic nerve and a caudal one for the inferior cardiac sympathetic nerve. To isolate the left inferior cardiac sympathetic nerve, heads of the first two ribs were removed. The bodies of ribs were then laterally retracted to expose the stellate ganglion and inferior cardiac sympathetic nerve, which was cut distally

and destheathed in some preparations. Rostrally, the phrenic nerve was isolated as it exited from the fourth cervical nerve root, cut distally and desheathed.

Left phrenic and inferior cardiac sympathetic nerves were placed on bipolar platinum electrodes for differential recording (Grass P9 amplifiers). The nerve signals were monitored on a storage oscilloscope and photographed at various stages in each experiment. After leaky integration, (Grass Model 7P3 A Integrator, low pass filter time constant = 0.5 sec.) the signals were displayed on the oscillograph and stored on magnetic tape (Precision Instruments model 6200 tape recorder) for later analysis.

3. Pontine Parabrachial Area Stimulation and Lesions

Stereotaxically placed (posterior 3.5, vertical -4.0, mediolateral $\pm$ 4.5) bipolar concentric electrodes were used to stimulate ipsilateral and/or contralateral pontine parabrachial areas during inspiration, post-inspiration, and expiration phases of the respiratory cycle (Fig. 6-1). Figure 6-2 illustrates the stimulation procedure. Amplified, integrated phrenic nerve activity triggered a level detector and variable delay circuit which then triggered the stimulator to deliver impulses (300 impulses/sec, 20 msec train, 0.5 msec/stim, 10-100 uA) through a stimulus

142

Figure 6-1

Inferior cardiac sympathetic nerve activity (Bottom) is characteristically enhanced during inspiratory and inhibited during post-inspiratory phases of phrenic nerve activity (Top). Pontine parabrachial areas were stimulated during inspiratory, post-inspiratory or expiratory phases of phrenic nerve activity.

EXP. INSP. POST INSP.

PHRENIC N. 417 μV|

INF. CARD. SYMP. N. 125 μV|

2 SEC.
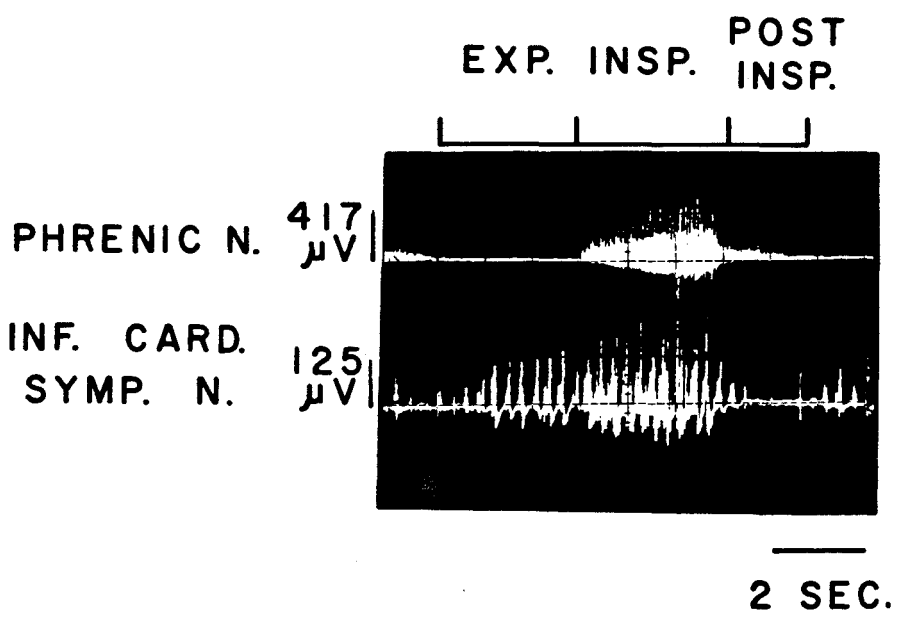
Figure 6-2

Diagrammatic illustration of method for stimulating medial parabrachial (PBM) and Kolliker-Fuse (KF) regions of the dorsolateral rostral pons during inspiration, post-inspiration or expiration. Amplified, integrated phrenic nerve activity was channeled through a level detector and variable delay circuit to trigger the stimulator which delivered stimuli to the pons during inspiration, post-inspiration, or expiration through a stimulus isolation unit, constant current unit, and coaxial electrodes.
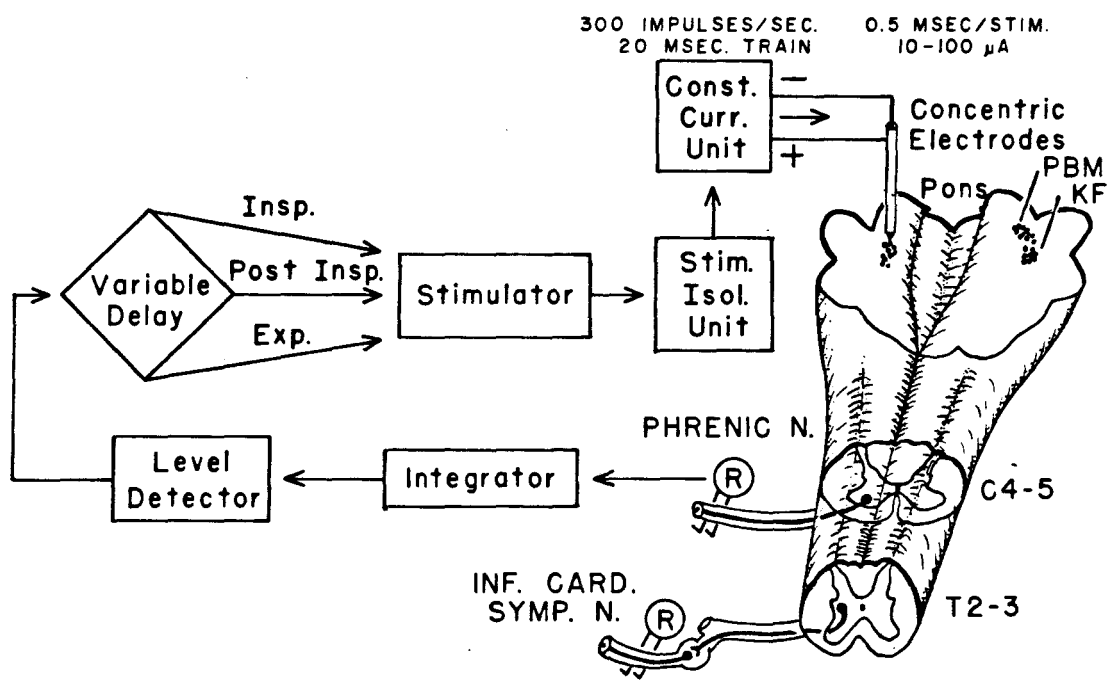
isolation unit and constant current device to the pontine parabrachial areas during different phases of the respiratory cycle. For comparison, data were also collected when the respiration-triggered stimulator output was not delivered to the brain and after DC lesions were made at the stimulation sites. Lesions were made at the stimulation sites by passing direct current (two milliamps for fifteen seconds) through the stimulating electrode. The lesions marked the stimulation sites and generated the apneustic breathing patterns characteristic of bilateral pneumotaxic lesions in vagotomized animals. Following the lesions in some animals, the stimulator was triggered by expiration or inspiration followed by a delay to further analyze respiratory effects on sympathetic activity during apneusis as described below.

4. Computer Summation Analysis

Stimulus triggered computer summations (Nuclear Chicago Data Retrieval Computer) of amplified, integrated, sympathetic activity (forty sweeps) were recorded during inspiration, post-inspiration, expiration, when the stimulator output was not delivered to the brain, and when the stimulus was delivered after making the lesions. Computer-summated areas (millivolt-seconds) were measured

with a graphics tablet (Bausch and Lomb) connected to a digital computer (Apple II Plus) and statistically compared using analysis of variance followed by tests for least significant differences (69, 163). Significance was defined at $P < 0.05$.

Computer summation techniques (Nuclear Chicago Data Retrieval Computer) were also used to determine how sympathetic nerve activity was affected by the onset and termination of inspiration after bilateral parabrachial area lesions. Amplified, integrated sympathetic and phrenic nerve activities (millivolts) were processed using respiration (phrenic nerve) triggered computer summation (twenty sweeps) to verify that respiratory modulation of sympathetic activity was present in all cats prior to pontine lesions. After parabrachial area lesions, the irregularity in both duration and frequency of the apneustic breathing pattern made it necessary to assess the inspiratory termination effects on sympathetic nerve activity in the following manner. At the time of the experiment, data was collected when the stimulator was triggered by expiration followed by a delay. These expiration triggered timing pulses were recorded on the tape recorder along with phrenic and sympathetic nerve activities. At the time of computer summation analysis, the tape recorder was played in reverse so that the timing

pulses triggered the summating computer to record (twenty sweeps) sympathetic and phrenic nerve activities after a fixed delay. When the computer summated sympathetic activity coincided with the phrenic nerve activity summation, it indicated a link between the termination of inspiration and sympathetic nerve activity. Similarly, a link between the onset of inspiration and sympathetic activity could be observed using inspiration triggered timing pulses.

5. Spectral Analysis

Spectral analysis (Rockland Real-Time Spectral Analyzer FFT 512/S) was used to determine the slow frequency characteristics of sympathetic nerve activity before and after pontine lesions. Prior to spectral analysis, the sympathetic nerve signals were low-pass filtered (Grass integrator TC = 0.5 sec) to facilitate assessment of the slow frequency components resulting from rhythmic bursts of sympathetic activity coinciding with the respiratory frequency. Although the higher frequency components of sympathetic activity (e.g. 2 to 6 Hz cardiac-related activity) were attenuated or eliminated by the low-pass filtering technique, low frequency bursts of sympathetic activity were more easily detected using this method. The "SLOW PEAK" was designated as the spectral peak of

sympathetic activity at the control respiratory frequency. The presence of the "SLOW PEAK" was assessed before and after pontine lesions for all cats. It should be noted that the higher background spectral amplitude in the lower frequencies is attributed to the low-pass signal filtering methods prior to spectral analysis and should not be mistakenly interpreted to indicate more physiological activity in the low rather than high frequency ranges.

6. Histology

The brain stems were placed in 10% buffered formalin for at least 3 days and then embedded in paraffin. Every tenth ten micron thin serial section was stained for fibers and cell bodies by the Kluver-Barrera method (103). The slides were projected onto paper for tracing of pontine stimulation/lesion sites.

7. Statistics

In addition to those already described, the following statistical applications were used. Latency of the stimulation evoked responses and duration of the inhibitory phase following the responses were compared for differences between phases of the respiratory cycle using

analysis of variance followed by tests for least significant differences. Differences in response latency between right and left sides were compared during the inspiratory or expiratory phase of respiration using t-tests (69, 163).

Blood pressure and blood pressure responses to bilateral carotid occlusion tests were statistically compared with values obtained after pontine parabrachial lesions using paired t tests. Significance was defined at P less than 0.05. All values were expressed as means $\pm$ standard error (SE) of the mean.

C. RESULTS

Stimulation of ipsilateral or contralateral pontine parabrachial areas evoked sympathetic activation followed by inhibition during inspiratory, post-inspiratory, and expiratory phases of the respiratory cycle. Figure 6-3 illustrates typically evoked sympathetic activation (5 sweeps) following ipsilateral (left) pontine stimulation (Cat #6). Amplitude of the evoked response and its latency were unaffected by the phase of the respiratory cycle. Varying stimulus current intensities in one of the cats from 12.5 to 100 uA did not alter response latencies, but larger stimulation currents did increase the amplitudes of evoked responses. Mean sympathetic response latency measured after ipsilateral stimulation during inspiration (9 cats), post-inspiration (5 cats) and expiration (9 cats) was not significantly ($P > 0.05$) affected by the phase of respiration (Fig. 6-3). In contrast, evoked phrenic nerve responses were present during inspiration and essentially absent during post-inspiration and expiration. Contralateral pontine stimulation results were similar to ipsilateral stimulation results. However, mean sympathetic response latency after ipsilateral stimulation during inspiration (41 $\pm$ 4 msec) was significantly ($P < 0.05$) shorter than the latency after contralateral stimulation (56

Figure 6-3

Oscilloscope tracings (five sweeps) from Cat #6 of left inferior cardiac sympathetic (Top) and phrenic (Bottom) nerve activities evoked after left parabrachial area stimulation during inspiratory, post-inspiratory, and expiratory phases of the respiratory cycle. Statistical analysis of the grouped data (MEAN SYMP. LATENCY) for the number of cats (No. of cats) in parentheses indicated that latencies of evoked responses were not significantly ($P < 0.05$) different when stimulations occurred during inspiration, post-inspiration, or expiration.

INSP.   POST INSP.   EXP.

STIM. LEFT

INF.
CARD.   400
SYMP. N.   μV
             800
PHRENIC N.   μV

40 msec

MEAN SYMP.
LATENCY (msec)   41±4   50±3   48±3

(No. of cats)   (9)   (5)   (9)
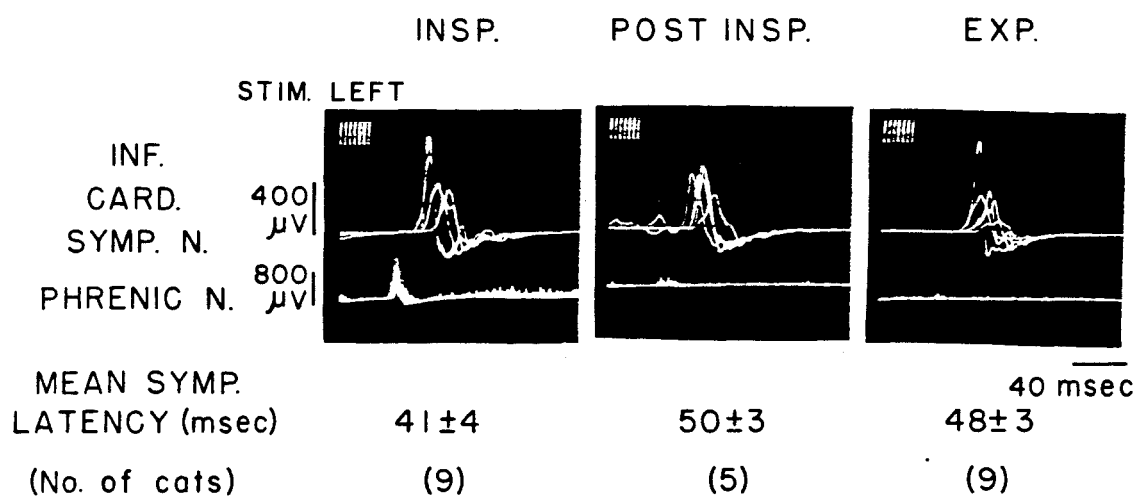
$\pm$ 4 msec). During expiration, sympathetic response latencies after ipsilateral stimulation (47 $\pm$ 4 msec) were not significantly (P > 0.05) different from latencies after contralateral pontine stimulation (52 $\pm$ 5 msec). The subtle ipsi- versus contralateral differences in response latency (not exceeding 15 msec during either inspiration or expiration) may be explained by longer contralateral pathway distances, or slight differences in electrode placement.

The longer time scale of Fig. 6-4 (Top) better illustrates the inhibition of sympathetic activity following evoked activation (Cat #6). Figure 6-4 (Bottom) contains group data from cats receiving ipsilateral pontine stimulation during inspiration (9 cats), post-inspiration (5 cats), and expiration (9 cats). Duration of the inhibitory period (Mean Duration Symp. Inhib.) after ipsi- or contralateral pontine parabrachial stimulation was not significantly (P > 0.05) affected by the respiratory cycle. The duration of the inhibition was increased in one of the cats by varying stimulus intensity from 12.5 to 100 uA.

Figure 6-5 (Top) illustrates typical computer-summated sympathetic activity (forty sweeps) evoked by ipsilateral pontine stimulation before and after ipsilateral pontine lesions. Areas of computer-summated sympathetic activity evoked above background activity levels (indicated by oblique lines under the curves) were compared during

Figure 6-4

Oscilloscope tracings (five sweeps) from Cat #6 of post-excitatory inhibition of left inferior cardiac sympathetic activity (Top) evoked by left pontine stimulation during inspiratory, post-inspiratory, and expiratory phases of the respiratory cycle. Phrenic nerve activity was recorded in the bottom trace. Statistical analysis of the grouped data (MEAN DURATION SYMP. INHIB.) for the number of cats (No. of cats) in parentheses indicated that the duration of the inhibitory period was not significantly (P < 0.05) affected by the phase of the respiratory cycle when stimuli were delivered.

INSP. POST INSP. EXP.

STIM. LEFT

INF.
CARD.   400
SYMP. N. μV

PHRENIC N. 800
μV

400 msec

MEAN
DURATION   442±90   720±242   578±106
SYMP. INHIB.
(msec)

(No. of cats)   (9)   (5)   (9)
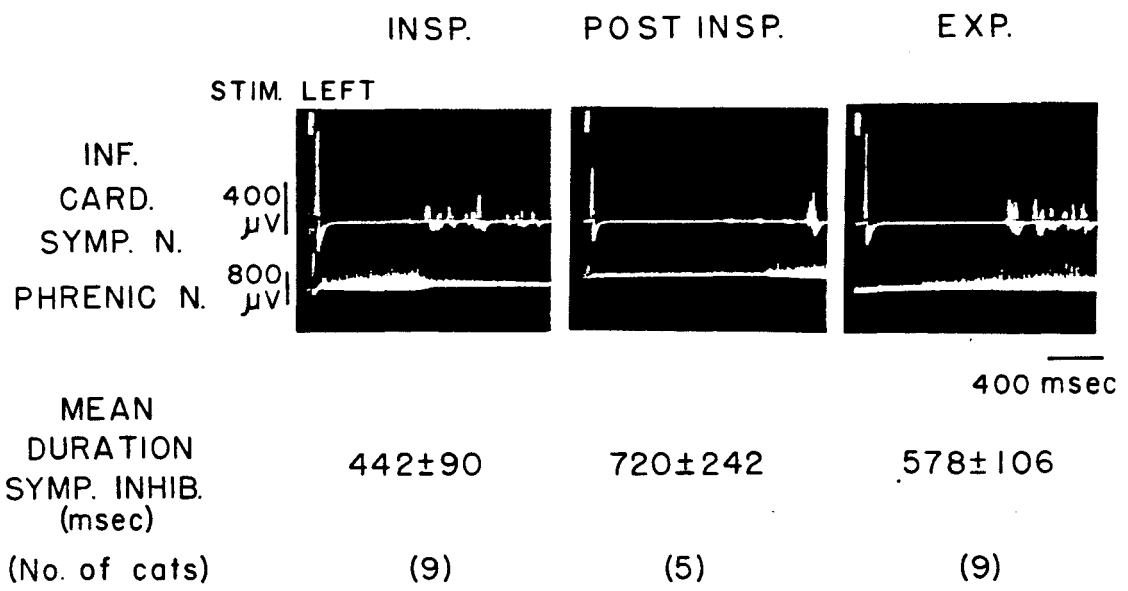
Figure 6-5

Stimulus triggered computer summations of evoked sympathetic activity (forty sweeps) from Cat #4 (top) during inspiration (INSP), post-inspiration (POST INSP), expiration (EXP), when respiration triggered stimuli were not delivered to the brain during the control period (NOT DELIVERED), and after direct current lesions of the stimulation site (POST LEFT LESION). Areas (mV-sec) of evoked sympathetic activity (oblique lines under each curve) were computed for Cat #4 and displayed above each curve. Areas evoked above the background activity (oblique lines under each curve) for the number of cats (N) indicated in parentheses are illustrated in the bar graph (bottom half of figure). The dashed horizontal and vertical lines under each curve (top) delineate the area of sympathetic activity evoked above a baseline of zero activity, which was also measured for comparison (see text).

CONTROL

INSP	POST INSP	EXP	NOT DELIVERED	POST LEFT LESION
AREA = 64 mV·sec	= 79 mV·sec	= 92 mV·sec	= 0 mV·sec	= 0 mV·sec

EVOKED SYMP. ACTIVITY (mV x1000) N = 1

2.5 2.0 1.5 1.0 0.5 0

MEAN AREA EVOKED SYMP. ACTIVITY (mV·sec)

100 75 50 25 0

N = 9   N = 5   N = 9   N = 5   N = 8

150 msec
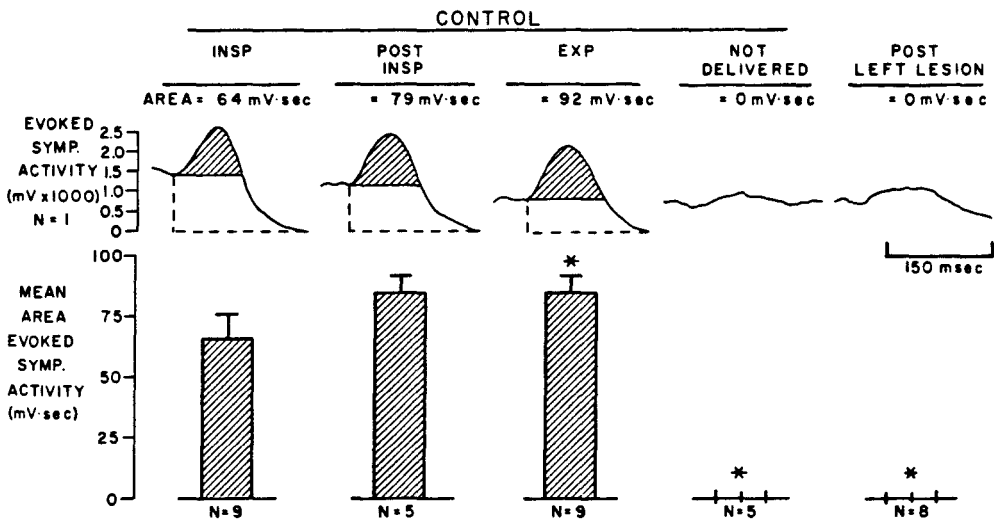
inspiration, post-inspiration, and expiration, when respiration triggered stimulator output was not delivered to the brain (NOT DELIVERED) and when the stimulus was delivered after ipsilateral pontine lesions. Group data comparisons (Fig. 6-5, Bottom) indicated no significant ($P >$ 0.05) differences between evoked areas during inspiration and post-inspiration. Area evoked during expiration was significantly ($P < 0.05$) larger than the area evoked during inspiration. The larger evoked area (above background activity) during expiration was attributed to less background sympathetic activity (i.e. lower baseline activity prior to stimulation) and not to respiratory gating of the evoked response. This interpretation was verified further when computer-summated evoked sympathetic areas were re-measured from a baseline of zero activity for comparison (i.e. area defined by dashed lines under evoked curves in Fig. 6-5, Top) and no significant ($P > 0.05$) differences in sympathetic responses to pontine stimulation during different phases of the respiratory cycle were found.

Stimulus triggered computer summations of non-evoked sympathetic activity served as controls for the computer summation technique (Fig. 6-5). Areas of evoked sympathetic activity (as measured above either background activity levels or a baseline of zero activity) during the three phases of the respiratory cycle were each significantly ($P <$

0.05) different from stimulus triggered computer summations of non-evoked activity occurring when stimulator output was not delivered to the brain (NOT DELIVERED) and after direct current lesions of the stimulation sites (POST LEFT LESION).

Histological analysis after bilateral parabrachial lesions indicated destruction of nuclei and/or pathways primarily from medial parabrachial nuclei (PBM) and/or Kolliker-Fuse nuclei (KF) regions (Fig.6-6). Left lesions (ipsilateral) in Cats #1,#2,#3,#4,#6,#7,#8, and #10 and right lesions in Cats #1,#2,#3,#4,#7 and #9 included regions of medial PBM and KF nuclei. More caudally placed lesions on the left side in Cat #5 and the right side in Cats #5 and #6 included pathways descending from the hypothalamus (35, 171) and parabrachial region (32, 129). More ventrally located paralemniscal tegmental fields (FTP) and lateral tegmental fields (FTL) which contain catecholaminergic pathways and cell groups (92) were included in the lesions on the left side in Cats #2,#3,#7,#8 and #10 and on the right side in Cats #2,#5,#7,#9, and #10. The asterisks above Cat #8 (right lesion) and Cat #9 (left lesion) indicate that stimulation of those locations prior to lesions did not evoke sympathetic responses. Lack of sympathetic response in those two cases was attributed to either suboptimal electrode placement during the attempted stimulations or electrode damage of surrounding tissue prior

Figure 6-6

Tracings of dorsolateral pontine stimulation/ lesion sites. Lesions were primarily localized in regions corresponding to stereotaxic rostrocaudal coordinates of Posterior 3-4 (e.g. Cat #1, left and right). The most caudal lesions were in regions corresponding to Posterior 6-6.5 (e.g Cat #6, right).

LEFT LESION   RIGHT LESION

CAT #   1   2   3   1   2   3

CAT #   4   5   6   4   5   6

CAT #   7   8   9*   7   8*   9

CAT #   10   10

4 mm
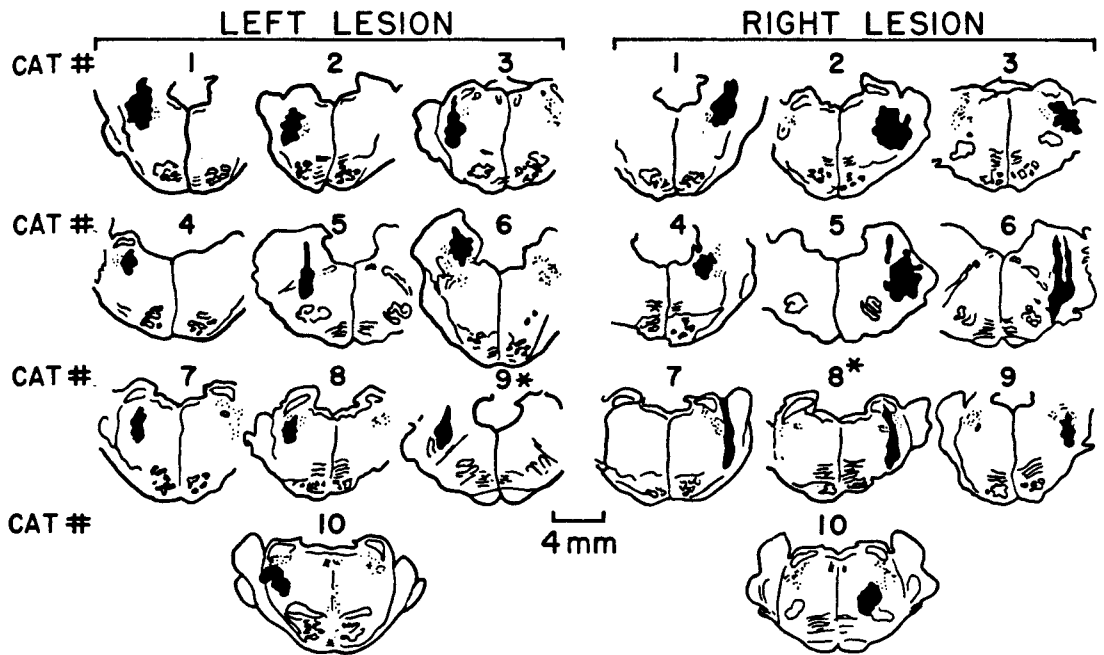
to stimulation. In all other cases, stimulation of parabrachial regions indicated by the lesions evoked sympathetic responses.

Bilateral parabrachial area lesions altered respiratory patterns in the 11 cats. Phrenic discharges became infrequent (3 respiratory cycles/15 minutes) in Cat #1 and phrenic activity was eliminated by lesions in Cat #6. Regularly occurring phrenic discharges were prolonged (i.e. apneusis occurred) in the other nine cats after bilateral parabrachial lesions. The duration of inspiration was significantly ($P < 0.05$) increased from 2.7 ± 0.2 seconds to 10.7 ± 2.6 seconds after the lesions.

Control blood pressures of 135 ± 5 mmHg were not significantly ($P > 0.05$) different from values of 133 ± 5 mmHg after pontine lesions. Blood pressure increases of 72 ± 6 mmHg during bilateral carotid occlusion were also not significantly ($P > 0.05$) different from 66 ± 4 mmHg increases after pontine lesions.

Oscillograph recordings in Figure 6-7 illustrate respiratory modulation of sympathetic activity before and after pontine lesions in Cat #5. In this example, the predominant respiratory influence on sympathetic activity during control recordings was post-inspiratory inhibition. Enhancement of sympathetic activity during inspiration was apparent for some breaths, but largely masked by high levels

Figure 6-7

The oscillograph tracings from Cat #5 illustrate (Top to Bottom) time, integrated inferior cardiac sympathetic activity, integrated phrenic activity, inferior cardiac sympathetic activity, phrenic nerve activity, blood pressure, and intratracheal pressure before and after pontine lesions. After pontine lesions, blood pressure waves and sympathetic activity followed the apneustic phrenic activity pattern. An additional faster sympathetic rhythm was superimposed on the apneustic pattern of sympathetic activity.

CONTROL

AFTER PONTINE
LESIONS

TIME MARKER
(sec)
INTEG.
SYMP. N.

INTEG.
PHRENIC N.

INF. CARD. 1
SYMP. N. mV

PHRENIC N. 1
mV

BP 200
(mm Hg) 100
0

ITP 5
(mm Hg) 0
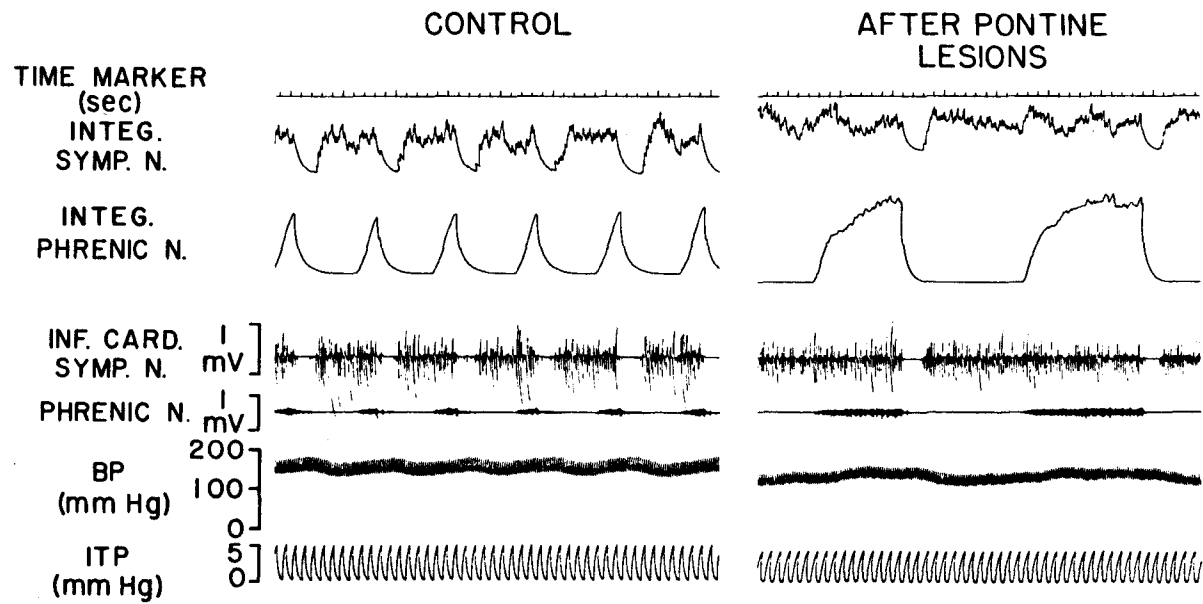
of sympathetic activity during the expiratory phase. Blood pressure waves in the control recording coincided with respiratory-related sympathetic rhythms which were independent from the lung inflations indicated by intratracheal pressure recordings. After pontine lesions, inspiratory and expiratory durations were more prolonged and variable (Fig. 6-7). Sympathetic activity and blood pressure oscillations followed apneustic patterns of phrenic activity. Sympathetic activity was predominantly enhanced at the onset and inhibited at the termination of the apneustic phrenic activity.

Figure 6-8 illustrates typical computer-summated sympathetic and phrenic nerve activities before and after pontine lesions (Cat #4). The control computer summation verified that slow sympathetic rhythms were respiratory-related prior to the lesions. Similar control computer summations were obtained for all cats used in the study. After pontine lesions, computer summation trace A. indicated a link between the start of inspiration and sympathetic activity. Computer summation B. indicated a link between the end of inspiration and sympathetic activity. Similar computer summations obtained for all cats after pontine lesions verified that sympathetic activity was enhanced at the onset and inhibited at the termination of phrenic activity.

Figure 6-8

Respiration triggered computer summation from Cat #4 illustrates respiratory related sympathetic activity before and after pontine lesions. After pontine lesions leading to apneusis, sympathetic activity was enhanced with the start of inspiration (A.) and inhibited at the end of inspiration (B.), indicated by the vertical arrows.

CONTROL   AFTER   PONTINE   LESIONS

| EXP. | INSP. | | INSP. | EXP. |

INTEG.
SYMP. N.
ACTIVITY

100
mV

20 SWEEPS   A. START   B. END
                       INSP.   INSP.

INTEG.
PHRENIC N.
ACTIVITY

5 sec
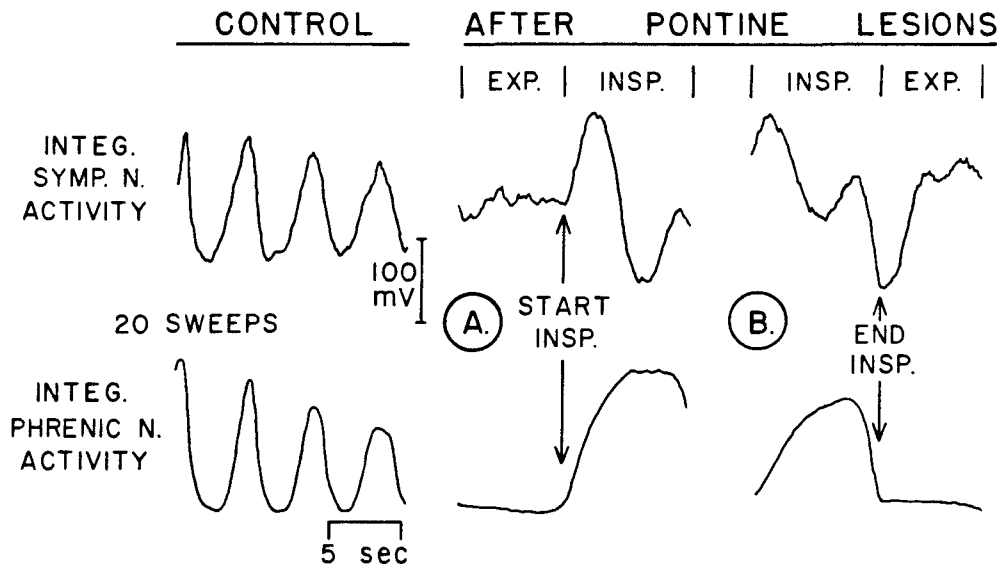
Additional rhythms were superimposed on apneustic patterns of sympathetic activity after pontine lesions in five of the eleven cats. Such superimposed sympathetic oscillations after pontine lesions were apparent in the oscillograph records from Cat #5 (Fig. 6-7) and Cat #11 (Fig. 6-9). Fig. 6-9 illustrates the most marked example of independent sympathetic rhythms observed after pontine lesions. Although sympathetic activity was enhanced at the onset of phrenic activity, sympathetic oscillations unrelated to phrenic activity continued into the long expiratory phase resulting after pontine lesions. When present, independent sympathetic oscillations after pontine lesions more frequently resembled the less marked oscillations superimposed on the apneustic activity pattern in Fig. 6-7. Subtle elevations of blood pressure waves during sympathetic inhibitions (negative deflection of integrated sympathetic activity) unrelated to respiration suggest baroreceptor-mediated inhibition of sympathetic activity.

Spectral analysis of sympathetic activity from Cat #11 (Fig. 6-10, Top) indicated that the independent sympathetic oscillations after pontine lesions ("SLOW PEAK") were the same frequency as the control respiratory oscillations in sympathetic activity ("SLOW PEAK (RESP)"). Spectral analysis of sympathetic nerve frequencies before

Figure 6-9

The oscillograph tracings of Cat #11 illustrate (top to
bottom) time, integrated inferior cardiac sympathetic
activity, integrated phrenic activity, inferior cardiac
sympathetic activity, phrenic nerve activity, blood
pressure, and intratracheal pressure before and after
pontine lesions. This recording illustrates an independent
sympathetic rhythm unrelated to phrenic nerve activity after
the pontine lesions indicated (far right). Inhibitions of
sympathetic activity (indicated by downward deflection of
integrated sympathetic activity) coinciding with subtle
increases in blood pressure suggested that the independent
oscillations were mediated by baroreceptors.

CONTROL AFTER PONTINE LESIONS PONTINE LESION SITES

TIME MARKER (sec)

INTEG. SYMP. N.

INTEG. PHRENIC N.

INF. CARD. SYMP. N.   250 μV

PHRENIC N.   200 μV

BP (mm Hg)   200 100 0

ITP (mm Hg)   5 0

5mm

CAT II
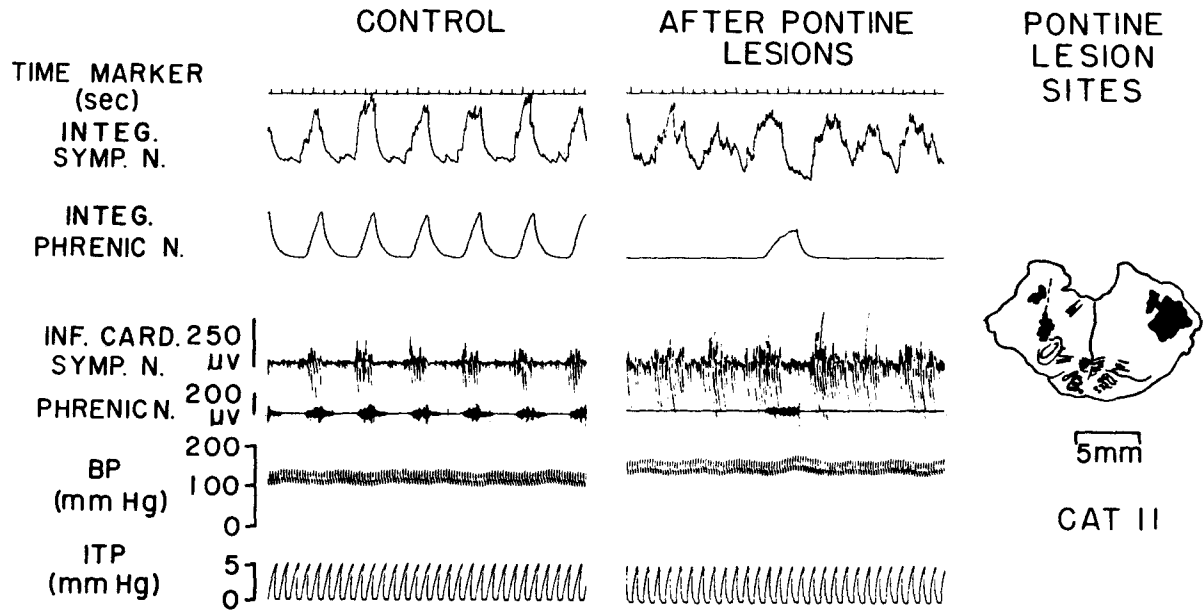
Figure 6-10

Spectral amplitude (ordinate) of sympathetic nerve
frequencies (abscissa) from two representative cats before
and after pontine lesions. The presence (top) and absence
(bottom) of slow spectral peaks ("SLOW PEAK") after lesions
are illustrated. The presence of a "SLOW PEAK" after pontine
lesions (top), illustrated for Cat #11, indicated that the
independent sympathetic oscillations depicted in Fig. 9 were
the same frequency as the control respiratory oscillations
in sympathetic activity ("SLOW PEAK (RESP)").
Alternatively, six of the eleven cats did not exhibit slow
spectral peaks after pontine lesions, as indicated for Cat
#7 (bottom).
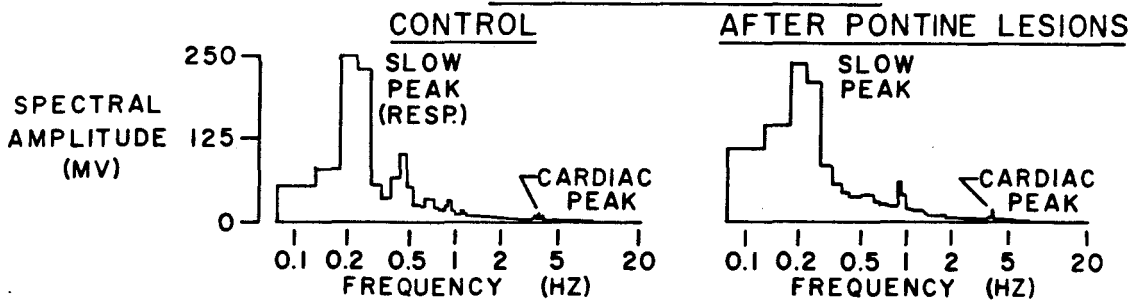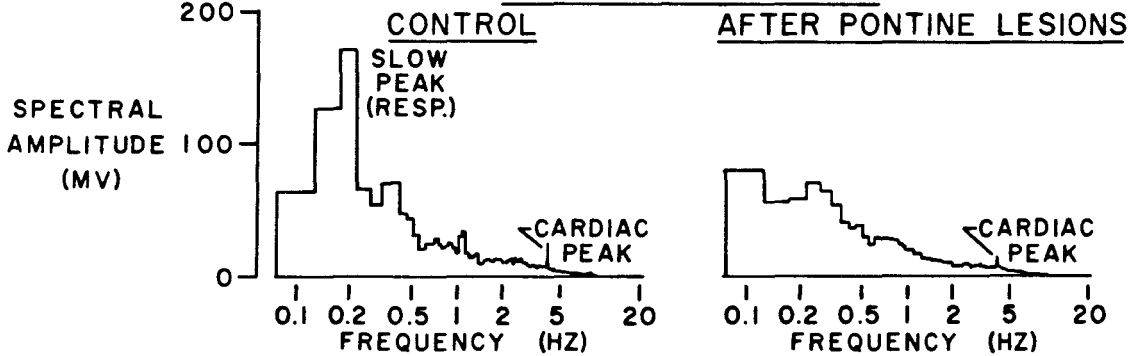
and after pontine lesions indicated that the "SLOW PEAK" was present when independent sympathetic rhythms were observed after pontine lesions in five out of the eleven cats. The "SLOW PEAK" was absent after pontine lesions in the other 6 cats, as indicated for Cat #7 at the bottom of Fig. 6-10.

After pontine lesions, prolonged and more variable inspiratory and expiratory times facilitated separate evaluation of inspiratory onset, inspiratory termination and possible baroreceptor-mediated influences on sympathetic rhythmicity (Figs. 6-9 and 6-11). In Fig. 6-11, enhanced sympathetic activity occurring with the onset of phrenic activity (after pontine lesions) resulted in elevation of blood pressure slightly preceding subsequent inhibition of sympathetic activity. Blood pressure elevations slightly preceding sympathetic inhibition and intact carotid sinus baroreceptors suggest that baroreceptor-mediated inhibition of sympathetic activity during the centrally (respiration) induced blood pressure elevation may best explain the pattern of sympathetic activity after pontine lesions in Cat #4. During the two longer breaths after pontine lesions in Fig. 6-11, the baroreceptor-mediated inhibition of sympathetic activity occurred before a second inhibition coinciding with the termination of inspiration. However, during the shorter breaths after pontine lesions (Figs. 6-9 and 6-11), only the baroreceptor reflex inhibition of

Figure 6-11

Oscillograph tracings (same abbreviations as Figs. 7 and 9) of interactions between respiratory and presumed baroreceptor influences on sympathetic rhythmicity which were easily visualized after pontine lesions disrupted the control respiratory pattern in Cat #4. After pontine lesions, the burst of sympathetic activity (upward deflection of integrated sympathetic activity) coinciding with the onset of phrenic activity was followed by an increase in blood pressure and simultaneous inhibition of sympathetic activity. Decreased sympathetic activity coinciding the with blood pressure elevation suggested carotid sinus baroceptor-mediated inhibition of sympathetic activity. Inhibition of sympathetic activity at the termination of phrenic activity was masked by the baroreceptor inhibition during the shorter apneustic breath, but was apparent at the termination of the longer two apneustic breaths after pontine lesions.

CONTROL

AFTER PONTINE
LESIONS

TIME MARKER
(sec)
INTEG.
SYMP. N.

INTEG.
PHRENIC N.

INF. CARD.   1
SYMP. N.   mV

PHRENIC N.   4
mV

BP   200
100
(mm Hg)   0

ITP   5
(mm Hg)   0
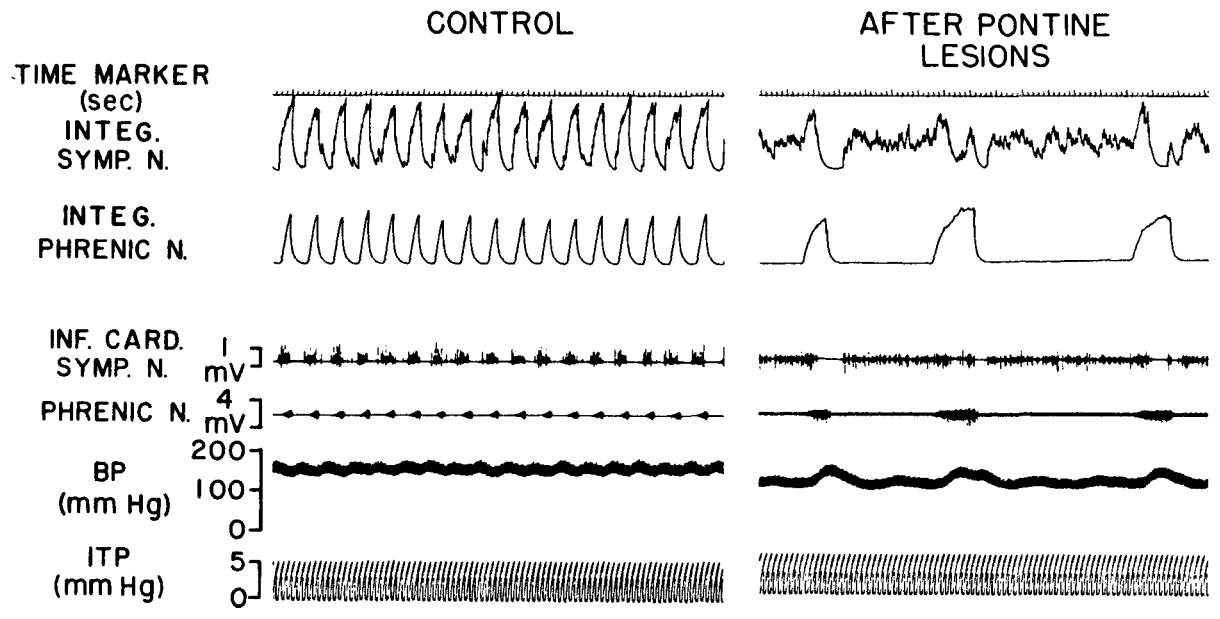
sympathetic activity was apparent.

D. DISCUSSION

Pontine parabrachial regions influence respiratory and cardiovascular control systems. In the present study dorsolateral regions of the rostral pons including medial parabrachial nuclei (PBM), Kolliker-Fuse nuclei (KF), brachium conjunctivum (BC), paralemniscal tegmental fields (FTP) and lateral tegmental fields (FTL) were designated as parabrachial areas. Those regions, which also correspond to the "pneumotaxic center" (26), were bilaterally stimulated and then lesioned in this study (Fig. 6-6) to further investigate pontine parabrachial region influences on sympathetic activity.

Consistent with findings of Cohen (39), parabrachial stimulations in the present experiment elicited excitation, inhibition, or no effect on phrenic discharges. Cohen (39) indicated that inspiratory-facilatory effects were elicited by stimulations in the region of PBM nuclei and expiratory-facilatory effects occurred with stimulations in more ventral paralemniscal tegmental (FTP) and lateral tegmental fields (FTL). Stimulations located between the facilatory and inhibitory regions of the pneumotaxic area evoked no response, indicating a transition zone. Projections extending from PBM nuclei to medullary respiratory neurons (11, 32, 51, 159) and directly to

phrenic motor neurons (162) provide an anatomical basis for pBM region influences on respiration.

The preliminary nature of previous observations concerning PBM region influences on sympathetic activity (71) warranted the current investigation. In their previous study involving stimulation of the medulla, Gootman and Cohen (71) briefly stated that single shock stimulations of some extramedullary sites, including "pneumotaxic regions" presumed to be PBM nuclei (2 cats), evoked splanchnic activity. More recently, Mraovitch, Kumada, and Reis (144) reported cardiovascular pressor responses elicited by PBM stimulation. Previous anatomical studies (110, 138) have indicated direct projections from PBM nuclei to regions of sympathetic preganglionic cell bodies in the intermediolateral cell column (IML). The present study supported results suggesting direct projections of PBM nuclei to sympathetic preganglionic nerves. However, stimulation of rostral pontine pathways and structures other than regions of PBM nuclei also elicited identical sympathetic response patterns. More specifically, Figure 6-6 illustrates that sympathetic responses were also evoked by stimulation of FTL and FTP regions with known anatomical projections to the IML (138). Parabrachial pathways (32, 129) and pathways from the hypothalamus which course through parabrachial regions of the dorsolateral rostral pons (35,

171) were also probably stimulated in the present and previous studies. Procedures such as glutamate application for stimulation (109) and kainic acid application for lesions (45) are necessary to state unequivocally that stimulation or lesions of CNS regions exclusively affect cell bodies and not fibers of passage. The present results suggest that stimulation of various structures in the dorsolateral rostral pons including PBM, FTL, FTP, and KF nuclei, in addition to hypothalamic and parabrachial descending pathways, evoked sympathetic responses.

Stimulation of ipsi- or contralateral parabrachial regions in the present study consistently elicited marked activation of inferior cardiac sympathetic activity followed by an inhibitory period, irrespective of the phase of respiration (Figs. 6-3, 6-4, and 6-5). In the present study, stimulus pulses of 0.5 msec duration and typical currents of 50 uA (10-100 uA range) allowed fairly localized stimulations. Amplitudes of the evoked responses and durations of post-stimulus inhibitory periods were proportional to stimulus currents. As increased stimulus currents activated a larger number of fibers, increased amplitudes of evoked sympathetic responses and longer periods of post-excitatory inhibition were probably due to spatial summation of more descending fiber inputs to sympathetic nerves. The pattern of evoked activation

followed by a period of inhibition was similar to that after medullary stimulation (71), and after stimulation of somatic afferent nerves evoking somatosympathetic reflexes (90). The mechanism behind the post-excitatory depression of sympathetic activity, also called the "silent period" (152), is not yet understood. Current theories suggest that the silent period is due to either a post-excitatory refractory period or to simultaneous stimulation of independent inhibitory pathways to sympathetic nerves.

The nature of the respiratory cycle influences during PBM region stimulations in the present study (Figs. 6-3, 6-4, and 6-5) indicated that evoked sympathetic responses are not gated through medullary respiratory neurons which receive afferent inputs from parabrachial areas (11, 32, 51, 159). Instead, parabrachial region stimulation may simultaneously activate separate respiratory and autonomic pathways. The slightly larger evoked sympathetic areas (above background activity) during expiration were attributed to decreased background sympathetic activity since absolute areas of the sympathetic responses (as measured from a baseline of zero sympathetic activity) were unaffected by the phase of the respiratory cycle. The subtle respiratory cycle influences on evoked responses indicated that PBM stimulation did not always mask ordinarily occurring respiratory influences on sympathetic

activity. These results support the contention that sympathetic activity patterns are derived from parallel inputs which have variable influences dependent on physiological conditions, i.e. strong extramedullary influences may overide medullary respiratory influences on sympathetic activity under certain conditions.

Lesions of parabrachial regions, which cause apneustic respiratory patterns in vagotomized cats (26, 27, 64, 176), also influenced sympathetic activity patterns in the present study. Sympathetic oscillations and blood pressure waves corresponded to the apneustic pattern of phrenic activity. Computer summation techniques verified that sympathetic activity was enhanced at the onset and inhibited at the termination of phrenic activity during apneusis (Fig. 6-8).

The appearance of additional sympathetic oscillations unrelated to phrenic activity after pontine lesions in five of the eleven cats may be attributed to pressoreceptor-autonomic oscillations (78). As in Fig. 6-9, for example, infrequent bursts of central respiratory input to sympathetic activity occurring after pontine lesions were adequate to cause subsequent blood pressure increases coinciding with baroreceptor-mediated negative feedback inhibition of sympathetic activity. Sympathetic inhibitions (negative deflections of integrated sympathetic nerve

activity) coinciding with elevations of blood pressure were attributed to baroreceptor inhibition of sympathetic activity since carotid sinus nerves and bilateral carotid occlusion responses were intact after pontine lesions. Because of the delay time inherent to baroreceptor feedback inhibition, such a blood pressure-sympathetic oscillation could help initiate or regenerate continuing oscillations in blood pressure and sympathetic activity to perpetuate a sympathetic rhythm apparently unrelated to respiratory oscillations. The occurrence of independent sympathetic oscillations with frequencies close to control respiratory frequencies (Fig. 6-10, Top) suggests that pressoreceptor-autonomic oscillations may potentiate respiratory influences on sympathetic activity during certain control conditions.

Baroreceptor-mediated inhibition of sympathetic activity coinciding with blood pressure elevations at the onset of inspiration may explain apparent phase changes between sympathetic and phrenic activities. As illustrated by Figs. 6-9 and 6-11 (after pontine lesions), inspiration-induced sympathetic activation was sufficient to increase blood pressure by 15-30 mmHG, causing subsequent reflex inhibition of sympathetic activity. Longer inspiratory durations after pontine lesions facilitated independent assessments of inhibitions resulting from

presumed baroreceptor reflex effects during inspiration and later occurring inhibitions coinciding with inspiratory termination (Fig. 6-11). During the shorter breaths in Fig. 6-9 and Fig. 6-11 (after pontine lesions), baroreceptor reflex inhibition during inspiration masked the inspiratory termination effects on sympathetic activity since both inhibitory influences overlapped in time. Depending on baroreceptor sensitivity and respiratory rate during control conditions, baroreceptor influences may potentiate the respiratory modulation of sympathetic activity or may alter apparent phase relations of sympathetic and phrenic activities by the same mechanism.

In conclusion, the present study indicated that parabrachial regions have bilateral influences on sympathetic nerve activity. Brain stem and/or spinal levels of intermediate synapses and crossed pathways were not addressed in the present study. The lack of respiratory cycle influences on evoked sympathetic activity suggested that parabrachial influences on sympathetic activity are independent from respiratory influences which also originate in parabrachial regions. Apneustic breathing patterns, resulting from the bilateral parabrachial lesions, influenced sympathetic activity primarily during the onset and termination of inspiration. Appearance of apparently independent sympathetic rhythms unrelated to the apneustic

phrenic pattern after pontine lesions may be attributed to pressoreceptor-autonomic oscillations. It was suggested that such pressoreceptor-autonomic oscillations may potentiate respiratory influences on sympathetic activity and/or alter phase relations between phrenic and sympathetic activities during normal breathing.

CHAPTER VII

EFFECTS OF MIDLINE MEDULLARY LESIONS ON THE
RESPIRATORY MODULATION OF SYMPATHETIC ACTIVITY

A. INTRODUCTION

In contrast to the bilateral bulbospinal projections to sympathetic preganglionic cell bodies; pathways to phrenic motor nuclei primarily arise from cell groups located in the contralateral medulla (56, 133, 134, 141). As described in detail in numerous reviews of central respiratory control (40, 95, 135, 189), the ventrolateral nucleus tractus solitarius (nTS) constitutes the dorsal respiratory group. Loewy and Burton (117) have demonstrated bilateral nTS projections to the C4-C5 motor horn containing phrenic motor neurons and the thoracic intermediolateral gray where sympathetic preganglionic cell bodies are located. A common respiratory pathway of contralateral medullary origin may innervate both sympathetic and phrenic nerves.

The possibility that midline connections influence medullary respiratory cell oscillations has not been

addressed until recently. Gromysz and Karczewski (76) reported that midline lesions in the cat medulla result in phrenic nerve quiescence during eupnea presumably due to interruption of pathways descending from brain stem respiratory neurons to the phrenic motor nerves. St. John (175) did a midline lesion experiment while recording right and left laryngeal nerves which have cell bodies located in the ipsilateral nucleus ambiguus and retrofacial nucleus (63, 97). St. John observed that respiratory oscillations in right and left halves of the brain became dissociated after midline medullary lesions. In addition, laryngeal nerve signals of some cats were attenuated or lost after the midline lesions, suggesting an overall depression of respiratory activity. Bainton and Kirkwood (10) similarly reported increased CO_2 thresholds for excitation of medullary inspiratory neurons after midline medullary lesions. This is consistent with current evidence suggesting that crossed brain stem pathways may be involved in respiratory rhythm generation (32, 96, 115, 136).

The above evidence indicates that loss of phrenic nerve activity after midline medullary lesions could be due to cutting either crossing bulbospinal or intrinsic brain stem pathways. The purpose of the present study was to determine effects of midline medullary lesions on the respiratory modulation of sympathetic nerve activity. Left

inferior cardiac and phrenic nerves were recorded to monitor sympathetic and respiratory activities, respectively. Respiratory modulation of sympathetic nerve activity was assessed using respiration triggered computer summation of sympathetic and phrenic nerve activities. Spectral analysis was also used to determine spectral frequencies of slow waves in sympathetic nerve activity before and after midline lesions. Left laryngeal nerves or brain stem dorsal respiratory group cells were extracellularly recorded in some sections of the study to monitor ipsilateral brain stem respiratory activity. Blood pressure responses to bilateral carotid occlusion tests were measured to determine the effects of midline lesions on baroreceptor reflexes, which are mediated by the nTS (93, 114, 150, 170). Supramedullary connections to sympathetic nerves were tested by stimulation of ipsilateral pontine parabrachial areas before and after midline lesions. ECG triggered computer summation was used to assess cardiac-related sympathetic nerve activity in some animals. Pontine stimulation sites, brain stem respiratory unit locations and midline lesions were histologically verified.

B. METHODS

1. General Preparation

Twenty-four cats were anesthetized with chloroform followed by intravenous infusion of alpha-chloralose (40-60 mg/kg). Femoral artery catheters were inserted for blood pressure, (Statham P23Db pressure transducer) and pH, pO_2, and pCO_2 measurements (Radiometer-Copenhagen BMS3-C Blood Microsystem). After tracheotomy, end-expiratory $\%CO_2$ was continuously monitored (Beckman LB1 analyzer). Positive pressure artificial ventilation was begun after neuromuscular blockade with continuous succinyl choline infusion (6 mg/kg/hr). A cannula was inserted into the trachea for measurement of intratracheal pressure (Statham P23Db pressure transducer) as an indicator of ventilator activity. Cervical vagi and aortic depressor nerves were cut to eliminate vagal stretch receptor and aortic baro- and chemoreceptor influences on sympathetic activity. When indicated, blood pressure, pH and/or blood gases were adjusted to normal with dextran, 8.4% sodium bicarbonate infusions or adjustment of ventilator rate and pressure. Rectal temperature was maintained at 38 $\pm$ 1 C with a servo-regulated heating pad.

Each cat was secured in a stereotaxic head frame

(David Kopf Instruments). The pelvic iliac crests and a thoracic spine were clamped to a hanging frame to minimize ventilator induced movement artifacts. The dorsal surface of the medulla was exposed by an occipital craniotomy. Once the dura was cut, the dorsal surface of the medulla was kept moist with warm mineral oil.

2. Experimental Protocols

The twenty-four cats were divided into three experimental groups. Group I, II, and III protocols are diagramatically illustrated in Figs. 7-1, 7-2, and 7-3, respectively.

Group I (Fig. 7-1): Left phrenic and inferior cardiac sympathetic nerves were recorded in the twelve Group I cats. Inflatable occluders (Rhodes Medical Instruments) were placed around common carotid arteries for tests of baroreceptor reflex integrity through the nTS region immediately adjacent to midline lesion locations. Extracellular microelectrodes were placed in the nTS region of the dorsal respiratory group to record respiratory cell activity before and after midline medullary lesions. Respiration (phrenic nerve or medullary respiratory unit) triggered computer summations of sympathetic activity were

Figure 7-1

Diagrammatic illustration of the Group I experimental
protocol as described in the methods.

MIDLINE
LESION

PARABRACHIAL
AREA

NTS
MICRO-
ELECTRODE

EXTERNAL
CAROTID
ARTERY

OCCLUDER

COMMON
CAROTID
ARTERY

PHRENIC
NERVE

INFERIOR
CARDIAC
NERVE
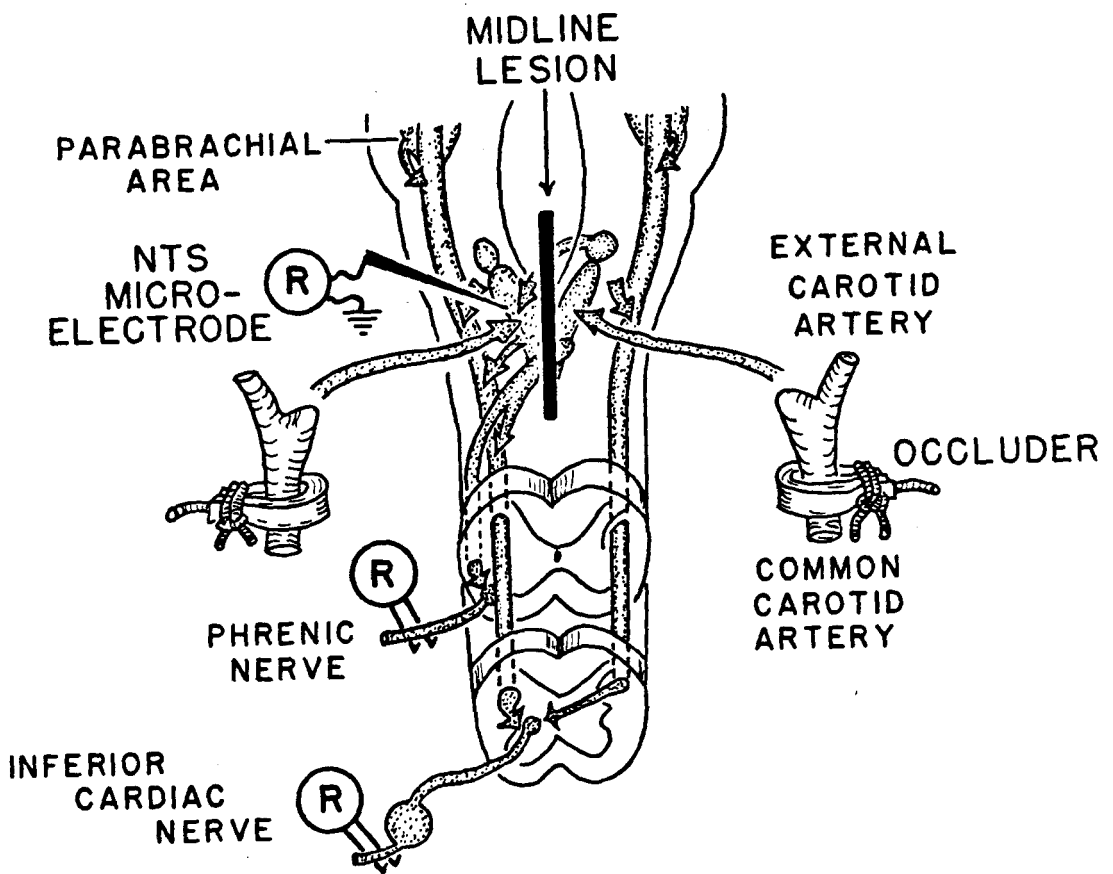
Figure 7-2

Diagrammatic illustration of the Group II experimental protocol as described in the methods.

MIDLINE LESION

PARABRACHIAL AREA

EXTERNAL CAROTID ARTERY

OCCLUDER

COMMON CAROTID ARTERY

PHRENIC NERVE

INFERIOR CARDIAC NERVE
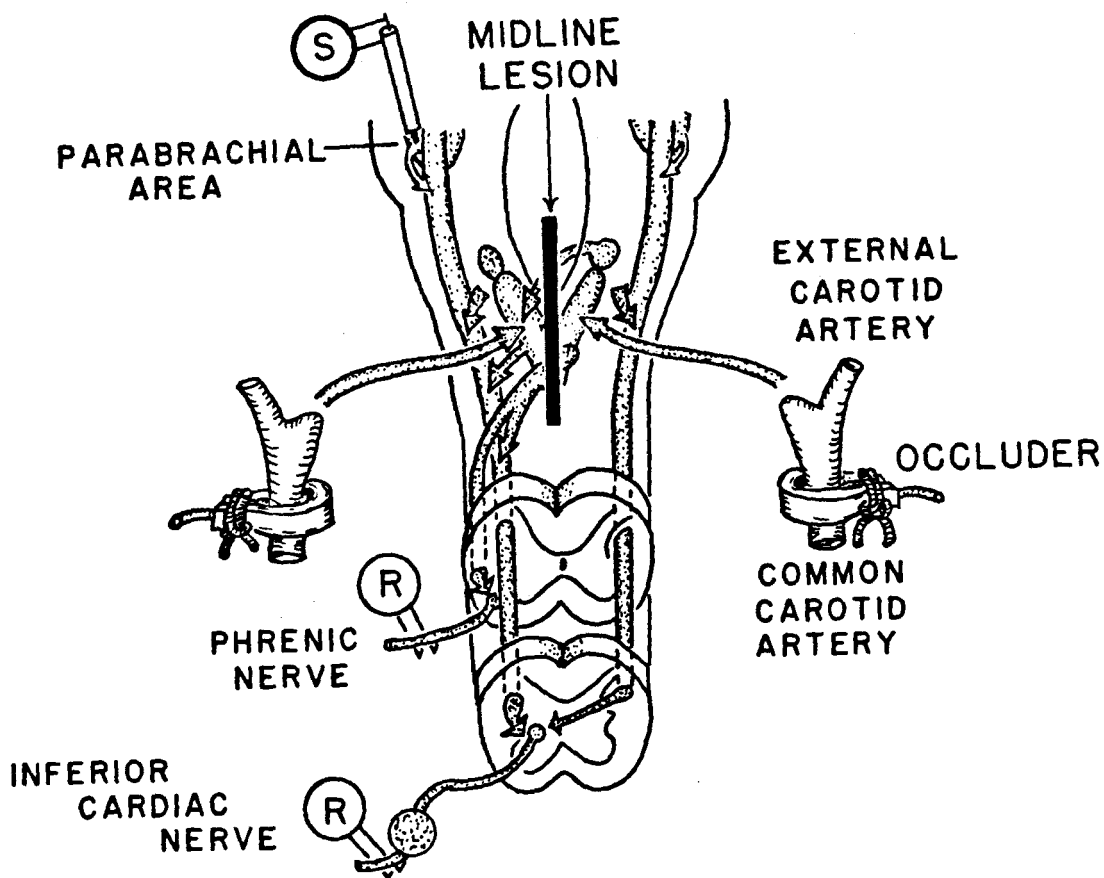
Figure 7-3

Diagrammatic illustration of the Group III experimental protocol as described in the methods.
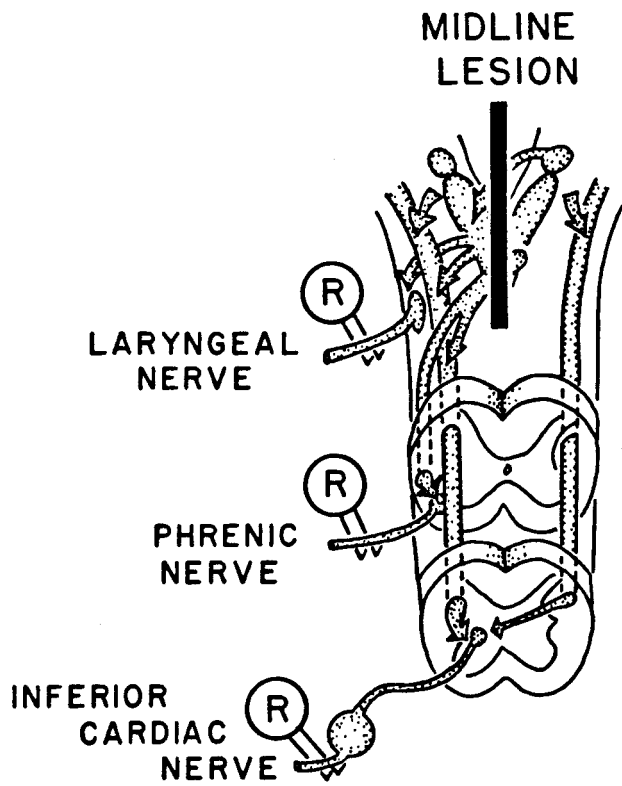
MIDLINE
LESION

LARYNGEAL
NERVE

PHRENIC
NERVE

INFERIOR
CARDIAC
NERVE

compared before and after medullary lesions. Using spectral analysis, sympathetic nerve frequencies from nine of the cats in this group were compared before and after midline lesions.

Group II. (Fig. 7-2): Activities of left inferior cardiac sympathetic and phrenic nerves were compared before and after midline medullary lesions in the eight Group II cats. Inflatable occluders (Rhodes Medical Instruments) were placed on common carotid arteries for bilateral carotid occlusion tests of baroreceptor reflex integrity through the nTS region immediately adjacent to midline lesion locations. Left pontine parabrachial areas were stimulated during inspiration, post-inspiration, expiration, when respiration triggered stimuli were not delivered to the brain and after midline medullary lesions. Stimulation triggered computer summations of evoked sympathetic activity were compared before and after midline medullary lesions to determine if ipsilateral pathways descending from supramedullary locations to sympathetic nerves were affected by the medullary lesions. Using spectral analysis, sympathetic nerve frequencies from four of the cats in this group were compared before and after midline lesions.

Group III (Fig. 7-3): Activities of left inferior cardiac

sympathetic, phrenic, and laryngeal nerves were compared before and after midline medullary lesions in the eight Group III cats. Due to the close proximity of the laryngeal nerve and common carotid artery, inflatable occluders were not placed around the common carotid arteries in these cats. Instead, baroreceptor reflex integrity was assessed using ECG (R-wave) triggered computer summation of sympathetic activity to determine effects of midline medullary lesions on cardiac-related sympathetic activity. Using spectral analysis, sympathetic nerve frequencies were compared before and after midline lesions.

3. Nerve and Electrocardiogram Recordings

A skin and muscle flap extending from the left ear to the second thoracic spine was pulled laterally and attached to a curved horizontal rod to create an oil bath for the nerves being recorded. To isolate the left inferior cardiac sympathetic nerve, the scapula was retracted exposing the ribs. The heads of the first two ribs were removed to expose the stellate ganglion and the ventrocaudally coursing inferior cardiac sympathetic nerve which was cut distally and desheathed in some preparations. Rostrally, the left phrenic nerve was isolated as it exited from the fourth cervical nerve root, cut distally, and

desheathed. In eight Group III cats, left laryngeal nerves were isolated in the cervical region and desheathed for recording.

The nerves were placed on bipolar platinum electrodes for differential recording (Grass P9 amplifiers). The nerve signals were monitored on a storage oscilloscope and photographed at various stages in each experiment. After rectification and leaky integration, (Grass Model 7P3 A Integrator, low pass filter time constant = 0.5 sec.) the signals were displayed on the oscillograph and stored on magnetic tape (Precision Instruments model 6200 tape recorder) for later analysis.

Lead II electrocardiogram activity was recorded in the Group III cats.

4. Lesions

Midline medullary lesions were made with fine dissecting scissors, and a blunt spatula. Lesions were begun either slightly rostral or caudal to the obex and then extended by millimeter increments until the phrenic nerve ceased firing. To avoid cutting the basilar artery, the deeper extensions of the lesions were made with a blunt spatula. When swelling or excessive bleeding occurred following the brain stem lesion, the experiment was

discontinued and the results not used. Lesions were extended until phrenic nerve activity could not be stimulated by chemoreceptor input induced by transiently discontinuing artificial ventilation for 10-30 seconds. Following the lesions, respiratory rhythmicity of sympathetic nerve activity was analyzed (computer summation and spectral analysis methods described below) and compared to control activity. In eight Group III cats, laryngeal nerve activity was also monitored and assessed before and after midline medullary lesions.

5. Ipsilateral Pontine Stimulation

Stereotaxically placed (posterior 3.5, vertical -4.0, mediolateral +4.5) bipolar concentric electrodes were used to stimulate ipsilateral pontine parabrachial areas in nine Group II cats during inspiration, post-inspiration, and expiration phases of the respiratory cycle during the control stage. Amplified, integrated phrenic nerve activity triggered a level detector and variable delay circuit which then triggered the stimulator to deliver impulses (300 impulses/sec, 20 msec train duration, 0.5 msec/stim, 10-100 uA) through a stimulus isolation unit and constant current device to the ipsilateral parabrachial area of the pons during different phases of the respiratory cycle. Following

midline medullary lesions, ipsilateral parabrachial regions were stimulated in eight of the cats using the same stimulation parameters. Since phrenic nerve activity was not present to trigger the stimulus trains after midline lesions, the trains were delivered at a set frequency ranging from 0.2 to 0.4 trains/sec. Stimulation sites were then marked by passing direct current (two milliamps for ten seconds) through the stimulating electrode. Stimulus triggered, computer summed (Nuclear Chicago) areas of amplified, integrated, sympathetic activity (forty sweeps) during inspiration, post-inspiration, expiration, and after midline medullary lesions were measured with a graphics tablet (Bausch and Lomb) connected to a digital computer (Apple II Plus). The areas were statistically compared using analysis of variance followed by tests for least significant differences (69, 163). Significance was defined at P < 0.05.

6. Respiratory Unit Recordings

In twelve control cats and seven of those cats after midline lesions (Group I), brain stem respiratory units were extracellularly recorded from the dorsal respiratory group (nucleus tractus solitarius) using tungsten microelectrodes with tip resistances of two to three megohms (Frederick

Haer). Brain stem respiratory unit signals were differentially amplified (Grass P9 amplifier) and then passed to a window device discriminating the signal from background noise. The spike output of the window device was used to generate histograms of brain stem respiratory unit activity. The spike output was additionally passed through a leaky integrator (Grass Model 7P3 A Integrator with low pass filter time constant = 0.5 sec.). The integrated spike output and histograms were displayed on the oscillograph and stored on a tape recorder for later data quantitation (see below). The location of one of the respiratory units in each experiment was marked by passing a 1 mA direct current through the recording electrode for 2-10 seconds. Locations of other recorded units were determined using relative coordinates.

7. Spectral Analysis

Spectral analysis (Rockland Real-Time Spectrum Analyzer FFT 512/S) was used to determine the effect of midline medullary lesions on the slow frequency characteristics of sympathetic nerve activity (15 cats). Prior to spectral analysis, the sympathetic nerve signals were low-pass filtered (Grass Integrator TC = 0.5 sec) to facilitate assessment of the slow frequency components due

to rhythmic bursts of sympathetic activity coinciding with the respiratory frequency ("Respiratory Peaks"). Amplitudes (millivolts) of control respiratory peaks in sympathetic activity were measured and compared with the amplitudes at the same frequency following midline medullary lesions. Paired t tests were used to compare amplitude differences. Significance was defined at $P < 0.05$.

8. Respiration Triggered Computer Summation

Computer summation techniques were used to analyze effects of midline medullary lesions on the respiratory modulation of sympathetic activity when respiratory units and sympathetic activity were simultaneously recorded following midline medullary lesions (five Group I cats). Amplified integrated sympathetic activity (millivolts) was processed using respiration (phrenic nerve or respiratory unit) triggered computer summation (Nuclear Chicago Data Retrieval Computer). Computer summated sympathetic and respiratory (phrenic nerve or respiratory unit) activities were analyzed before and after lesions. Areas of computer summated sympathetic activity were measured using a graphics tablet (Bausch and Lomb) connected to a digital computer (Apple II plus). Net sympathetic inspiratory amplitude (NSIA) was then calculated to quantitate the respiratory

modulation of sympathetic nerve activity (Fig.7-4):

$$NSIA= (Area\ Insp/\ TI) - (Area\ Exp/\ TE)$$

Area Insp= computer-summed area (twenty sweeps) of amplified integrated sympathetic activity during inspiration (millivolt-seconds)

Area Exp= computer-summed area (twenty sweeps) of amplified integrated sympathetic activity during expiration (millivolt-seconds)

TI= duration of inspiration (seconds)

TE= duration of expiration (seconds)

When sympathetic activity has a respiratory related discharge, the derived net sympathetic inspiratory amplitude is a positive value. Net sympathetic inspiratory amplitude approaches zero when phrenic nerve triggered sympathetic activity summates into a straight line, indicating no respiratory modulation. As an alternative to only presenting single cat data, the NSIA analysis procedure was devised as a quantitative means to assess the respiratory modulation of sympathetic activity.

Figure 7-4

Diagrammatic · illustration   of the data analysis method used to quantitate computer summation data.
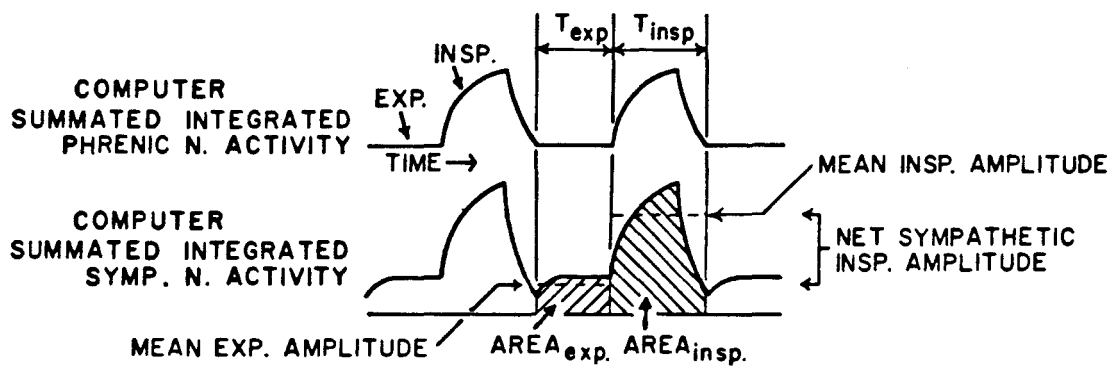
COMPUTER
SUMMATED INTEGRATED
PHRENIC N. ACTIVITY

COMPUTER
SUMMATED INTEGRATED
SYMP. N. ACTIVITY

INSP.

EXP.

TIME →

T_{exp} T_{insp}

MEAN INSP. AMPLITUDE

NET SYMPATHETIC
INSP. AMPLITUDE

MEAN EXP. AMPLITUDE

$AREA_{exp.}$ $AREA_{insp.}$

$$\text{MEAN EXP. AMPLITUDE} = \frac{AREA_{exp.}}{T_{exp.}}$$

$$\text{MEAN INSP. AMPLITUDE} = \frac{AREA_{insp.}}{T_{insp.}}$$

$$\begin{array}{l} \text{NET SYMPATHETIC} \\ \text{INSP. AMPLITUDE} \end{array} = \begin{array}{l} \text{MEAN INSP. AMPLITUDE} - \\ \text{MEAN EXP. AMPLITUDE} \end{array}$$

9. ECG Triggered Computer Summation

Cardiac related sympathetic activity was assessed using ECG (R-wave) triggered computer summation (Nuclear Chicago Data Retrieval Computer) of amplified, integrated sympathetic nerve activity. Areas (millivolt-seconds) of computer summated sympathetic activity (100 sweeps) were measured using a graphics tablet (Bausch and Lomb) connected to a digital computer (Apple II plus). Areas were divided by the duration (seconds) to correct for cardiac cycle time differences between cats. Mean area/time was compared before and after midline medullary lesions using paired t tests (69, 163). Significance was defined at $P < 0.05$.

10. Histology

Brain stems were removed and placed in 10% buffered formalin for at least 3 days. The tissues were then processed and embedded in paraffin. Every fifth ten micron thin serial section was stained for fibers and cell bodies by the Kluver-Barrera method (103). The slides were projected onto paper for tracing of the midline medullary lesions, pontine stimulation sites, and respiratory unit locations.

11. Statistics

In addition to the statistical methods already described, control blood pressure and blood pressure responses to bilateral carotid occlusion tests were statistically compared with values obtained after midline lesions using paired t tests (69, 163). Significance was defined at P < 0.05. Values were expressed as means $\pm$ standard error (SE) of the mean.

C. RESULTS

1. Group I Results

Effects of midline medullary lesions on the respiratory modulation of sympathetic activity, phrenic activity, brain stem respiratory unit activity and blood pressure oscillations are illustrated in Fig. 7-5. The control recordings from Cat #R4 (Fig. 7-5) indicate typical respiratory oscillations of integrated left inferior cardiac sympathetic activity coinciding with left respiratory unit (RESP. UNIT SPIKES) and phrenic activities. Slow respiratory-related waves and faster waves related to artificial ventilation (indicated by the ITP recording) are apparent in the control blood pressure recording. After the midline medullary lesion, phrenic nerve activity ceased and the respiratory modulation of sympathetic activity was no longer apparent. Rhythmic unit activity (RESP UNIT SPIKES) recorded from the dorsal respiratory group (ventrolateral nTS) after midline medullary lesions was unrelated to either artificial ventilation (ITP) or sympathetic activity. Mechanically induced blood pressure waves due to artificial ventilation were still present after the medullary lesions while slower blood pressure waves related to respiration were absent.

Figure 7-5

Polygraph tracings from a Group I cat before and after
midline medullary lesions. Illustrated are (top to bottom)
integrated respiratory unit spikes from the window device,
time (seconds), integrated inferior cardiac sympathetic
activity, integrated phrenic activity, the respiratory unit
spike histogram, respiratory unit spike output from the
window device, blood pressure, and intratracheal pressure.
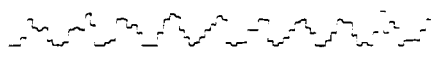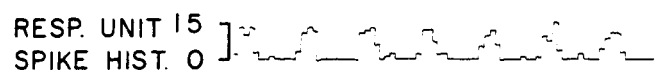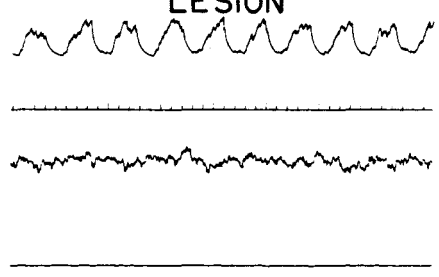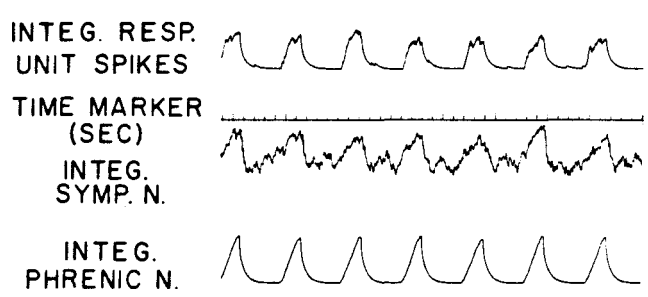
In the absence of phrenic nerve activity following midline medullary lesions, rhythmic unit activity was recorded from the nTS region ipsilateral to the recorded nerves in seven of the twelve Group I cats. Respiratory units recorded before and after medullary lesions in those seven cats were located in the ventrolateral nTS, i.e. dorsal respiratory group (Fig. 7-6). The same respiratory unit was not necessarily recorded before and after the lesions. The control respiratory rate (12.1 $\pm$ 1.6 breaths/min) was not significantly (P > 0.05) different from the rate of rhythmic brain stem unit activity recorded after medullary lesions (16.1 $\pm$ 2.5 breaths/min). However, respiratory units were more difficult to locate after than before midline medullary lesions. Evidence of respiratory unit activity was not found in the other five Group I cats after midline lesions. No systematic differences were noted between midline lesions in cats with respiratory units recorded (Fig. 7-7) as compared to those without respiratory units recorded after lesions (Fig. 7-8). Only Cat #R11 (Fig. 7-8, Section C) appeared to have more extensive nTs region damage.

Respiration (phrenic nerve or brain stem unit) triggered computer summation verified that control oscillations in sympathetic activity were related to respiration and that the respiratory modulation of

Figure 7-6

Locations of respiratory unit activities recorded before and after midline medullary lesions in seven Group I cats. Abbreviations: DMV, dorsal motor nucleus of the vagus; IN, nucleus intercalatus; SL, lateral nucleus of the solitary tract; SM, medial nucleus of the solitary tract; 5st, spinal trigeminal tract; 12N, hypoglossal nucleus; 12n, 12th nerve.

CAT # R1 R2 R3

CAT # R4 R5 R6

CAT # R7

5 mm

Figure 7-7

Dorsal and cross-sectional views of midline medullary lesions in the seven Group I cats in which respiratory units were recorded before and after midline medullary lesions. Dorsal views of the brain stems were drawn after removal from the body and fixation in formalin. The dashed lines (labeled A,B,C, and D) through each dorsal view of the brain stem indicate relative locations of the corresponding cross sections labeled A,B,C, and D.
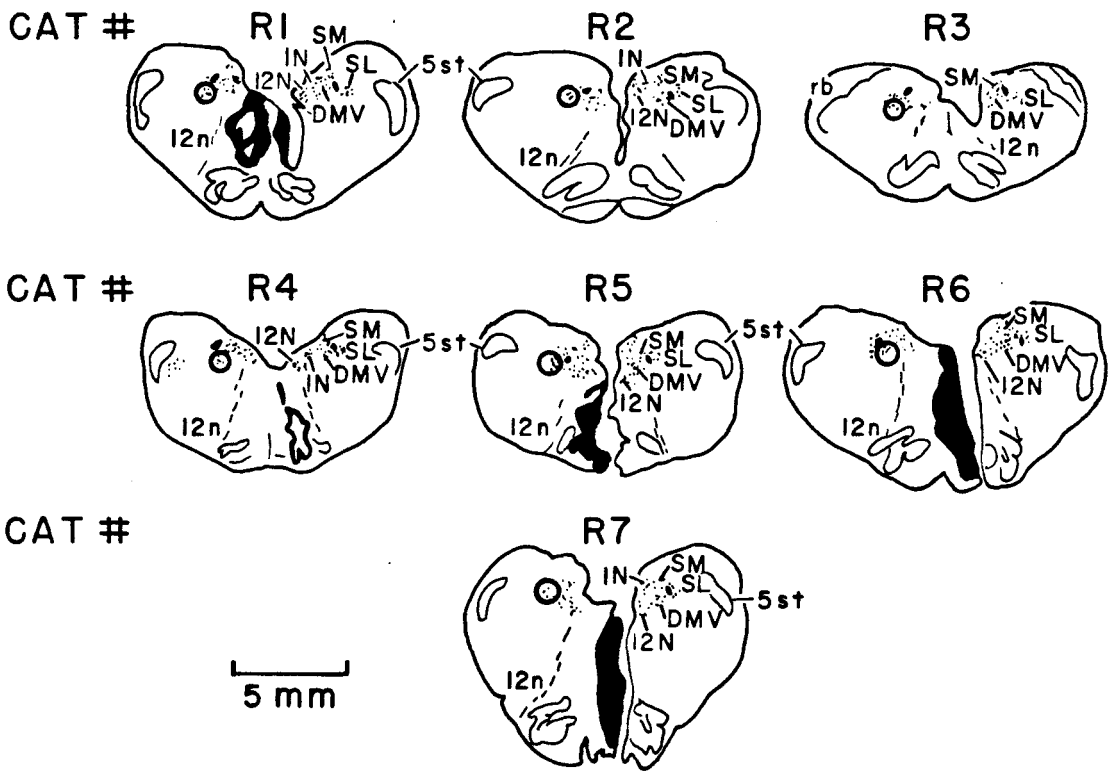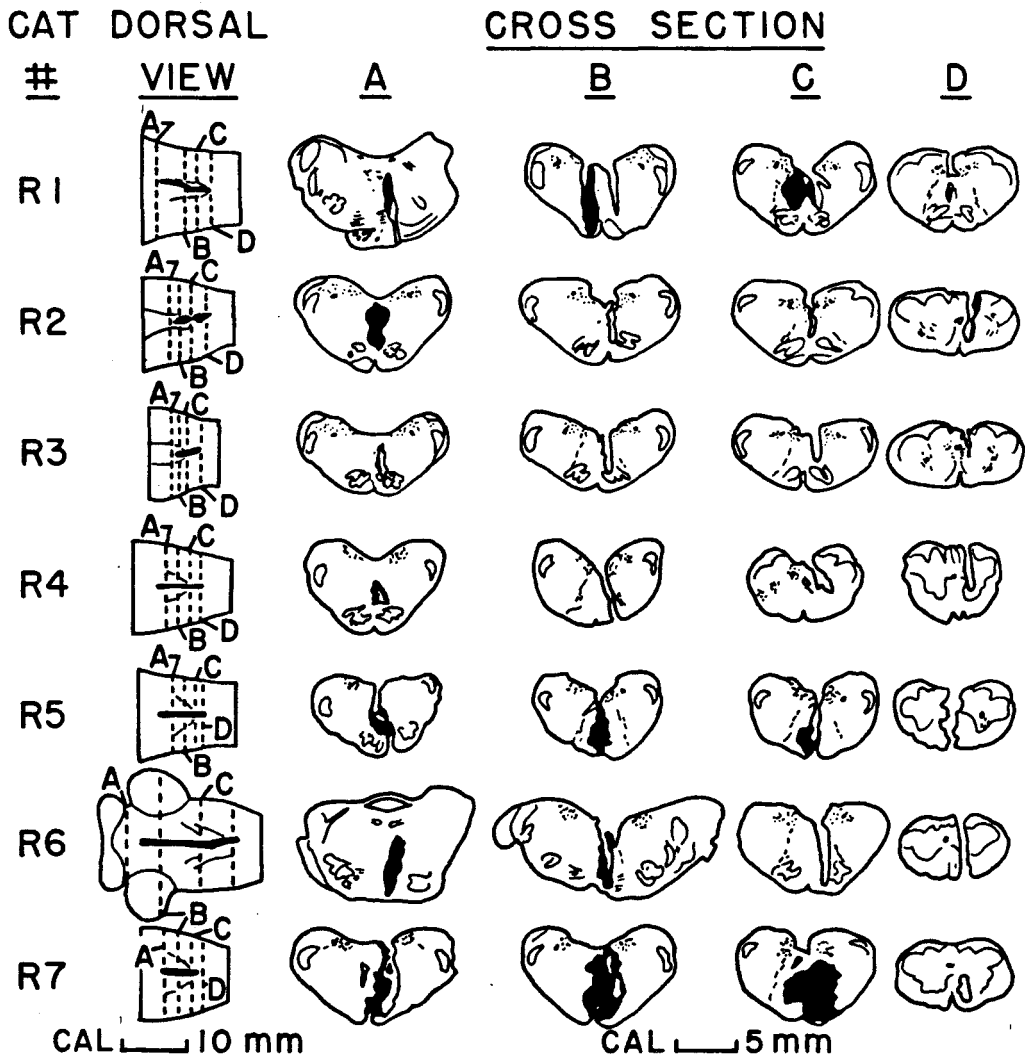
216

UNITS AFTER LESION

Figure 7-8

Dorsal and cross-sectional views of midline medullary lesions in the five Group I cats in which rhythmic units were not found after midline medullary lesions.

NO UNITS AFTER LESION

CAT DORSAL   CROSS SECTION

\#   VIEW   A   B   C   D

R8

R9

R10

R11

R12

CAL └──┘ 10 mm   CAL └──┘ 5 mm
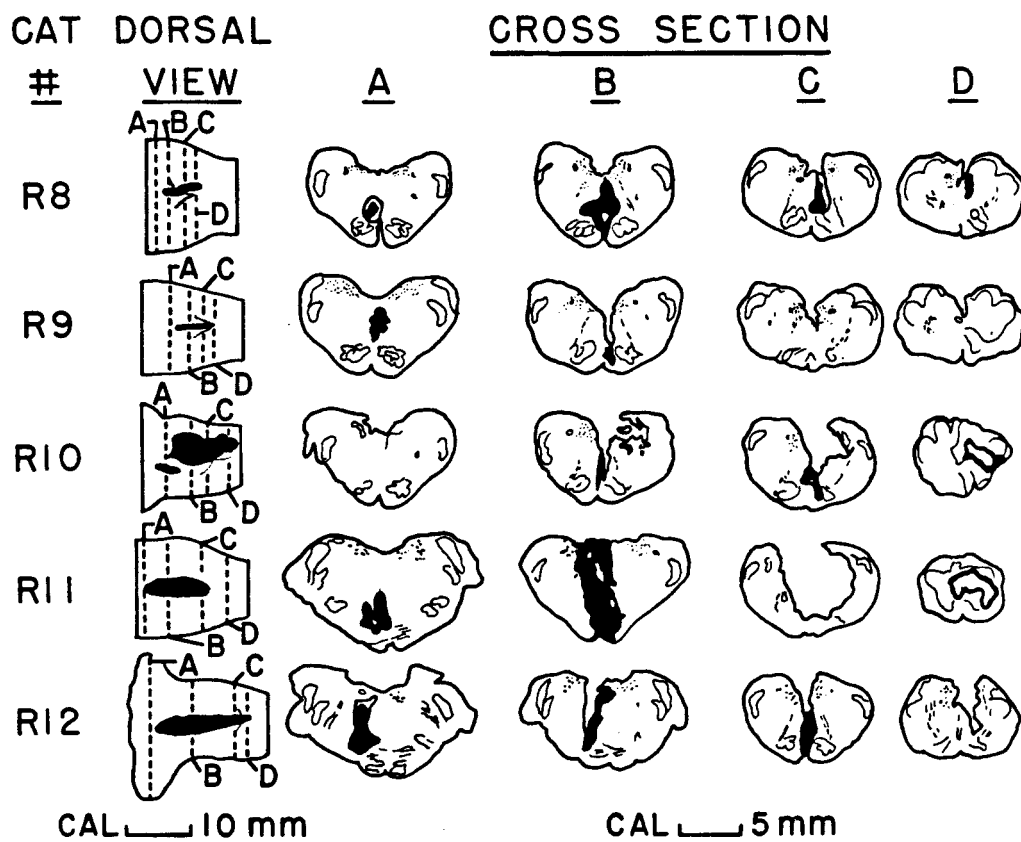
sympathetic activity was absent after midline medullary lesions (Fig. 7-9). Sympathetic activity patterns related to phrenic nerve activity in Cat #R4 were indicated by the control respiration (phrenic nerve) triggered computer summations (Fig. 7-9, left). In contrast, respiration (brain stem unit) triggered computer summation of sympathetic activity into a relatively straight horizontal line indicated absence of respiratory modulation after midline medullary lesions (Fig. 7-9, right). To quantitatively assess the respiratory modulation of sympathetic activity before and after midline medullary lesions, NSIA was calculated using computer summation data obtained from five cats (Cats #R3, #R4, #R5, #R6, and #R7) in which both sympathetic and brain stem respiratory unit activities were recorded (Fig. 7-10, top). NSIA after midline lesions (18 $\pm$ 11 mV) was significantly (P < 0.05) lower than control NSIA (423 $\pm$ 64 mV), substantiating that the respiratory modulation of sympathetic activity was eliminated by midline medullary lesions.

Blood pressure and blood pressure responses to bilateral carotid occlusion were not significantly (P > 0.05) altered by midline medullary lesions in any of the Group I cats. Blood pressure data from the five cats with respiratory units recorded from the nTS before and after midline lesions is illustrated in Fig. 7-10 (bottom).

Figure 7-9

Respiration triggered computer summation (20 sweeps) of integrated sympathetic and respiratory activities from Group I Cat #R4 before and after midline medullary lesions. Respiratory activities used for this analysis were phrenic activity before and brain stem rhythmic unit activity recorded from the dorsal respiratory group after midline medullary lesions.
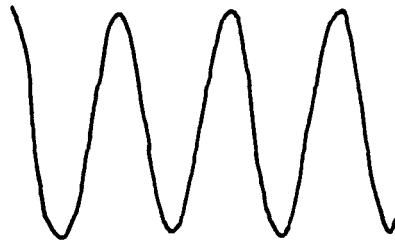
Figure 7-10

NSIA (top), blood pressure (bottom, solid bars, left scale), and blood pressure response to bilateral carotid occlusion (bottom, horizontal bars, right scale) before and after midline medullary lesions. Results were obtained from the five Group I cats in which respiratory unit activity was recorded before and after midline lesions. The asterisk indicates that NSIA was significantly (P < 0.05) decreased after the lesions.
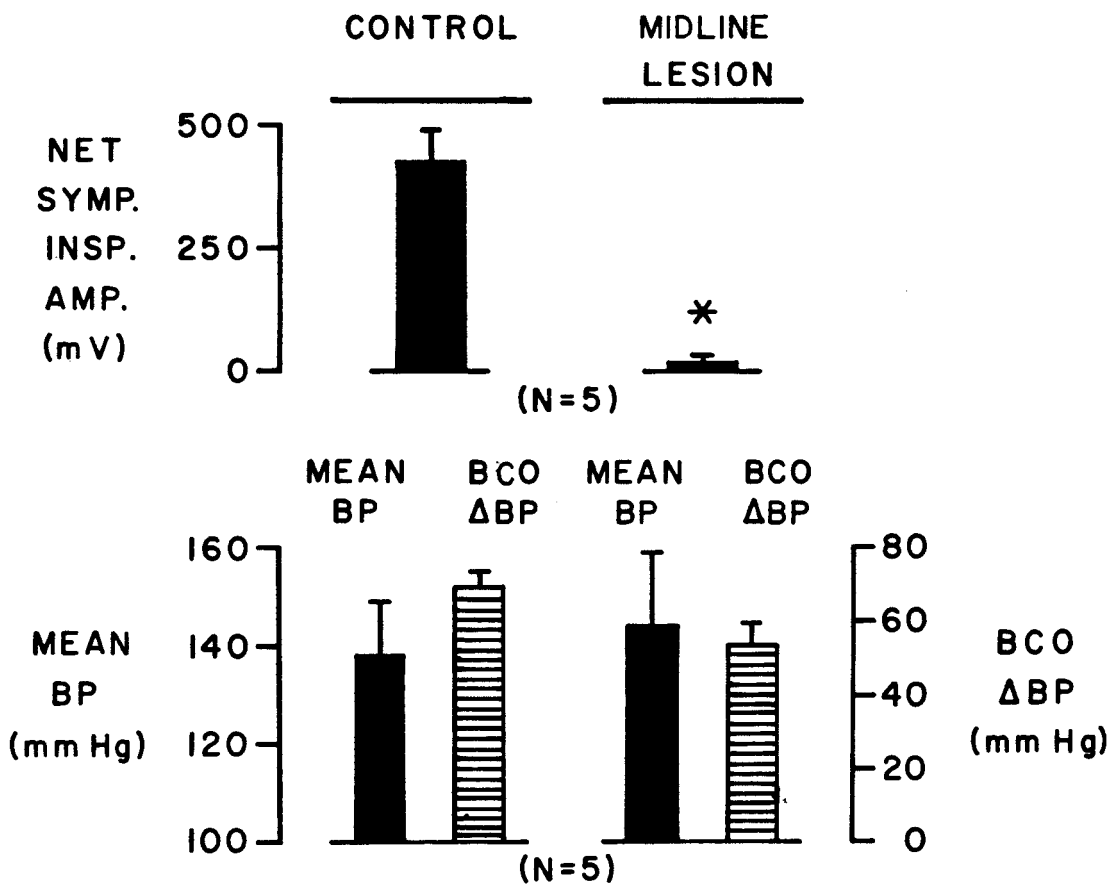
In summary, Group I results indicated that the respiratory modulation of sympathetic activity was absent after midline medullary lesions eliminated phrenic nerve activity. Evidence of respiratory unit activity in the nTS ipsilateral to the recorded nerves was observed in seven out of twelve Group I cats. General difficulty locating respiratory unit activity after midline medullary lesions suggested a decreased population of rhythmically active respiratory neurons resulting from the lesions. Blood pressure and bilateral carotid occlusion data indicated that lesions did not cause general depression of medullary brain stem function or affect close neighboring nTS structures mediating baroreceptor responses.

2. Group II Results

Effects of pontine parabrachial stimulations ipsilateral to recorded sympathetic nerves were assessed during inspiration, post-inspiration, and expiration and after midline medullary lesions (POST MIDLINE) which eliminated phrenic activity and the respiratory modulation of sympathetic activity. Stimulus triggered computer summation of sympathetic activity from Cat #S4 (Fig. 7-11, top) indicated that activity was evoked during inspiration, post-inspiration, expiration and after midline medullary

lesions. In contrast, when no stimulus was delivered (NOT DELIVERED) computer summation of non-evoked sympathetic activity indicated no response. The oblique lines under each curve indicate areas of evoked activity (mV-sec). Computed values (mV-sec) for Cat #S4 are represented above each curve in Fig. 7-11 (top). When areas of evoked sympathetic activity from all the cats were statistically compared, no differences (P < 0.05) were found between activities evoked during inspiration, post-inspiration, expiration or after midline medullary lesions (Fig. 7-11, bottom). However, all evoked sympathetic activities before and after midline lesions were significantly (P < 0.05) different from non-evoked activity (NOT DELIVERED).

Histological analysis of the pontine stimulation sites indicated that pathways and nuclei located in the dorsolateral rostral pons were stimulated (Fig. 7-12). Stimulation sites were located in regions of medial parabrachial (PBM), Kolliker-Fuse (KF), lateral tegmental field (FTL) and paralemniscal tegmental field (FTP) nuclei which all have direct anatomical projections to spinal locations of sympathetic preganglionic cell bodies (138). Pathways, such as those descending from hypothalamic and parabrachial nuclei, were probably also stimulated.

Dorsal and cross-sectional views of the midline medullary lesions in Group II cats (Fig. 7-13) indicated

Figure 7-11

Sympathetic activity evoked by pontine parabrachial stimulation during inspiration, post-inspiration, expiration, when the stimulus was not delivered to the brain, and after midline medullary lesions in Group II Cat #S4 (top). Evoked areas indicated by the oblique lines are displayed above each curve. Group data from the cats is indicated by the bar graphs in the bottom half of the figure. The asterisk indicates a significant ($P < 0.05$) difference from the control area. The bars represent the mean area $\pm$ standard error (SE) for the number of cats (N) represented in the brackets.
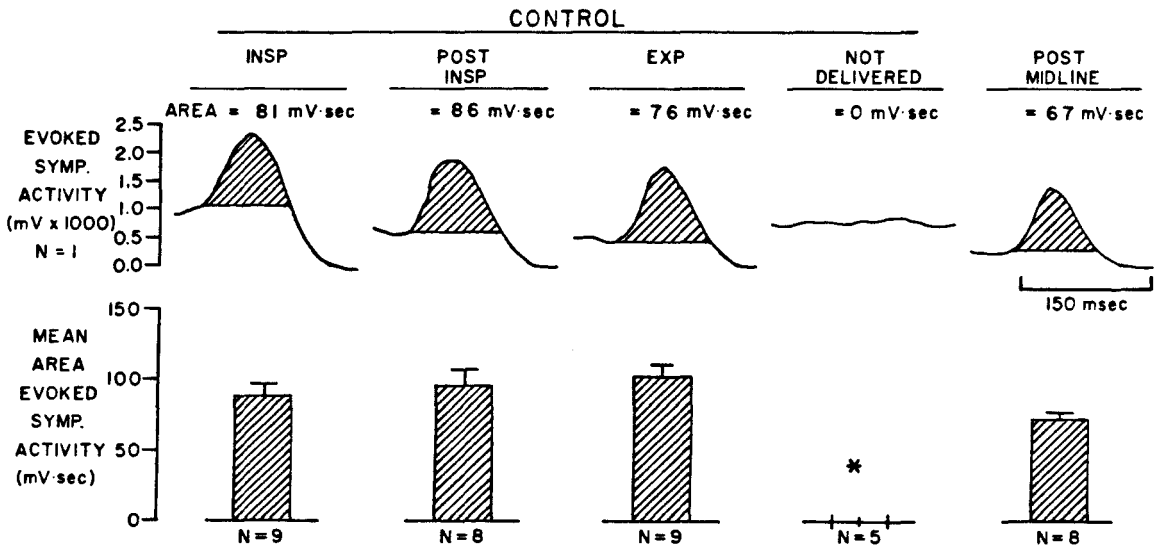
Figure 7-12

Stimulation sites in the pontine parabrachial region. The horizontal arrows point to darkened lesion zones indicating the stimulation sites. Abbreviations: bc, brachium conjunctivium; bp, brachium pontis: KF, Kolliker-Fuse nucleus; ml, medial lemniscus; PBM, medial parabrachial nucleus; PG, pontine gray; rb, restiform body; SOL, lateral nucleus of the superior olive; SOM, medial nucleus of the superior olive; 5M, trigeminal motor nucleus; 5n, 5th nerve; 5SP, spinal trigeminal nucleus; 5st, spinal trigeminal tract; 6N abducens nucleus; 6n, 6th nerve; 7g, genu of facial nerve; 7n, 7th nerve; 8n, 8th nerve.
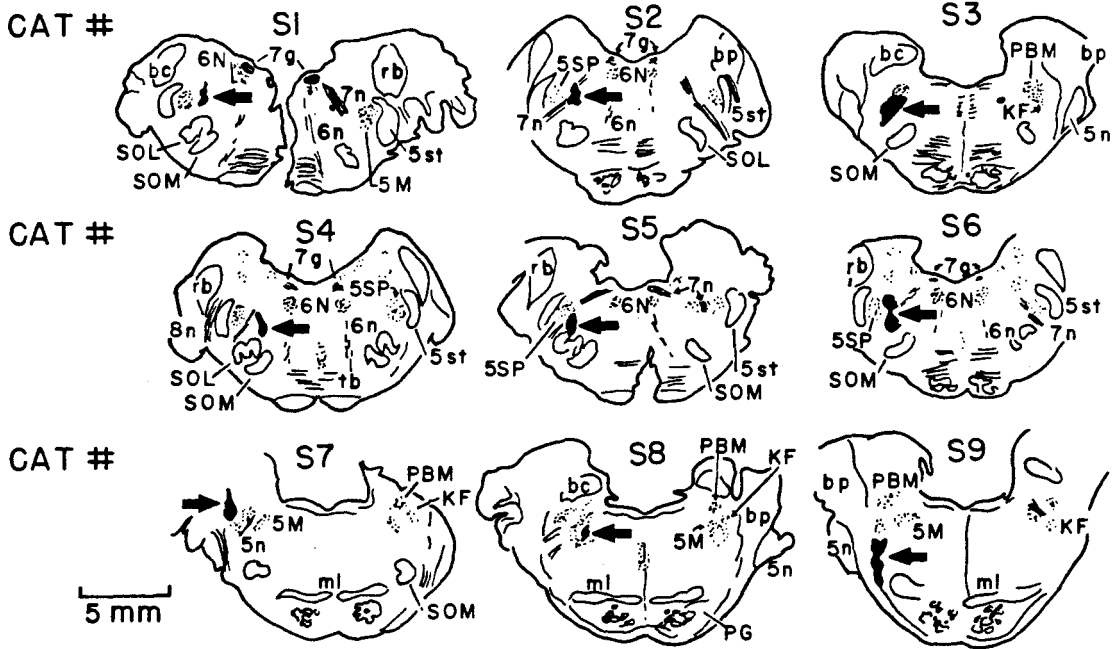
Figure 7-13

Dorsal and cross-sectional views of midline medullary lesions in Group II cats.

CAT DORSAL

#	VIEW	CROSS SECTIONS			
		A	**B**	**C**	**D**

S1

S2

S3

S4

S5

S6

S7

S8

CAL ⊢——⊣ 10mm

CAL ⊢——⊣ 5mm
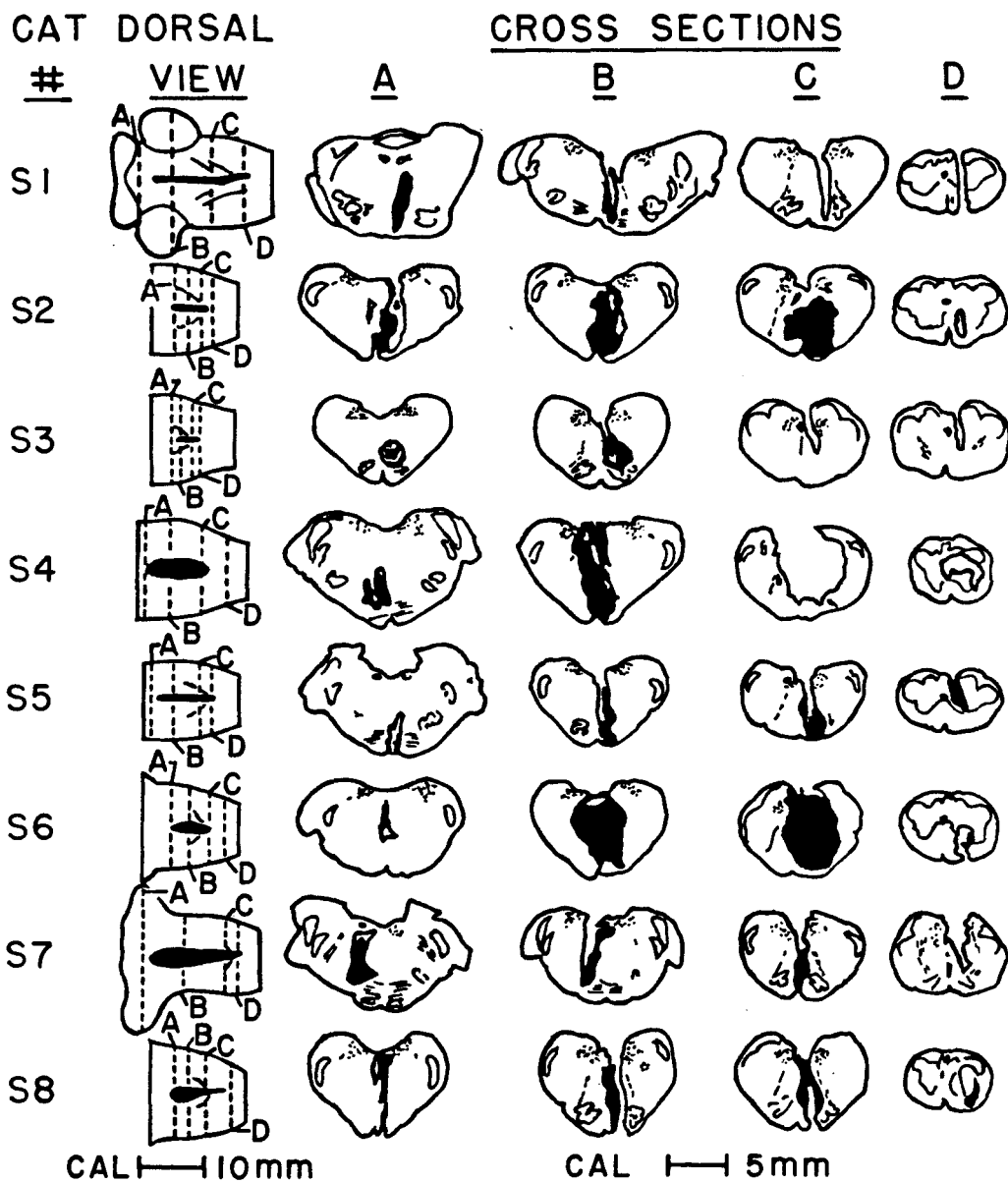
that lateral medullary structures and pathways were intact. Regions of the nTS immediately adjacent to the lesions were also spared by the lesions in all but Cats #S4 and #S6. Thus, the lesions primarily affected pathways and nuclei located in medial regions of the medulla near the obex.

As in Group I, blood pressure and bilateral carotid occlusion responses of the Group II cats were not significantly (P > 0.05) affected by midline medullary lesions (Fig. 7-14).

In summary, the Group II results indicated that sympathetic responses evoked by ipsilateral stimulation of supramedullary structures were unaffected by midline medullary lesions which eliminated phrenic activity and the respiratory modulation of sympathetic activity. Blood pressure and bilateral carotid occlusion responses were also unaffected by the midline medullary lesions.

3. Group III Results

Representative oscillograph tracings from Cat #L1 indicate left laryngeal, sympathetic, and phrenic nerve activities before and after midline medullary lesions (Fig. 7-15). Phrenic, laryngeal and sympathetic activity patterns were all related prior to the lesions. Respiratory oscillations were also apparent in the control blood

Figure 7-14

Mean blood pressure (solid bars, left scale) and amount of increase in blood pressure during bilateral carotid occlusion (horizontal bars, right scale) before and after midline medullary lesions in Group II cats.
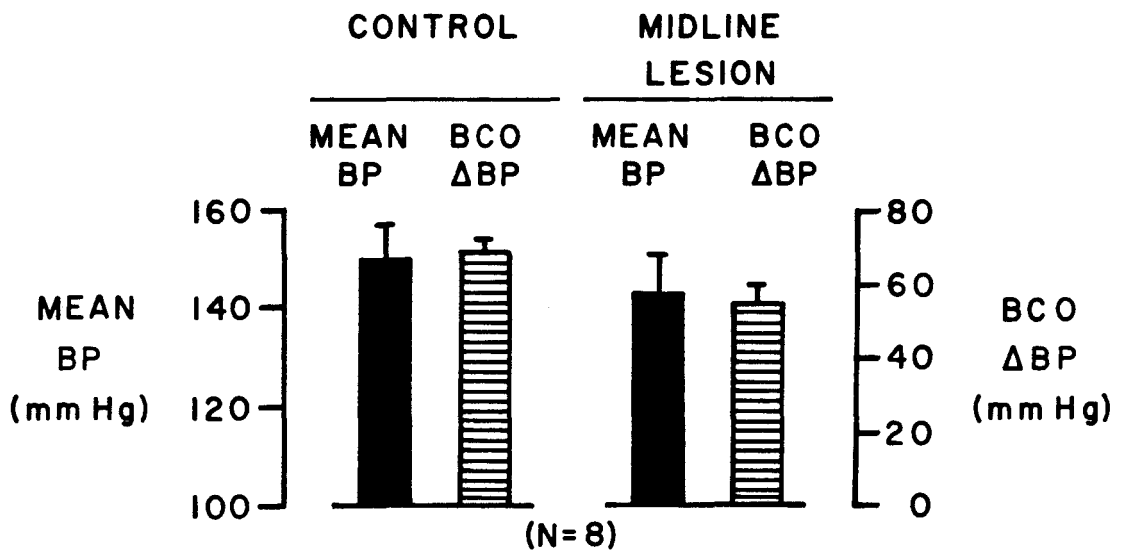
Figure 7-15

Oscillograph tracing from Group III Cat #L1 before and after midline medullary lesions. Illustrated are (top to bottom) integrated laryngeal nerve activity, time marker (seconds), integrated inferior cardiac sympathetic activity, integrated phrenic activity, inferior cardiac sympathetic activity, phrenic activity, blood pressure, and intratracheal pressure.

CONTROL   MIDLINE MEDULLARY
                                  LESION

INTEG.
LARYNGEAL N.

TIME MARKER
(SEC)

INTEG.
SYMP. N.

INTEG.
PHRENIC N.

INF. CARDIAC   120
SYMP. N.   µV

PHRENIC N.   250
                µV

BP   200
(mm Hg)   100
                0

ITP.   5
(mm Hg)   0
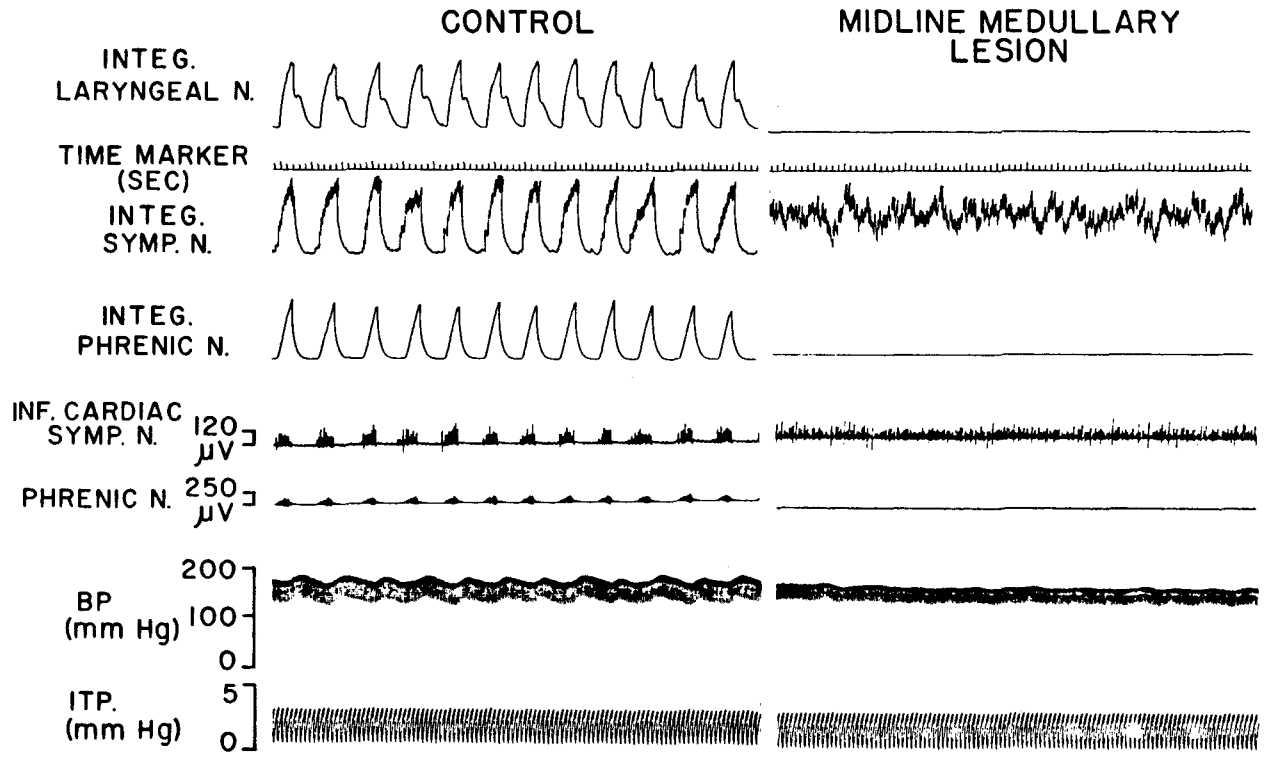
pressure tracing. The respiratory modulation of sympathetic activity and respiratory oscillations in the blood pressure waves were no longer present after midline medullary lesions eliminated phrenic and laryngeal nerve activities. Similar results were obtained in the other Group III cats. Although respiratory related blood pressure oscillations were absent after the lesions, mean blood pressure was not significantly ($P > 0.05$) affected (Fig. 7-16, bottom).

ECG-triggered computer summation of cardiac related sympathetic activity was used to assess baroreceptor reflex integrity before and after midline lesions in Group III cats. ECG-triggered computer summations from six of the Group III cats were similar to those of Cat #L5 (Fig. 7-16, top). The computer summation data from Cat #L5 indicated that cardiac related sympathetic activity was still present and slightly enhanced after midline lesions. Results from Cat #L7 were eliminated from the study since the ECG-triggered computer summation of sympathetic activity, resulting in a straight line after the midline lesion, indicated that the lesion affected more brain stem structures (e.g. nTS) than intended. ECG-triggered computer summations of sympathetic activity were not obtained for Cat #L8. To quantitatively assess the ECG-triggered computer summation data, areas indicated by the oblique lines under each curve (Fig. 7-16, top) were divided

Figure 7-16

Cardiac-related sympathetic activity and blood pressure before and after midline lesions in six Group III cats. Illustrated are ECG triggered computer summations of sympathetic activity for Cat #L5 (top), the mean area/time of ECG triggered sympathetic activity (middle), and mean blood pressure (bottom) before and after midline lesions in six Group III cats. The asterisk indicates a significant (P < 0.05) difference from control.

CONTROL   MIDLINE LESION

ECG TRIG. SYMP. ACTIVITY (mV)

$\dfrac{AREA}{TIME}$ = 1794 mV

$\dfrac{AREA}{TIME}$ = 2542 mV

100 SWEEPS

250 msec.

ECG TRIG. SYMP. ACTIVITY $\dfrac{AREA}{TIME}$ (mV)

(N = 6)

MEAN BP (mm Hg)
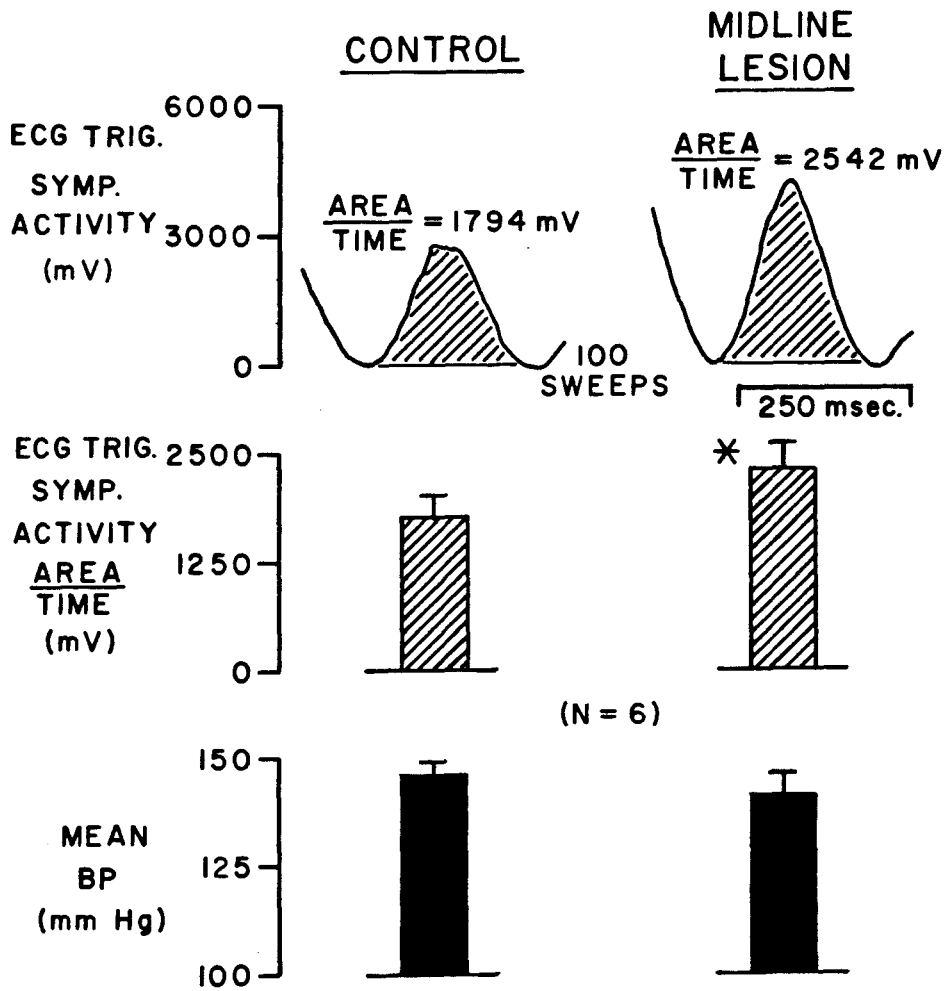
by the cardiac cycle time (AREA/TIME) and then statistically compared (N = 6 cats). Area/time of ECG triggered sympathetic activity was significantly (P < 0.05) increased after midline lesions (Fig. 7-16, middle).

Dorsal and cross-sectional views of midline lesions in the Group III cats are illustrated in Fig. 7-17. The lesions were similar to those previously observed in the Group I and II cats. Results from Cat #L8 were eliminated from the study since the attempted midline lesions extended so far laterally into caudal medullary regions (represented by cross-section C in Fig. 7-17) and ECG-triggered computer summation data for Cat #L8 was not available to otherwise verify brain stem integrity after the lesions.

In summary, Group III results indicated that laryngeal nerve activity ceased when midline medullary lesions eliminated phrenic activity and the respiratory modulation of sympathetic activity. ECG-triggered computer summations indicated that baroreceptor reflex effects on sympathetic activity (mediated by the nTS) were intact before and after midline lesions in six of the Group III cats.

4. Spectral Analysis Results; Groups I,II, and III

Using spectral analysis, frequencies of sympathetic

Figure 7-17

Dorsal and cross-sectional views of midline medullary lesions in the Group III cats.

CAT DORSAL VIEW — CROSS SECTIONS

CAL ⊢——⊣ 10 mm   CAL ⊢——⊣ 5 mm
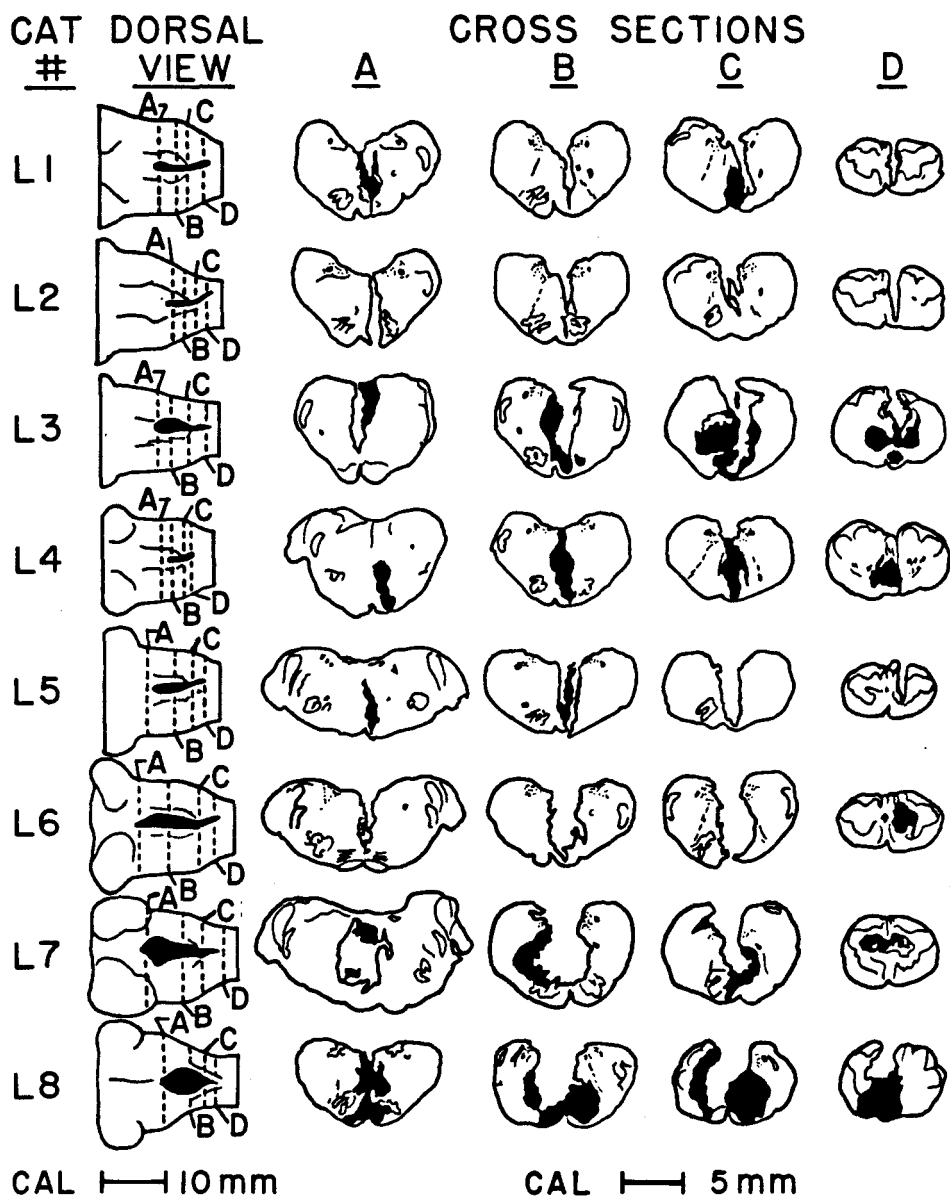
nerve activities from Group I (N = 5), combined Group
I/Group II (N = 4) and Group III (N = 6) cats were assessed
before and after midline medullary lesions (Fig. 7-18). In
the control frequency spectrum of representative Cat #R3
(Fig. 7-18, top), the prominent spectral peak at the
respiratory frequency (RESP. PEAK) indicated respiratory
modulation of sympathetic activity prior to any lesions.
Absence of the respiratory peak (RESP. PEAK) after the
midline medullary lesion indicated that respiratory
modulation of sympathetic activity was no longer present.
Spectral analysis data from the fifteen cats was grouped by
comparing the heights of the respiratory peaks (SPECTRAL
AMPLITUDE AT RESP. FREQ.) before and after midline lesions.
Due to the absence of respiratory peaks (RESP. PEAK),
spectral amplitude at the respiratory frequency was
significantly (P < 0.05) decreased after midline medullary
lesions (Fig. 7-18, bottom). Cardiac related and artificial
ventilator related influences on sympathetic activity,
indicated by the labeled cardiac and ITP peaks, were
unaffected by midline medullary lesions.

In summary, spectral analysis of sympathetic
activity from fifteen cats indicated that the respiratory
modulation of sympathetic activity was eliminated by midline
medullary lesions.

Figure 7-18

Spectral analysis of sympathetic nerve frequencies before and after midline medullary lesions. Illustrated are (top) sympathetic frequency spectra from representative Group I Cat #R3 and (bottom) spectral amplitude of the respiratory peak in fifteen cats before and after midline medullary lesions. Respiratory peaks, intratracheal pressure peaks (indicating ventilator influences on sympathetic activity), and cardiac peaks are labeled. The asterisk indicates a significant ($P < 0.05$) difference from control.
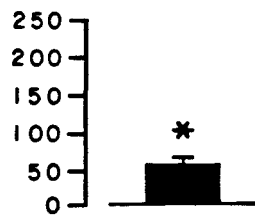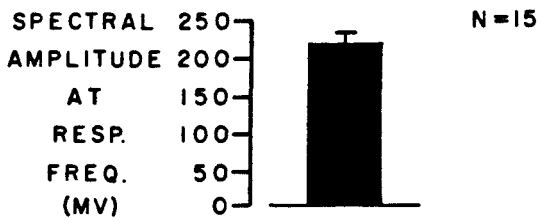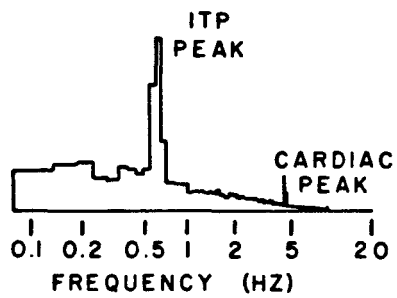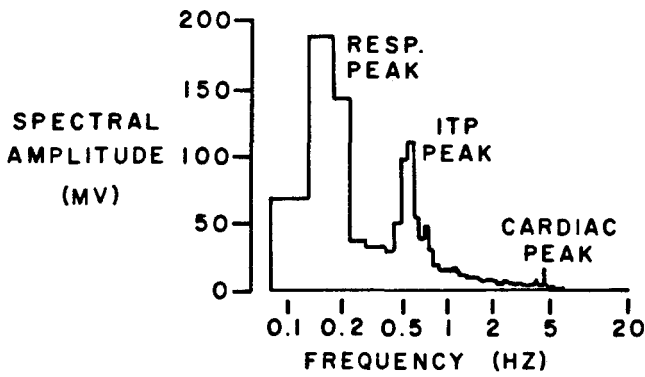
D. DISCUSSION

The present investigation established that phrenic
nerve activity and the respiratory modulation of sympathetic
activity were eliminated after midline medullary lesions.
Cessation of phrenic activity after midline medullary
lesions in the cat brain stem is well-documented (76, 167,
178) and has been attributed to interruption of bulbospinal
respiratory pathways which decussate in the medulla (56,
133, 134, 141). In contrast, bulbospinal pathways to
sympathetic nerves are bilateral, with an ipsilateral
predominance (1, 71, 81, 138). Since most bulbospinal input
to sympathetic neurons is mediated by ipsilateral pathways,
we predicted that the respiratory modulation of sympathetic
activity would be unaffected by midline medullary lesions
which eliminate phrenic nerve activity. However, as the
results clearly indicated (Figs. 7-5, 7-9, 7-10, 7-15,
7-18), the respiratory modulation of sympathetic activity
was eliminated after midline medullary lesions. Laryngeal
nerve recordings, supramedullary pontine stimulations and
brain stem unit recordings were incorporated into this
investigation to clarify why the respiratory modulation of
sympathetic activity was eliminated after midline medullary
lesions. Two ancillary questions addressed by these
experiments were 1) Did midline medullary lesions affect all

brain stem influences on sympathetic activity or just the respiratory modulation? and 2) Did midline medullary lesions merely interrupt descending bulbospinal pathways to phrenic nerves or did they also affect respiratory rhythm generation in the brain stem?

Although midline medullary lesions eliminated the respiratory modulation of sympathetic activity, other non-respiratory influences on sympathetic activity were unaffected. Mean arterial pressure did not change after midline lesions (Figs. 7-10, 7-13, 7-16), indicating that supraspinal inputs to sympathetic nerves were intact. If medullary function had been traumatized by the midline lesions, blood pressure would have fallen due to loss of bulbospinal influences on sympathetic nerves (4). Furthermore, intact bilateral carotid occlusion responses and cardiac related sympathetic activity after midline medullary lesions (Figs. 7-10, 7-13, 7-16) indicated functional integrity of dorsomedial nTS structures which mediate baroreceptor responses (93, 114, 150, 170). Thus, non-specific depression of medial medullary structures adjacent to the lesions did not occur. In addition, results from the pontine stimulation study (Group II) indicated that supramedullary pathways descending through the medulla were not significantly ($P < 0.05$) affected by the midline lesions (Fig. 7-11). Therefore, medullary influences other than

central respiratory input and supramedullary influences coursing through the medulla to sympathetic nerves were unaffected by the midline medullary lesions.

The primary effect of the medial medullary lesions was to depress rhythmicity of brain stem respiratory cells. Depression of respiratory rhythm generation was hypothesized since rhythmically firing units in the dorsal respiratory group was observed were more difficult to find after than before midline medullary lesions (Group I). This hypothesis was tested in the Group III study by recording the laryngeal nerve before and after midline lesions. The laryngeal nerve has cell bodies located in ipsilateral ambiguus and retrofacial nuclei (63, 97). Cessation of laryngeal nerve activity after midline medullary lesions substantiated the hypothesis that respiratory rhythm generation at the brain stem level was depressed by the midline lesions. Loss of laryngeal nerve activity after medullary lesions is consistent with reports by Bainton and Kirkwood (10) indicating increased CO_2 thresholds for respiratory rhythm generation in expiratory brain stem neurons after midline medullary lesions. At normal CO_2 levels, the expiratory neurons discharged in a tonic pattern after midline medullary lesions. Although Salmoiraghi and Burns concluded in an earlier study that brain stem respiratory activity was unaffected after midline medullary lesions, those

observations were based on results obtained after stimulation with 7% CO_2 (167). In a different study, St. John (175) reported that right and left laryngeal nerve activities became dissociated after midline medullary lesions. However, St. John also observed that laryngeal nerve activity was attenuated or eliminated after the midline lesions were extended in some cats. Although the elimination of laryngeal nerve activity may have been interpreted as brain stem trauma induced by the lesion, results from the present study clearly indicate that midline medullary lesions which depressed respiratory activity did not significantly affect other functions in close neighboring brain stem structures. Specifically, the dorsomedial nTS nuclei involved in baroreceptor reflexes were not affected when rhythmic respiratory activities in the contiguous ventrolateral nTS (dorsal respiratory group) and more laterally located laryngeal nerve cell bodies were decreased after the midline lesions. It is suggested that rhythmic oscillations of respiratory brain stem units located in right and left halves of the brain stem first become dissociated and then lose rhythmic oscillations after midline medullary lesions.

Loss of respiratory brain stem activity after midline medullary lesions is consistent with current evidence suggesting that crossed intrinsic brain stem

connections may be involved in respiratory rhythm generation (115, 135). Reciprocal inhibition between medullary inspiratory and expiratory neurons has been hypothesized as one explanation of central respiratory rhythmogenesis (31, 137, 189). However, no functional evidence of expiratory neuron inhibitory contacts with nTS inspiratory neurons existed prior to a recent study by Merrill, Lipski, Kubin, and Fedorko (136). In their investigation (136), inhibitory post synaptic potentials were intracellularly recorded in nTS inspiratory neurons following stimulation of contralateral Botzinger Complex expiratory neurons. Anatomical studies also confirmed that Botzinger Complex neurons project to the contralateral ventrolateral nTS (32, 96). A diagramatic illustration of the Botzinger Complex in relation to nTS nuclei and other brain stem structures is provided in Fig. 7-19. The demonstrated existence of crossed brain stem connections between medullary inspiratory and expiratory respiratory cells may provide some basis for the loss of respiratory rhythmogenesis observed after midline medullary lesions in the present study.

It is concluded that the primary interaction between respiration and central sympathetic pathways occurs in the medulla. The present study indicated that the respiratory modulation of sympathetic activity was eliminated after midline medullary lesions depressed central respiratory

Figure 7-19

Diagrammatic illustration of neuroanatomical structures and pathways involved in central control of sympathetic and respiratory functions which are discussed in the text.
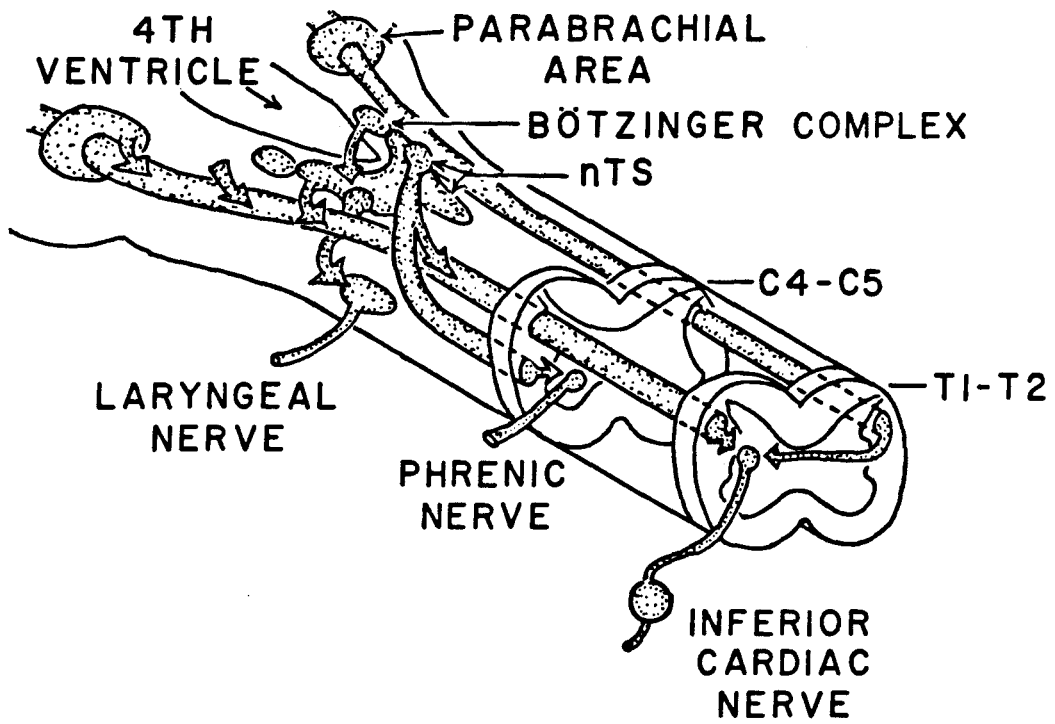
rhythmogenesis. In fact, the tonic sympathetic activity pattern and spectral analysis of sympathetic nerve frequencies after midline medullary lesions resembled sympathetic activity patterns and frequency spectra observed during respiratory depression induced by hyperventilation (Chapter III). During either hyperventilation or midline lesion induced central respiratory depression, sympathetic activity retained its other characteristics (e.g. response to baroreceptor input or supramedullary stimulation). Whether or not medullary sympathetic pathways receive ipsi-, contra-, or bilateral respiratory inputs could not be determined from the present study since ipsilateral respiratory cell (e.g. nTS) influences would not be detected after depression of ipsilateral brain stem respiratory neurons. In contrast with the respiratory-sympathetic interactions occurring at medullary levels, the lack of respiratory cycle or midline lesion effects on stimulation of supramedullary parabrachial regions (Fig. 7-11) suggested that those pontine influences on central respiratory and sympathetic functions are separate. Similarly, spinal pathways mediating the respiratory modulation of sympathetic activity are independent from the spinal respiratory pathways (Chapter IV). It is concluded, therefore, that central respiratory input on sympathetic activity primarily occurs at medullary levels.

CHAPTER VIII

SUMMARY AND CONCLUSIONS

Central nervous system levels of interaction between respiratory and cardiovascular control systems were studied in the five projects of this dissertation. Specifically, experiments were designed to assess the central neural organization of pathways and/or structures influencing the respiratory modulation of sympathetic nerve activity.

Sympathetic activity is ordinarily enhanced at the onset of inspiration and inhibited during the short post-inspiratory period between active inspiration and expiration. The first study was designed to assess the respiratory nature of the sympathetic oscillations related to phrenic nerve activity. This was a necessary preliminary study since the existence of independent sympathetic and respiratory oscillators was recently postulated. In the first study, external intercostal, phrenic and inferior cardiac sympathetic nerves were recorded in cats which were hyperventilated (by increasing the depth of artificial ventilation) until phrenic and external intercostal respiratory activities ceased. As respiratory activity

254

ceased during hyperventilation, sympathetic activity simultaneously lost its respiratory modulation and became tonically active. Although sympathetic activity lost its respiratory modulation during hyperventilation, bilateral carotid occlusion responses and ECG (R-wave) triggered computer summation of sympathetic activity were unaffected. Spectral analysis of sympathetic nerve frequencies during control, hyperventilation (resulting in phrenic nerve quiescence), and recovery stages indicated that the spectral peaks in sympathetic activity with control respiratory frequencies disappeared during hyperventilation, and reappeared with the return of phrenic activity during the recovery stage (i.e. after blood gases and pH returned to control levels). It was concluded that the respiratory modulation of sympathetic activity was due to central respiratory input and that carotid sinus baroreceptor mediated inputs may explain the occasional presence of apparently independent sympathetic rhythms.

The second study assessed the spinal location of descending pathways responsible for the respiratory modulation of sympathetic activity. Descending brain stem pathways to sympathetic nerves are located in dorsal and ventral regions of the spinal cord whereas descending pathways to respiratory nerves are located in the ventral spinal cord. In this study, phrenic (C4-C5), external

intercostal (T1), and inferior cardiac sympathetic (T2-T10) nerves were recorded while cumulative lesions were made in the C6-C7 region of the spinal cord. Following ventral spinal cord hemisection, intercostal activity was eliminated and sympathetic activity retained its respiratory modulation. Since phrenic nerve activity remained intact above the C6-C7 level of spinal lesions, respiration (phrenic nerve) triggered computer summation of sympathetic activity was used to assess the respiratory modulation of sympathetic activity after each spinal lesion. The respiratory modulation of sympathetic activity was eliminated after bilateral lesions of dorsolateral funiculus regions of the spinal cord. The above results were verified when the order of lesions was reversed, i.e. when lesions of the dorsal cord preceded ventral cord lesions in another group of cats. It was concluded that influences mediating the respiratory modulation of sympathetic activity descend bilaterally in dorsolateral funiculus regions of the spinal cord.

Effects of medial cerebellar lesions on sympathetic rhythmicity were assessed in the third study. Stimulation of medial cerebellar (fastigial) nuclei is known to cause a significant blood pressure elevation (50 mmHg) mediated by the sympathetic nervous system. Thus, this study was necessary to determine cerebellar influences on sympathetic

rhythmicity before proceeding to the other dissertation studies in which portions of medial cerebellar structures were to be routinely removed (e.g. to facilitate recording brain stem respiratory units). The results from respiration (phrenic nerve) triggered computer summation of sympathetic activity verified that midline cerebellar lesions eliminating fastigial nuclei had no influence on the respiratory modulation of sympathetic activity. In addition, respiration and bilateral carotid occlusion responses were unaffected by the extensive midline cerebellar lesions. In conclusion, this control study indicated that removal of medial cerebellar structures did not affect rhythmicity of sympathetic nerve activity, baroreceptor responses, or respiration.

Since pontine parabrachial areas have known influences on both respiratory and cardiovascular systems, effects of pontine parabrachial stimulation and lesions on the respiratory modulation of sympathetic activity were assessed in the fourth study. This experiment tested the hypothesis that parabrachial influences on sympathetic nerve activity are gated through the respiratory system. Stimulation during inspiration, post-inspiration, and expiration evoked activation of sympathetic activity followed by a period of inhibition (silent period). Latencies of evoked responses and silent period durations

were unaffected by the phase of the respiratory cycle when stimuli were delivered. Stimulus triggered computer summation of evoked sympathetic activity indicated that amplitudes of the responses were slightly, but significantly ($P < 0.05$), enhanced during expiration when evoked activities were measured above the background level of sympathetic activity. The enhancement of evoked sympathetic activity during expiration was attributed to the lower background sympathetic activity during expiration due to respiratory modulation. If pontine parabrachial influences on sympathetic activity were gated through the respiratory system, a markedly decreased or absent evoked sympathetic response would be anticipated during expiration. It was concluded from the stimulation studies that parabrachial area influences on sympathetic activity were not gated exclusively through respiratory inputs on sympathetic activity.

Lesions of the parabrachial areas resulted in apneusis (i.e. prolonged inspiratory duration) which is known to occur in vagotomized animals after bilateral parabrachial area lesions. Sympathetic activity was enhanced at the onset and inhibited at the termination of apneustic phrenic nerve activity. Additional rhythms superimposed on the apneustic pattern of sympathetic activity were observed in five of the eleven cats and were

attributed to baroreceptor feedback oscillations occurring between sympathetic activity and blood pressure waves. Depending on baroreceptor sensitivity and respiratory rate, it was concluded that baroreceptor influences may similarly potentiate the respiratory modulation of sympathetic activity or alter apparent phase relations between sympathetic and phrenic activities during normal breathing.

The fifth study assessed whether midline medullary pathways and/or structures were necessary for respiration and/or the respiratory modulation of sympathetic activity. Brain stem pathways from the dorsal respiratory group (ventrolateral nTS) cross the midline of the medulla before descending in the ventral spinal cord to contralateral phrenic motor nerves. In contrast, respiratory nerves to the larynx (laryngeal nerves) arise from ipsilaterally projecting brain stem nuclei. Descending pathways to sympathetic nerves are primarily ipsilateral. In this study, midline medullary lesions were made while recording left phrenic and inferior cardiac sympathetic nerves. Laryngeal nerve activity and brain stem respiratory unit activity ipsilateral to the recorded nerves were also assessed before and after midline medullary lesions in some cats. In other cats, ipsilateral pontine parabrachial regions were stimulated before and after midline medullary lesions.

After midline medullary lesions, phrenic activity ceased and the respiratory modulation of sympathetic activity was no longer present, as determined using spectral analysis of sympathetic nerve frequencies. Laryngeal nerve activity also ceased after midline medullary lesions, indicating that medullary respiratory cell activity was depressed. After midline medullary lesions, rhythmic brain stem units in the dorsal respiratory group were more difficult to locate than control respiratory units. However, when rhythmic brain stem unit and sympathetic activities were recorded in five cats before and after midline medullary lesions, respiration (brain stem unit) triggered computer summation further substantiated that the respiratory modulation of sympathetic activity was eliminated after the lesions.

In contrast, blood pressure, bilateral carotid occlusion tests of baroreceptor reflex integrity, ECG (R-wave) triggered computer summation of cardiac-related sympathetic activity, and sympathetic responses evoked by ipsilateral supramedullary stimulation of pontine parabrachial areas were not significantly affected by the midline medullary lesions.

It was concluded that midline medullary lesions eliminated the respiratory modulation of sympathetic activity by decreasing the population of rhythmically active

brain stem respiratory units. Although respiration and the respiratory modulation of sympathetic activity were eliminated by midline medullary lesions, other influences on sympathetic activity (e.g. baroreceptor and supramedullary stimulation) remained intact.

In overview, it is concluded that the primary interaction between respiration and central sympathetic pathways occurs in the medulla. When medullary respiratory cell activity was depressed during hyperventilation or after midline medullary lesions, sympathetic activity lost its respiratory modulation. Central respiratory input is represented by the ipsi- and contralateral nTS projections onto descending sympathetic pathways in Fig. 8-1. Botzinger Complex projections to contralateral nTS inspiratory neurons may provide some basis for the loss of respiratory rhythmogenesis observed after midline medullary lesions. In contrast with respiratory-sympathetic interactions occurring at medullary levels, the lack of respiratory cycle or midline lesion effects on stimulation of supramedullary parabrachial regions suggested that those pontine influences on sympathetic and respiratory functions are separate. As illustrated in Fig. 8-1, the bilateral pathways descending from pontine parabrachial and suprapontine (e.g. hypothalamic) regions are not gated through respiratory (e.g. nTS) centers. Similarly, spinal pathways mediating

Figure 8-1

Diagrammatic illustration of neuroanatomical structures and pathways involved in central control of respiratory and sympathetic functions discussed in the text.
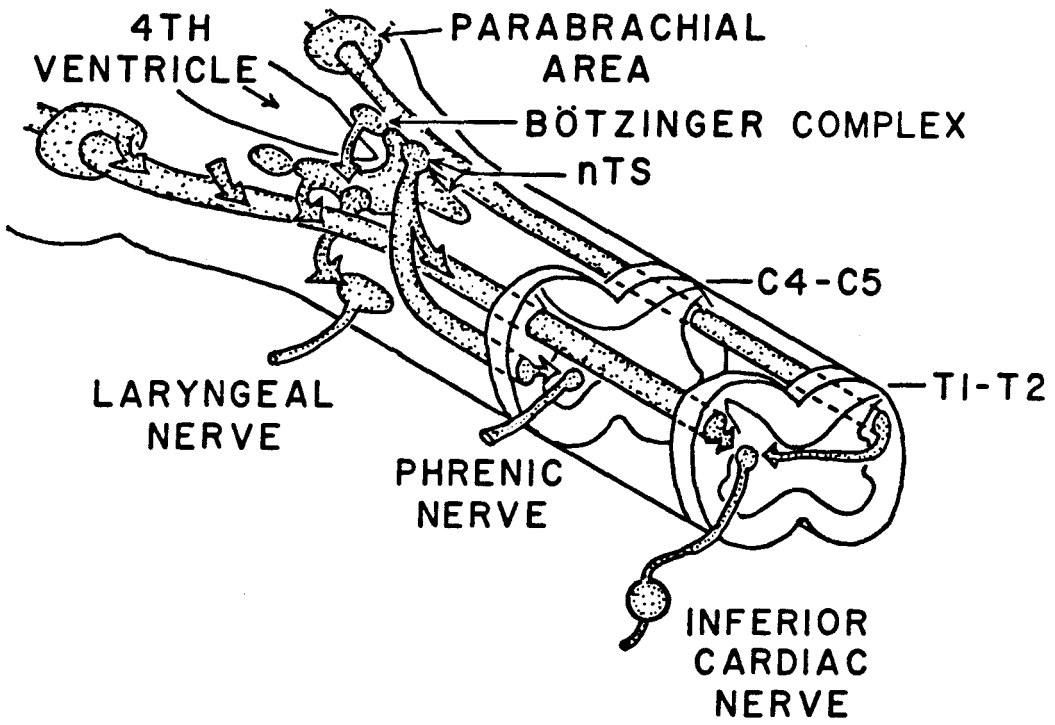
4TH VENTRICLE

PARABRACHIAL AREA

BÖTZINGER COMPLEX

nTS

C4-C5

T1-T2

LARYNGEAL NERVE

PHRENIC NERVE

INFERIOR CARDIAC NERVE

the respiratory modulation of sympathetic activity are
independent from the spinal respiratory pathways. Pathways
mediating the respiratory modulation of sympathetic activity
are located in the dorsolateral funiculus whereas central
respiratory pathways are in the ventrolateral spinal cord.
Since the cerebellum had no influence on the respiratory
modulation of sympathetic activity, it was excluded from
summary Fig. 8-1.

Specific conclusions drawn from the results of these
studies are the following:

1. Respiratory-related sympathetic rhythms were due to
central respiratory input which ceased during
hyperventilation-produced phrenic and intercostal nerve
quiescence.

2. Central respiratory input on sympathetic activity was
markedly attenuated after the midline medullary lesions
depressed the population of rhythmically active units in the
dorsal respiratory group. As a result, the respiratory
modulation of sympathetic activity was eliminated after
midline medullary lesions.

3. In the absence of central respiratory input, during
hyperventilation or after midline medullary lesions, other

influences on sympathetic activity (e.g. baroreceptor and supramedullary stimulation) are intact.

4. Lesions of medial cerebellar structures had no influence on the respiratory modulation of sympathetic activity, respiration, or baroreceptor reflex integrity.

5. Delivering pontine parabrachial stimuli during different phases of the respiratory cycle or after midline medullary lesions (which eliminated respiration and the respiratory modulation of sympathetic activity) did not consistently affect the evoked sympathetic response latency, amplitude, or silent period duration. Thus, pontine parabrachial influences on sympathetic activity are not exclusively gated through the respiratory system.

6. Spinal pathways mediating the respiratory modulation of sympathetic activity are located bilaterally in dorsolateral funiculus regions of the spinal cord.

BIBLIOGRAPHY

1. Achari N.K., Al-Ubaidy, S.S., and C.B.B. Downman. Spinal sympathoexcitatory pathways activated by stimulating fastigial nuclei, hypothalamus, and lower brain stem in cats. Exp. Neurol. 62: 230-240, 1978.

2. Achari N.K., and C.B.B. Downman. Autonomic effector responses to stimulation of nucleus fastigius. J. Physiol. 210: 637-650, 1970.

3. Adrian E.D., Bronk D.W. and G. Phillips. Discharges in mammalian sympathetic nerves. J. Physiol.(London) 74: 115-133, 1932.

4. Alexander, R.S. The effects of blood flow and anoxia on spinal cardiovascular centers. Amer. J. Physiol. 143: 698-708. 1945.

5. Alexander, R.S. Tonic and reflex functions of medullary sympathetic cardiovascular centers. J. Neurophysiology 9: 205-217, 1946.

6. Amendt, K., Czachurski, J., Dembowsky, K, and H. Seller. Neurones within the "chemosensitive area" on the ventral surface of the brainstem which project to the intermediolateral column. Pfluegers Arch. 375: 289-292, 1978.

7. Aminoff, M.J. and T.A. Sears. Spinal integration of segmental, cortical and breathing inputs to thoracic respiratory motoneurones. J. Physiol. (Lond.). 215: 557-575, 1971.

8. Anden N-E., Haggendal, J., Magnussen, T. and E. Rosengren. The time course of the disappearance of noradrenaline and 5-hydroxytryptamine in the spinal cord after transection. Acta. Physiologica Scandinavica. 62: 115-118, 1964.

9. Ardell, J.F., Barman, S.M., and G.L. Gebber. Sympathetic discharge in chronic spinal cat. Amer. J. Physiol. 243: H463-H470, 1982.

10. Bainton, C.R., and P.A. Kirkwood. The effect of carbon dioxide on the tonic and rhe rhythmic discharges of expiratory bulbospinal neurones. J. Physiol. 296: 291-314, 1979.

11. Baker, J.P.. Jr., and J.E. Remmers. Response of medullary respiratory neurons to rostral pontine stimulation. Resp. Physiol. 50: 197-208, 1982.

12. Balis, G.U. and R.R. Monroe. The pharmacology of chloralose; A review. Psychopharmacologia. 6: 1-30, 1964.

13. Barman S.M. and G.L. Gebber. Basis for synchronization of sympathetic and phrenic nerve discharges. Amer. J. Physiol. 231: No.5, 1601-1607, 1976.

14. Barman, S.M. and G.L. Gebber. Hypothalamic neurons with activity patterns related to sympathetic nerve discharge. Amer. J. Physiol. 242: R34-R43, 1982.

15. Basbaum, A.I., Clanton, C.H., and H.L. Fields. Three bulbospinal pathways from the rostral medulla of the cat.: an autoradiographic study of pain modulating systems. J. Comp. Neurol. 178: 209-224, 1978.

16. Bassal, M., and A.L. Bianchi. Inspiratory onset or termination induced by electrical stimulation of the brain. Resp. Physiol. 50: 23-40, 1982.

17. Batton, R.R., Jayaraman, A., Ruggiero, D., and M.B. Carpenter. Fastigial efferent projections in the monkey; an autoradiographic study. J. Comp. Neurol. 174: 281-306, 1977.

18. Baumgarten, R. von and E. Kanzow. The interaction of two types of inspiratory neurons in the region of the tractus solitarious of the cat. Arch. ital. Biol. 96: 361-378, 1958.

19. Beacham, W.S. and E.R. Perl. Background and reflex discharge of sympathetic preganglionic neurons in the spinal cat. J. Physiol.(London). 172: 400-416, 1964.

20. Bentivoglio, M. The organization of the direct cerebellospinal projections. Progr. Brain Res. Vol. 57, Anatomy of Descending Pathways to the Spinal Cord. H.G.J.M. Kuypers and G.F. Martin (Eds.), Elsevier, Amsterdam, 1982, p. 279-291.

21. Berger, A.J. Dorsal respiratory group neurons in the medulla of the cat: spinal projections, responses to

lung inflation and superior laryngeal nerve stimulation. Brain Res. 135: 231-254, 1977.

22. Berger, A.J., Averill, B.B., and W.E. Cameron. Morphology of inspiratory neurons located in the ventrolateral nucleus of the tractus solitarious of the cat. J. Comp. Neurol. 224: 60-70, 1984.

23. Berman, A.L. The Brain Stem of the Cat; a Cytoarchitectonic Atlas with Sterotaxic Coordinates.Madison. University of Wisconsin Press, 1968.

24. Bernard C., Lecons sur la physiologie et la pathlogie du systeme nerveux. Vol. 1, Bailliere et ils, Paris, 1863.

25. Bernthal, T.G., Motley, H.E., Schwind, F.J. and W.F. Weeks. The efferent pathway of chemoreflex vasomotor reactions arising from the carotid body. Amer. J. Physiol. 143: 220-225, 1945.

26. Bertrand, F., and A. Hugelin. Respiratory synchronizing function of nucleus parabrachialis medialis: pneumotaxic mechanisms. J. Neurophysiol. 34: 189-207, 1971.

27. Bertrand, R., Hugelin, A., and J.F. Vibert. A stereologic model of pneumotaxic oscillator based on spatial and temporal distributions of neuronal bursts. J. Neurophysiol. 37: 91-107, 1974.

28. Blessing, W.W., Frost, P., and J.B. Furness. Catecholamine cell groups of the cat medulla oblongata. Brain Res. 192: 69-75, 1980.

29. Bowker, R.M., Westlund, K.N., Sullivan, M.C., and J.D. Coulter. Organization of descending serotonergic projections to the spinal cord. Progr. Brain Res. 57: 239-265, 1982.

30. Breckenridge, C.G. and H.E. Hoff. Pontine and medullary regulation of respiration in the cat. Amer. J. Physiol. 160: 385-394, 1950.

31. Burns, B.D. and G.C. Salmoiraghi. Repetitive firing of respiratory neurones during their burst activity. J. Neurophysiol. 23: 27-46, 1960.

32. Bystrzycka, E.K. Afferent projections to the dorsal and ventral respiratory nuclei in the medulla oblongata of the cat studied by the horseradish peroxidase technique. Brain Res. 185: 59-66, 1980.

33. Carlsson, A., Falk, B., Fuxe, K., and N-A Hillarp. Cellular localization of monoamines in the spinal cord. Acta Physiol. Scandinavica. 60: 112-119, 1964.

34. Chu, N.S. and F.E. Bloom. The catecholamine containing neurons in the cat dorsolateral pontine tegmentum: distribution of the cell bodies and some axonal projections. Brain Res. 66: 1-21, 1974.

35. Ciriello, J. and F.R. Caleresu. Descending hypothalamic pathways with cardiovascular function in the cat: a silver impregnation study. Exp. Neurol. 57: 561-580, 1977.

36. Cohen F.L. Effects of various lesions on crossed and uncrossed descending inspiratory pathways in the cervical spinal cord of the cat. J. Neurosurg. 39: 589-595, 1973.

37. Cohen, M.I. Intrinsic periodicity of the pontile pneumotaxic mechanism. Amer. J. Physiol. 195: 23-27, 1958.

38. Cohen, M.I. Discharge patterns of brainstem respiratory neurons in relation to carbon dioxide tension. J. Neurophysiol. 31: 142-165, 1968.

39. Cohen, M.I. Switching of the respiratory phases and evoked phrenic responses produced by rostral pontine electrical stimulation. J. Physiol. (London). 217: 133-158, 1978.

40. Cohen, M.I. Central determinants of respiratory rhythm. Ann. Rev. Physiol. 43: 91-104, 1981.

41. Cohen, M.I., and P.M. Gootman. Periodicities in efferent discharge of the splanchnic nerve of the cat. Amer. J. Physiol. 218: No. 4, 1092-1101, 1970.

42. Cohen, M.I., Piercey, M.F., Gootman, P.M. and P. Wolotsky. Synaptic connections between medullary inspiratory neurons and phrenic motoneurons as revealed by cross-correlation. Brain Res. 81:

319-324, 1974.

43. Cohen, M.I. and S.C. Wang. Respiratory neuronal activity in the pons of the cat. J. Neurophysiol. 22: 33-50, 1959.

44. Coote, J.H. and V.H. Macleod. The spinal route of sympatho-inhibitory pathways descending from the medulla oblongata. Pfluegers Arch. 359: 335-347, 1975.

45. Coyle, J.T., Molliver, M.E., and M.J. Kuhar. In situ injection of kainic acid: a new method for selectively lesioning neuronal cell bodies while sparing axons of passage. J. Comp. Neurol. 180: 301-324, 1978.

46. Dahlstrom, A., and K. Fuxe. Evidence for the existence of monoamine neurons in the central nervous system. II. Experimentally induced changes in the intraneuronal amine levels of bulbospinal neuron systems. Acta Physiologica Scandinavica. 64: Suppl. 247, 1-36, 1965.

47. Daly, I. DE B. and M. DE B. Daly. The effects of stimulation of the carotid body chemoreceptors on the pulmonary vascular bed in the dog: The vasosensory controlled perfused living animal preparation. J. Physiol. (London). 148: 201-219, 1959.

48. Daly, M. DE B. and M.J. Scott. Analysis of the primary cardiovascular reflex effects of stimulation of the carotid body chemoreceptors in the dog. J. Physiol. (Lond.). 162: 555-573, 1962.

49. Decima, E.E. and C. von Euler. Intercostal and cerebellar influences on efferent phrenic activity in the decerebrate cat. Acta Physiol. Scand. 76: 148-158, 1969.

50. Dembowsky, K., Czachurski, J., Amendt, K., and H. Seller. Bulbospinal inhibitory influences on sympathetic preganglionic neurones. In: Integrative Functions of the Autonomic Nervous System. C. McCBrooks, K. Koizumi, and A. Sato (Eds.), Amsterdam, Elsevier, 376-384, 1974.

51. Denavit-Saubie, M. and D. Riche. Descending input from the pneumotaxic system to the lateral

respiratory nucleus of the medulla. An anatomical study with the horseradish peroxidase technique. Neurosci. Lett. 6: 121-126, 1977.

52. Dittmar C. Ein neur beweis fur die reizbarkart der centripetalen faser des ruckenmarks. Ber. Verh. Sachs Ges. Wiss. Lepzig Math Phys. K1 22: 18-48, 1870.

53. Doba, N., and D.J. Reis. Cerebellum; role in reflex cardiovascular adjustment to posture. Brain Res. 39: 495-500, 1972.

54. Doba, N., and D.J. Reis. Role of the cerebellum and the vestibular apparatus in regulation of orthostatic reflexes in the cat. Circulat. Res. 34: 9-18, 1974.

55 Dormer, K.J., Foreman, R.D., and H.L. Stone. Glutamate-induced fastigial pressor response in the dog. Neuroscience 2: 577-584, 1977.

56. Euler, C. Von, Hayward, J.N., Martilla, I., and R.J. Wyman. Respiratory neurons of the ventrolateral nucleus of the solitary tract of the cat: vagal input, spinal connections and morphological identification. Brain Res. 61: 1-22, 1973.

57. Euler, C. Von, Hayward J.N., Marttila, I., and R.J. Wyman. The spinal connections of the ventrolateral nucleus of the cat's tractus solitarious. Brain Res. 61: 23-33, 1973.

58. Euler, C. Von, and T. Trippenbach. Excitability changes of the inspiratory 'off-switch' mechanism tested by electrical stimulation in nucleus parabrachialis in the cat. Acta Physiol. Scand. 97: 175-188, 1976.

59. Fedorko, L. Axonal projections from Botzinger expiratory neurones to other medullary nuclei and spinal cord in the cat. J. Physiol. (Lond.) 332: 80P, 1982.

60. Feldberg, W.,The ventral surface of the brain stem: a scarcely explored region of pharmacological sensitivity. Neuroscience 1: 427-441, 1976.

61. Feldberg, W., and P.G. Guertzenstein. Vasodepressor effects obtained by drugs acting on the ventral

surface of the brain stem. J. Physiol. (Lond.).,
258: 337-355, 1976.

62.   Foreman R.D. and R.D. Wurster. Localization and
      functional characteristics of descending sympathetic
      spinal pathways. Amer. J. Physiol. 225: No. 1,
      212-217, 1973.

63.   Gacek, R.R. Localization of laryngeal motoneurons in
      the kitten. Laryngoscope 85: 1841-1861, 1975.

64.   Gautier, F. and F. Bertrand. Respiratory effects of
      pneumotaxic lesions and subsequent vagotomy in
      chronic cats. Resp. Physiol. 23: 71-85, 1975.

65.   Gautier, H., J.E. Remmers, and D. Bartlett, Jr.
      Control of the duration of expiration. Resp. Physiol.
      18: 205-221, 1973.

66.   Gebber, G.L. Central oscillators responsible for
      sympathetic nerve discharge. Amer. J. Physiol. 239:
      H143-H155, 1980.

67.   Gebber, G.L. and S.M. Barman. Brain stem neurons
      governing the discharges of sympathetic nerves. J.
      Auton. Nerv. Syst. 5: 55-61, 1982.

68.   Gerber, U. and C. Polosa. Some effects of superior
      laryngeal nerve stimulation on sympathetic
      preganglionic neuron firing. Can. J. Physiol.
      Pharmacol. 57: 1073-1081, 1979.

69.   Glantz, S.A. Primer of Biostatistics. McGraw Hill,
      St. Louis. 1981.

70.   Glasser, R.L., Tippett, J.W., and V.A. Davidian, Jr.
      Cerebellar activity, apneustic breathing and neural
      control of respiration. Nature 209: 810-812, 1966.

71.   Gootman, P.M., and M.I. Cohen. Evoked splanchnic
      potentials produced by electrical stimulation of
      medullary vasomotor regions. Exp. Brain Res. 13:
      1-14, 1971.

72.   Gootman, P.M. and M.I. Cohen. The interrelationships
      between sympathetic discharge and central respiratory
      drive. Central Rhythmic and Regulation. Hippokrates,
      Stuttgart, 195-209, 1974.

73.   Gootman P.M. and M.I. Cohen.   Origins of rhythms
       common to sympathetic outflows at different spinal
       levels. In: Arterial Baroreceptors and Hypertension.
       P. Sleight (Ed.),   Oxford Medical Publications,
       England, 155-160, 1980.

74.   Gootman, P.M., and M.I. Cohen. Sympathetic rhythms
       in spinal cats. J. Auton. Nerv. Syst. 3: 379-387,
       1981.

75.   Gootman, P.M., Cohen, M.I., Piercey, M.P., and P.
       Wolotsky.   A search for medullary neurons with
       activity patterns similar to those in sympathetic
       nerves. Brain Res. 87: 395-406, 1975.

76.   Gromysz,   H.,   and   W.A.   Karczewski.   Phrenic
       motoneurone activity in split-brainstem cats and
       monkeys. Resp. Physiol. 50: 51-61, 1982.

77.   Guertzenstein, P.G., and A. Silver. Fall in blood
       pressure produced from discrete regions of the
       ventral surface of the medulla by glycine and
       lesions. J. Physiol. (Lond.). 242: 489-503, 1974.

78.   Guyton, A.C. and J.W. Harris. Pressoreceptor-autnomic
       oscillation: a probable cause of vasomotor waves.
       Amer. J. Physiol. 165: 158-166, 1951.

79.   Guyton, A.C. and J. H. Satterfield. Vasomotor waves
       possibly resulting from CNS ischemic reflex
       oscillation. Amer. J. Physiol. 170: 601-605, 1952.

80.   Harper,R.M. and G.C. Sieck. Discharge correlations
       between neurons in nucleus parabrachialis medialis
       during sleep-waking states. Brain Res. 199: 343-358,
       1980.

81.   Harrison, F., Wang, S.C., and E. Berry. Decussations
       of sympathetic efferent pathways from the
       hypothalamus. Amer. J. Physiol. 125: 449-456, 1939.

82.   Henry, J.L. and F.R. Caleresu. Origin and course of
       crossed medullary pathways to spinal sympathetic
       neurons in the cat. Exp. Brain Res. 20: 515-526,
       1974.

83.   Hoff, H.E. and C.G. Breckenridge. The medullary
       origin of respiratory periodicity in the dog. Amer.
       J. Physiol. 158: 157-72, 1949.

84. Holstege, G., and H.G.J.M. Kuypers. The anatomy of brain stem pathways to the spinal cord in cat. A labeled amino acid study. Progr. in Brain Res. 57: 145-175, 1982.

85. Holstege, G., Kuypers, H.G.J.M., and R.C. Boer. Anatomical evidence for direct brain stem projections to the somatic motoneuronal cell groups and autonomic preganglionic cell groups in cat spinal cord. Brain Res. 171: 329-333, 1979.

86. Huang, T.F. Cardiac arrythmia induced by electrical stimulation of the fastigial nucleus in cats. Jap. J. Physiol. 27: 565-576, 1977.

87. Huang, T.F., Carpenter, M.B., and S.C. Wang. Fastigial nucleus and orthstatic reflex in cat and monkey. Amer. J. Physiol. 232 (6): 676-681, 1977.

88. Illert, M. and M. Gabriel. Descending pathways in the cervical cord of cats affecting blood pressure and sympathetic activity. Pfluegers Arch. 335: 109-124, 1972.

89. Illert, M. and H. Seller. A descending sympathoinhibitory tract in the ventrolateral column of the cat. Pfluegers Arch. 313: 343-360, 1969.

90. Iwamura, Y., Uchino, Y., Ozawa, S., and N. Kudo. Excitatory and inhibitory components of somato-sympathetic reflex. Brain Res. 16: 351-358, 1969.

91. Janig, W., H. Kummel, and L. Wiprich. Respiratory rhythmicities in vasoconstrictor and sudomotor neurones supplyiny the cat's hindlimb. In: Koepchen, H.P., S.M. Hilton, and A. Trzebski. Central Interactions between Respiratory and Cardiovascular Control Systems. Springer-Verlag. New York. pp. 128-136, 1980.

92. Jones, B.E., and L. Friedman. Atlas of catecholamine perikarya, varicosities and pathways in the brainstem of the cat. J. Comp. Neurol. 215: 282-396, 1983.

93. Jordan, D. and K.M. Spyer. Studies on the termination of sinus nerve afferents. Pfluegers Arch. 69: 65-73, 1977.

94. Kahn, N., and E. Mills. Centrally evoked sympathetic discharge; a functional study of medullary vasomotor areas. J. Physiol. (Lond.). 191: 339-352, 1967.

95. Kalia, M. Anatomical organization of central respiratory neurons. Ann. Rev. Physiol. 43: 105-120, 1981.

96. Kalia, M., Feldman, J.L., and M.I. Cohen. Afferent projections to the inspiratory neuronal region of the ventrolateral nucleus of the tractus solitarious in the cat. Brain Res. 171: 135-141, 1979.

97. Kalia, M. and M.M. Mesulam. Intramedullary course of afferent and efferent fibers of the vagus nerve: a study using tetramethylbenzidine reaction for horseradish peroxidase. In: Central Nervous Control Mechanisms in Breathing. C. von Euler and H. Lagercrantz (Eds.). London: Pergamon, 1979, pp. 273-285.

98. Kaminski, R.J., G.A. Meyer, and D.L. Winter. Sympathetic unit activity associated with mayer waves in the spinal dog. Amer. J. Physiol. 219: 1768-1771, 1970.

99. Kell, J.F., and E.C. Hoff. Descending spinal pathways mediating pressor responses of cerebral origin. J. Neurophysiol. 15: 299-311, 1952.

100. Kerr, F.W., and S. Alexander. Descending autonomic pathways in the spinal cord. Arch. Neurol. (Chic). 10: 249-261, 1964.

101. Kezdi, P., and E. Geller. Baroreceptor control of preganglionic sympathetic nerve discharge. Amer. J. Physiol. 214: 427-435, 1968.

102. King, G.W. Topology of ascending brainstem projections to nucleus parabrachialis in the cat. J. Comp. Neurol. 191: 612-638, 1980.

103. Kluver, H., and E. Barrera. A method for the combined staining of cells and fibers in the nervous system. J. Neuropathol. Exp. Neurol. 12: 400-403, 1953.

104. Koepchen, H.P., Hilton, S.M. and A. Trzebski (Eds). Central Interaction Between Respiratory and

Cardiovascular Control Systems. Springer-Verlag, New York, 1980.

105.   Koepchen, H.P., Klussendorf, D., and D. Sommer. Neurophysiological background of central neural cardiovascular-respiratory coordination: Basic remarks and experimental approach. _J. Auton. Nerv. Sys_. 3: 335-368, 1981.

106.   Koepchen, H.P., Langhorst, P. and H. Seller. The problem of identification of autonomic neurons in the lower brain stem. _Brain Res._ 87: 375-393, 1975.

107.   Koepchen, H.P. and K. Thurau. Untersuchungen uber Zusammenhange zwischen Blutdruckwellen und Atemminnervation. _Plfuegers Arch_. 267: 10-26, 1958.

108.   Koizumi, K., Seller, H., Kaufman, A., and C. McCBrooks. Pattern of sympathetic discharges and their relation to baroreceptor and respiratory activities. _Brain Res._ 27: 281-294, 1971.

109.   Krnjevic, K. Chemical nature of synaptic transmission in vertebrates. _Physiol. Rev._ 54: 418-540, 1974.

110.   Kuypers H.G.J.M. and V. Maisky. Retrograde axonal transport of horseradish peroxidase from spinal cord to brain stem cell groups in the cat. _Neurosci. Lett._ 1: 9-14, 1975.

111.   LeGallois, J.C.C. Experiences sur le principe de la vie d'hautel, D'Hautel, Paris, 1812.

112.   Levy, M.N., DeGeest, H., and H. Zieske. Effects of respiratory center activity on the heart. _Circ. Res._ 18: 67-78, 1966.

113.   Lipski, J., Kubin, L., and J. Jodkowski. Synaptic action of R beta neurons on phrenic motoneurons studied with spike-triggered averaging. _Brain Res._ 288: 105-118, 1983.

114   Lipski, J., McAllen, R.M., and K.M. Spyer. The sinus nerve and baroreceptor input to the medulla of the cat. _J. Physiol. (London)_. 251: 61-78, 1975.

115.   Lipski, J. and E.G. Merrill. Electrophysiological demonstration of the projection from expiratory neurons in the rostral medulla to contralateral

dorsal respiratory group. Brain Res. 197: 521-524, 1980.

116. Lisander, B., and J. Martner. Interaction between the fastigial pressor response and the baroreceptor reflex. Acta Physiol. Scand. 83: 505-515, 1971.

117. Loewy A. and H. Burton. Nuclei of the solitary tract: efferent connections to the lower brain stem and spinal cord of the cat. J. Comp. Neurol. 181: 421-450, 1978.

118. Loewy, A.D. and S. McKellar. The neuroanatomical basis of central cardiovascular control. Fed. Proc. 39: 2495-2503, 1980.

119. Long, S.E. and J. Duffin. The medullary respiratory neurons: a review. Can. J. Physiol. Pharmacol. 62: 161-182, 1984.

120. Lovfing, B. Cardiovascular adjustments induced from the rostral cingulate gyrus. Acta Physiol. Scand. (Suppl.) 184: 1-82, 1961.

121. Lumsden, T. Observations on the respiratory centres in the cat. J. Physiol. (London). 57: 153-160, 1923.

122. Lumsden, T. Observations on the respiratory centres. J. Physiol. (London) 57: 354-367, 1923.

123. Lumsden, T. The regulation of respiration, Part I. J. Physiol. (London). 58: 81-91, 1923.

124. Lumsden, T. The regulation of respiration, Part II. Normal type. J. Physiol. (London) 58: 111-126, 1923.

125. Lutherer, L.O., Lutherer, L.B.C., Dormer, K.J., Janssen, H.F, and C.D. Barnes. Bilateral lesions of the fastigial nucleus prevent recovery of blood pressure following hypotension induced by hemmorhage or administration of endotoxin. Brain Res. 269: 251-257, 1983.

126. Magoun, H.W., Ranson, S.W., and A. Hetherington. Descending connections from the hypothalamus. Arch. Neurol. Psychol. 39: 1127-1149, 1939.

127. Mannard, A. and C. Polosa. Analysis of background

firing of single sympathetic preganglionic neurons of cat cervical nerve. J. Neurophysiol. 36: 398-408, 1973.

128. Martin, R.F., Jordan, L.M., and W.D. Willis. Differential projections of cat medullary raphe neurons demonstrated by retrograde labeling following spinal cord lesions. J. Comp. Neurol. 182: 77-88, 1978.

129. McBride, R.L. and J. Sutin. Projections of the locus coeruleus and adjacent pontine tegmentum in the cat. J. Comp. Neurol. 165: 265-284, 1976.

130. McLachlan, E.M., and G.D. S. Hirst. Some properties of preganglionic neurons in the upper thoracic spinal cord of the cat. J. Neurophysiol. 43: 1251-1265, 1980.

131. McLachlan, E.M. and B.J. Oldfield. Some observations on the catecholaminergic innervation of the intermediate zone of the thoracolumbar spinal cord of the cat. J. Comp. Neurol. 200: 529-544, 1981.

132. Mendelson, M. Oscillator neurons in crustacean ganglia. Science 171: 1170-1174, 1971.

133. Merrill, E.G. The lateral respiratory neurons of the medulla: Their association with nucleus ambiguus, nucleus retroambigualis, the spinal accessory nucleus and the spinal cord. Brain Res. 24: 11-28, 1970.

134. Merrill, E.G. Finding a respiratory function for the medullary respiratory neurons. In: Essays on the Nervous System. R. Bellairs and E.G. Gray (eds.) Oxford: Clarendon, 451-486, 1974.

135. Merrill, E.G. Where are the real respiratory neurons? Fed. Proc. 40: 2389-2394, 1981.

136. Merrill, E.G., Lipski, J., Kubin, L., and L. Fedorko. Origin of the expiratory inhibition of nucleus tractus solitarius neurones. Brain Res. 263: 43-50, 1983.

137. Mitchell, R.A. and A.J. Berger. Neural Regulation of Respiration. Amer. Rev. Respir. Dis. 111: 206-224, 1975.

138.   Miura, M., Onai, T., and K. Takayama. Projections of
        upper structure to the spinal cardioacceleratory
        center   in   cats: an   HRP   study using a new
        microinjection method. J. Auton. Nerv. Syst. 7:
        119-139, 1983.

139.   Miura, M., and D.J. Reis.   Cerebellum: a pressor
        response elicited from the fastigial nucleus and its
        efferent pathway in the brain stem. Brain Res. 13:
        595-599, 1969.

140.   Miura, M., and D.J. Reis. A blood pressure response
        from fastigial nucleus and its relay pathway in the
        brainstem. Amer. J. Physiol. 219: No. 5, 1330-1336,
        1970.

141.   Morest, D.K. Experimental study of the projections
        of the nucleus of the tractus solitarious and the
        area postrema in the cat. J. Comp. Neurol. 130:
        277-300, 1967.

142.   Morrison, S.F. and G.L. Gebber. Classification of
        raphe neurons with cardiac-related activity. Amer. J.
        Physiol. 12: R49-R59, 1982.

143.   Moruzzi, G. Paleocerebellar inhibition of vasomotor
        and respiratory carotid sinus reflexes. J.
        Neurophysiol. 3: 20-32, 1940.

144.   Mraovitch, S., Kumada, M., and D.J. Reis. Role of
        the nucleus parabrachialis in cardiovascular
        regulation in cat, Brain Res. 232: 57-75, 1982.

145.   Ngai, S.H. and S.C. Wang. Organization of central
        respiratory mechanisms in the brain stem of the cat:
        localization by stimulation and destruction. Amer. J.
        Physiol. 190: 343-349, 1957.

146.   Okada, H. and I.J. Fox.   Respiratory grouping of
        abdominal sympathetic activity in the dog. Amer. J.
        Physiol. 213: 48-56, 1967.

147.   Oldfield, B.J. and E.M. McLachlan. The segmental
        origin of preganglionic axons in the upper thoracic
        rami of the cat. Neurosci. Lett. 18: 11-17, 1980.

148.   Oldfield, B.J. and E.M. McLachlan. An analysis of the
        sympathetic preganglionic neurons projecting from the
        upper thoracic spinal roots of the cat. J. Comp.

Neurol. 196: 329-345, 1981.

149. Owsjannikow, P. Die tonischen und reflectorischen centren der gefassnerven. Ber. Verh. K. Saechs. Ges. Wiss., Math.-Phys. Kl. 23: 135-147, 1871.

150. Panneton, W.M. and A.D. Loewy. Projections of the carotid sinus nerve to the nucleus of the solitary tract in the cat. Brain Res. 191: 239-244, 1980.

151. Pitts, R.F. The respiratory center and its descending pathways. J. Comp. Neurol. 72: 605-625, 1940.

152. Polosa, C. The silent period of sympathetic preganglionic neurons. Can. J. Physiol. Pharmacol. 45: 1033-1045, 1967.

153. Polosa, C., Gerber, U. and R. Schondorf. Central mechanisms of interaction between sympathetic preganglionic neurons and the respiratory oscillator. In: Central Interaction Between Respiratory and Cardiovascular Control Systems. Springer, Berlin, HP Koepchen, SM Hilton and A Trzebski (eds.), 137-142, 1980.

154. Preiss, G., Kirchner, F., and C. Polosa. Patterning of sympathetic preganglionic neuron firing by central respiratory drive. Brain Res. 87: 363-374, 1975.

155. Preiss, G., and C. Polosa. The relation between end-tidal CO_2 and discharge patterns of sympathetic preganglionic neurons. Brain Res. 122: 255-267, 1977.

156. Pryzbyla, A.C. and S.C. Wang. Neurophysiological characteristics of cardiovascular neurons in the medulla oblongata of the cat. J. Neurophysiol. 30: 645-660, 1967.

157. Ranson, S.W. and P.R. Billingsley. Vasomotor reactions from stimulations of the floor of the fourth ventricle. Amer. J. Physiol. 41: 85-90, 1916.

158. Remmers, J.E. and W.G. Tsiaris. Effect of lateral cervical cord lesions on the respiratory rhythm of anaesthetized decerebrate cats after vagotomy. J. Physiol. (Lond.). 233: 63-74, 1973.

159. Riche, D., Denavit-Saubie, M., and J. Champagnat.

Pontine afferents to the medullary respiratory system: anatomicofunctional correlation. Neurosci. Lett. 13: 151-155, 1979.

160. Richter, D.W. Generation and maintenance of the respiratory rhythm. J. Exp. Biol. 100: 93-107, 1982.

161. Richter, D.W. and D. Ballantyne. A three phase theory about the basic respiratory pattern generator. In: Central Neurone Environment and the Control Systems of Breathing and Circulation. M.E. Schlafke, H.P. Koepchen, and W.R. See (Eds.) Berlin, Springer-Verlag, 1983, pp. 164-174.

162. Rikard-Bell, G.C. Bystrzycka, E.K., and B.S. Nail. Brainstem projections to the phrenic nucleus; an HRP study in the cat. Neurosci. Lett. Suppl. 11: S70, 1983.

163. Rimm, A., Hartz, A., Kalbefleisch, J., Anderson, A., and R. Hoffman. Basic Biostatistics in Medicine and Epidemiology. Appleton-Century-Crofts. New York, 1980.

164. Rohlicek, C.V. and C. Polosa. Hypoxic responses of sympathetic preganglionic neurons in the acute spinal cat. Amer. J. Physiol. 241: H679-H683, 1981.

165. Rohlicek, C.V. and C. Polosa. Hypoxic responses of sympathetic preganglionic neurons in sino-aortic denervated cats. Amer. J. Physiol. 244: H681-H686, 1983.

166. Salmoiraghi, G.C. "Cardiovascular" neurons in the brain stem of the cat. J. Neurophysiol. 25: 182-197, 1962.

167. Salmoiraghi, G.C., and B.D. Burns. Notes on mechanism of rhythmic respiration. J. Neurophysiol. 23: 14-26, 1960.

168. Schlaefke, M.E. Koepchen, H.P. and W.R. See (Eds). Central Neurone Environment and the Control Systems of Breathing and Circulation. Springer-Verlag, New York. 1983.

169. Schlaefke, M.E., See, W.R., and H.H. Loeschke. Ventilatory response to alterations of H+ ion concentration in small areas of the ventral medullary

surface. Resp. Physiol. 10: 198-212, 1970.

170.   Seller, H. and M. Illert. The localization of the
        first synapse in the carotid sinus baroreceptor
        reflex pathway and its alteration of afferent input.
        Pfluegers Arch. 306: 1-19, 1969.

171.   Smith, O.A. Anatomy of central neural pathways
        mediating cardiovascular function.   In: Nervous
        Control of the Heart. W.C. Randall (Ed.), Williams
        and Wilkins, Baltimore, 1965, pp. 34-52.

172.   Speck, D.F. and C.L. Webber. Cerebellar influence on
        the termination of inspiration by intercostal nerve
        stimulation. Respir. Physiol. 47: 231-238, 1982.

173.   Spyer, K.M. Neural organization and control of the
        baroreceptor reflex.   Rev. Physiol. Biochem.
        Pharmacol. 88: 23-124, 1981.

174.   Spyer, K.M. and R.M. McAllen. Interaction of central
        and peripheral inputs onto vagal cardiomotor
        neurones. In: Koepchen, H.P., Hilton, S.M., and A.
        Trzebski. (Eds).

175.   St. John, W.M., Independent brain stem sites for
        ventilatory neurogenesis.   J. Appl. Physiol. 55:
        433-439, 1983.

176.   St. John, W.M., Glasser, R.L. and R.A. King.
        Apneustic breathing after vagotomy in cats with
        chronic pneumotaxic center lesions. Resp. Physiol.
        12: 239-250, 1971.

177.   Stroh-werz, M., Langhorst, P., and H. Camerer.
        Neuronal activity with relation to cardiac rhythm in
        the lower brain stem of the dog. Brain Res. 106:
        293-305, 1976.

178.   Tabatabai, M., Ovassapian, A., Etemadi, A.A., and B.
        Turner.   Respiratory arrest induced by unilateral
        lesion (s) of the medullary inspiratory center in
        cats. Proc. Soc. Exp. Biol. and Med. 145: 1333-1338,
        1974.

179.   Takeuchi, Y., Uemura, M., Matsuda, K., Matsushima,
        R., and N. Mizuno. Parabrachial nucleus neurons
        projecting to the lower brain stem and spinal cord. A
        study in the cat by the Fink-Heimer and the

horseradish peroxidase methods. Exp. Neurol. 70: 403-412, 1980.

180. Tang, P.C., Maire, T.W., and V.E. Amassian. Respiratory influence on the vasomotor center. Amer. J. Physiol. 191: 218-224, 1957.

181. Taylor, D.G. and G.L. Gebber. Sympathetic unit responses to stimulation of cat medulla. Amer. J. Physiol. 225: 1138-1146, 1973.

182. Thomas, D.M., Kaufman, R.P., Sprague, J.M. and W.W. Chambers. Experimental studies of the vermal cerebellar projections in the brain stem of the cat (fastigiobulbar tract). J. Anat. (Lond.), 90: 371-385, 1956.

183. Tohyama, M., Sakai, K., Touret, M., Salvert, D., and M. Jouvet. Spinal projections from the lower brain stem in the cat as demonstrated by the horseradish peroxidase technique. II. Projections from the dorsolateral pontine tegmentum and raphe nuclei. Brain Res. 176: 215-231, 1979.

184. Umbach, W. and H.P. Koepchen (Eds). Central Rhythmic and Regulation. Hippocrates, Stuttgart, 1974.

185. Wang, S.C., Ngai, S.H., and M.J. Frumin. Organization of central respiratory mechanisms in the brain stem of the cat: genesis of normal respiratory rhythmicity. Amer. J. Physiol. 190: 333-342, 1957.

186. Wang, S.C. and S.W. Ranson. Autonomic responses to electrical stimulation of the lower brainstem. J. Comp. Neurol. 71: 437-455, 1939.

187. Ware, C.B., and E.J. Mufson. Spinal cord projections from the medial cerebellar nucleus in tree shrew (Tupaia glis). Brain Res. 171: 383-400, 1979.

188. Westlund, K.N., Bowker, R.M., Ziegler, M.G., and J.D. Coulter. Origins of spinal noradrenergic pathways demonstrated by retrograde transport of antibody to dopamine-beta-hydroxylase. Neurosci. Lett. 25: 243-249, 1981.

189. Wyman, R.J. Neural generation of the breathing rhythm. Ann. Rev. Physiol. 39: 417-48, 1977.

APPENDIX I

NERVE RECORDING TECHNIQUE

A simple model was devised to illustrate fundamental principles of signal recording which apply to methods used in this dissertation (Fig. A-1, Bottom). To mimic nerve activity, trains of 1 msec impulses were produced by a square wave stimulator and isolation unit (SIU). Prior to amplification, these signals were passed through a RC circuit to simulate the effects of nerve impedence (due to the nerve fibers, epineural sheath, etc.) on extracellularly recorded action potentials. A nerve placed on a bipolar electrode is analogous to the RC circuit in this model. The nerve or the RC circuit functions as a "leaky" integrator (low pass filter) of the extracellularly recorded action potentials or the stimulator impulse trains, respectively.

Signal B closely approximated the wave form of the input signal to the amplifiers (Amp A and Amp B) following the RC circuit stage (Fig. A-1, Top). The wide frequency filter characteristics of Amp B minimally filtered slow potentials from the RC circuit stage and allowed passage of the relatively high frequency (50 Hz) stimulus trains. When Method B is used for recording nerves, the extracellularly recorded signals represent high frequency bursts of action potential activity along with some integration of that activity resulting from impedence of the nerve. The term
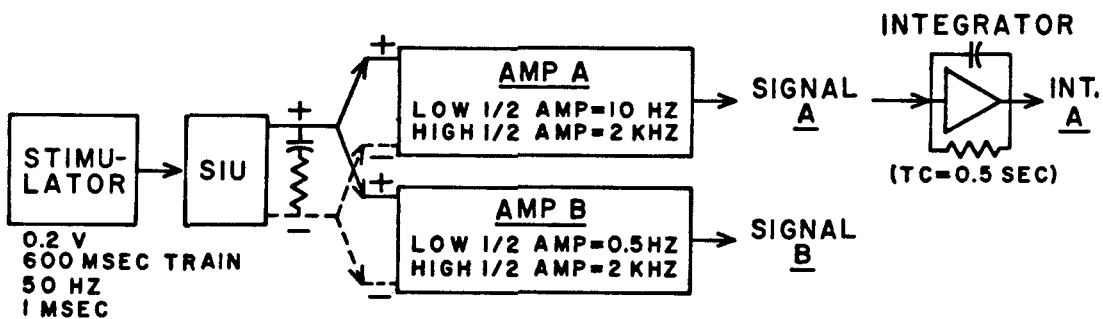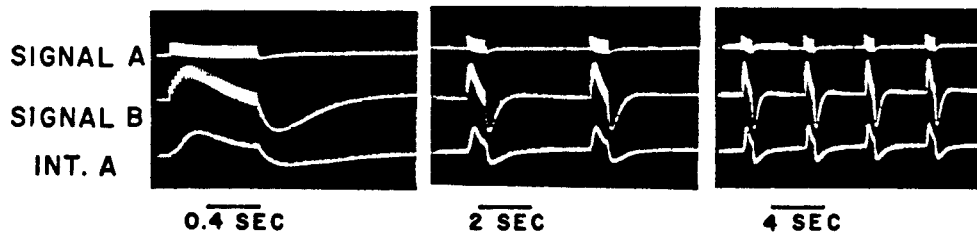
Figure A-1

Electronic model illustrating differences between two signal
filtering methods, A and B (see text).

SIGNAL A
SIGNAL B
INT. A

0.4 SEC   2 SEC   4 SEC

INTEGRATOR

STIMU-LATOR → SIU

0.2 V
600 MSEC TRAIN
50 HZ
I MSEC

AMP A
LOW 1/2 AMP=10 HZ
HIGH 1/2 AMP=2 KHZ

→ SIGNAL A

AMP B
LOW 1/2 AMP=0.5HZ
HIGH 1/2 AMP=2 KHZ

→ SIGNAL B

→ INT. A

(TC=0.5 SEC)

"envelope of spikes" has been used to describe this type of recorded nerve activity.

Alternatively, slow potentials due to either the impedence properties of the nerve, or the RC circuit in the analogous electronic model, are eliminated by high pass filters. The effect of high pass filtering the input signal at the primary amplification stage is illustrated by the wave form of Signal A. Slow potentials were filtered from the signal and high frequency activity was retained. The slow potential activity was regenerated by low pass filtering Signal A at a later stage (ie. the integrator) to produce Int. A. The wave form of Int. A closely approximated the slow potential wave form of Signal B and also accurately represented an RC integration of Signal A. When nerves are extracellularly recorded using Method A, the amplified high pass filtered signals represent action potential activity. A "leaky" integration of the action potentials is produced by passing the amplified output through a low pass filter.

In conclusion, this electronic model graphically illustrates that there is no fundamental problem with recording extracellular nerve signals using either Method A or B. Both methods provide accurate representations of nerve activity. For this dissertation, nerve signals were recorded using Method A. Method A was preferred for these

particular studies because Method B is more susceptible to mechanical artifacts which are potentially of great concern when recording from the inferior cardiac nerve (isolated under partially removed T2-T3 ribs). When using Method B, slow wave potentials due to impedence changes resulting from mechanical respiratory and cardiac movements could be recorded. Use of Method A for these projects easily insured that the respiratory and cardiac rhythms in the sympathetic nerve signals being studied were specifically due to nerve activity. For all the studies, analogous equivalents of Signal A and Int. A were recorded and assessed.

APPROVAL SHEET

The dissertation submitted by Caroline Ann Connelly has been read and approved by the following committee:

Robert D. Wurster, Ph.D., Director
Professor, Physiology
Loyola, Stritch School of Medicine

Clarence N. Peiss, Ph.D.
Professor, Physiology
Loyola, Stritch School of Medicine

John X. Thomas, Jr., Ph.D.
Associate Professor, Physiology
Loyola, Stritch School of Medicine

Charles Robinson, D.Sci.
Adjunct Assistant Professor, Physiology, Loyola
Assoc. Dir. Rehab. Res. Dev. Ctr., V.A. at Hines

Edward J. Neafsey, Ph.D.
Assistant professor, Anatomy
Loyola, Stritch School of Medicine

Susan M. Barman, Ph.D.
Assistant Professor, Pharmacology
Michigan State University

The final copies have been examined by the director of the dissertation and the signature which appears below verifies the fact that any necessary changes have been incorporated and that the dissertation is now given final approval by the committee with reference to content and form.

The dissertation is therefore accepted in partial fulfillment of the requirements for the degree of Doctor of Philosophy.

Aug 28, 1984
_____
Date

Robert D. Wurster
_____
Director's Signature